EFFICIENT MULTICHANNEL METHODS FOR HIGH-RATE DATA TRANSMISSION WITH APPLICATION TO ISDN

(OR)

POURING WATER TO GET MORE OUT OF COPPER

Thesis by

Rajaram Ramesh

In Partial Fulfillment of the Requirements

for the Degree of

Doctor of Philosophy

California Institute of Technology

Pasadena, California

1992

(Submitted August, 1991)

Acknowledgements

It is a pleasant task to acknowledge the support of various people who have, in a way, influenced the growth of this thesis. However, it is simply impossible to thank each and every person who had a contribution to the development of this thesis and to my development as a person; I shall try to do my best.

First and foremost, I would like to thank my adviser, Dr.E.C.Posner for his support through the years. He was the person who steered me in the direction of the ISDN local loop. I am particularly indebted to him for the flexibility he allowed me in defining my research; I am sure it will be invaluable to me in the years to come.

The inspiration to use Multirate Signal Processing in the thesis came as a result of a course I did with Dr.P.P.Vaidyanathan. I would like to thank him for this, and also for the various discussions I had with him in the course of my research. His colossal knowledge of signal processing has benefitted me to a great extent. The friendship and technical help of David Koilpillai and Vinay Sathe, members of Dr.Vaidyanathan's research group, is appreciated.

It has been a pleasure to have been a student of Dr.Joel Franklin. I enjoyed his courses immensely, and was able to use some of the concepts he taught me in my research. He was readily available for discussions and was a member of the committee for my defense. For these, I am grateful to him.

I thank the other members of my committee: Dr.R.J.McEliece, Dr.Y.S.Abu-Mostafa and Dr.M.K.Simon.

The professors in the Department of Electrical Engineering at the Indian Institute of Technology, Madras were primarily responsible for whetting my appetite

for my field of research, and I thank Dr.Bhaskar Ramamurthi, Dr.V.Venkata Rao, Dr.M.Anthony Reddy and Dr.K.Radhakrishna Rao for their guidance.

I would like to acknowledge the help of Dr.Kamran Sistanizadeh of Bellcore in obtaining the impulse responses of representative loops from the ISDN local loop plant. I would also like to thank Dr.B.R.Petersen and Dr.D.D.Falconer of Carleton University for providing me with data on crosstalk impulse responses.

The music of the great composers, Mozart in particular, has kept me company through times good and bad. I classify the music of Mozart into beautiful and more beautiful. In a similar vein, I could broadly classify the people I have come across during my stay at Caltech into nice and nicer. Barring isolated incidents, my personal experiences at Caltech have been pleasant, and I thank the people who made them so.

I am grateful to my friends in and around Caltech who did their part to enrich my life. Of them, John Miller, Ian Galton, Kerry Galton, Janet McWaid and Kathleen Kramer receive honourable mention for their companionship and support. The unnamed few, I hope, will not take umbrage at the fact that their names have been left out.

I would also like to thank my roommates (at one time or the other) primarily for sharing culinary responsiblities, which made existence more bearable. These people include Girish Pendse, Sanjay Kumar, Kumar Sivarajan, Kannan Rangaramanujam and Rajesh Panchanathan. I also thank Kumar Sivarajan for TEX help.

I thank Bette Linn for helping me deal with the morass of paperwork to be done in order to fulfill my administrative responsiblities. I am also thankful to other members of the secretarial and support staff in the EE department at Caltech, particularly Linda Dosza, Su McKinley, Janice Tucker, Illiana Salazar, Pamela Jones, Debbie McGougan, Paula Samazan, Sandi Dawson, Cynthia Stewart and Gloria,

for providing scintillating conversation.

I would like to thank my family for their love and understanding.

Financial support for this research was provided by a grant form Pacific Bell; their support in this respect is gratefully acknowledged.

Abstract

In this thesis, we are concerned with the transmission of data over channels with intersymbol interference. We consider input signals which are multiplexed versions of several parallel input signals, with the aim of splitting the input signal spectrum into disparate frequency bands and shaping the input spectrum by adjusting the power on each of the frequency bands. We introduce a multirate signal processing framework for the representation of the channel under these conditions and derive simple equivalents for the channel and the associated processors.

Using the equivalent circuits, we derive simple equalization schemes for the channel by drawing from the theory of polynomial matrices. We show that vector equalization can be reduced to a combination of prefiltering, postfiltering and scalar equalization of a few of the parallel input signals. We also discuss several interesting properties of this decomposition.

In the case when the channel is corrupted by colored noise, we derive expressions for the optimum prefilters and postfilters with decision feedback equalization that minimize the mean-squared error between the input and the output, given a constraint on the input power. For uncorrelated inputs, the scheme leads to a set of parallel independent scalar channels with the optimum postfilter whitening the noise, which permits the optimal use of trellis codes for data transmission.

We apply the scheme to a special channel, viz., the ISDN digital subscriber loop. The main impairments on this channel are intersymbol interference and crosstalk due to adjacent loops in the same binder group. Crosstalk is an especially interesting case of noise since it depends on the signal being transmitted; we assume that all loops in a binder group transmit using the same scheme. We consider two

cases of crosstalk noise: when transmission between different loops in a binder group is synchronized, the crosstalk noise is wide-sense cyclostationary, and with a lack of synchronization between loops, the crosstalk noise is wide-sense stationary. We present methods to determine the optimum filters for data transmission and the optimum input power distributions for both these cases. We demonstrate the possibility of data transmission at the T1 rate, i.e., 1.544 Mb/s over most loops in the local loop plant. We also find that synchronizing transmission between different loops in a binder group does not get us much; the difference in the throughputs for the cases of cyclostationary crosstalk and wide-sense stationary crosstalk does not seem to justify the effort involved in synchronization.

Table of Contents

Chapter 1 Introduction

Communication is essentially the transfer of information from one point to another. The information conveyed by a modern communication system comes in many forms—voice, video, music, fax, etc. In most cases, this information has been represented accurately by an analog waveform; hence it seemed natural to use an analog communication system and this is what is still in use in the case of radio and television. However, it is well known that a digital communication system has several advantages over an analog one, a main one being repeatability. Thus it is of primary interest to transmit the analog waveform in a digital format and try to recover the analog information only at the receiving end. However, communication channels really only permit the passage of continuous waveforms. Hence, we have to transmit analog waveforms over the channel. These analog waveforms have to be obtained from digital data and have to be reconverted back to digital data at the receiving end to ensure more efficient processing. The processed digital data is then used to recover the original transmitted source signal. In this chapter, we shall briefly go over the various steps involved in the transfer of information using a digital communication system. We shall give some historical perspective about the various components and identify the parts of the system that we address in this thesis.

1.1 A Digital Communication System

A block diagram of a typical digital communication system is given in Fig. 1.1.

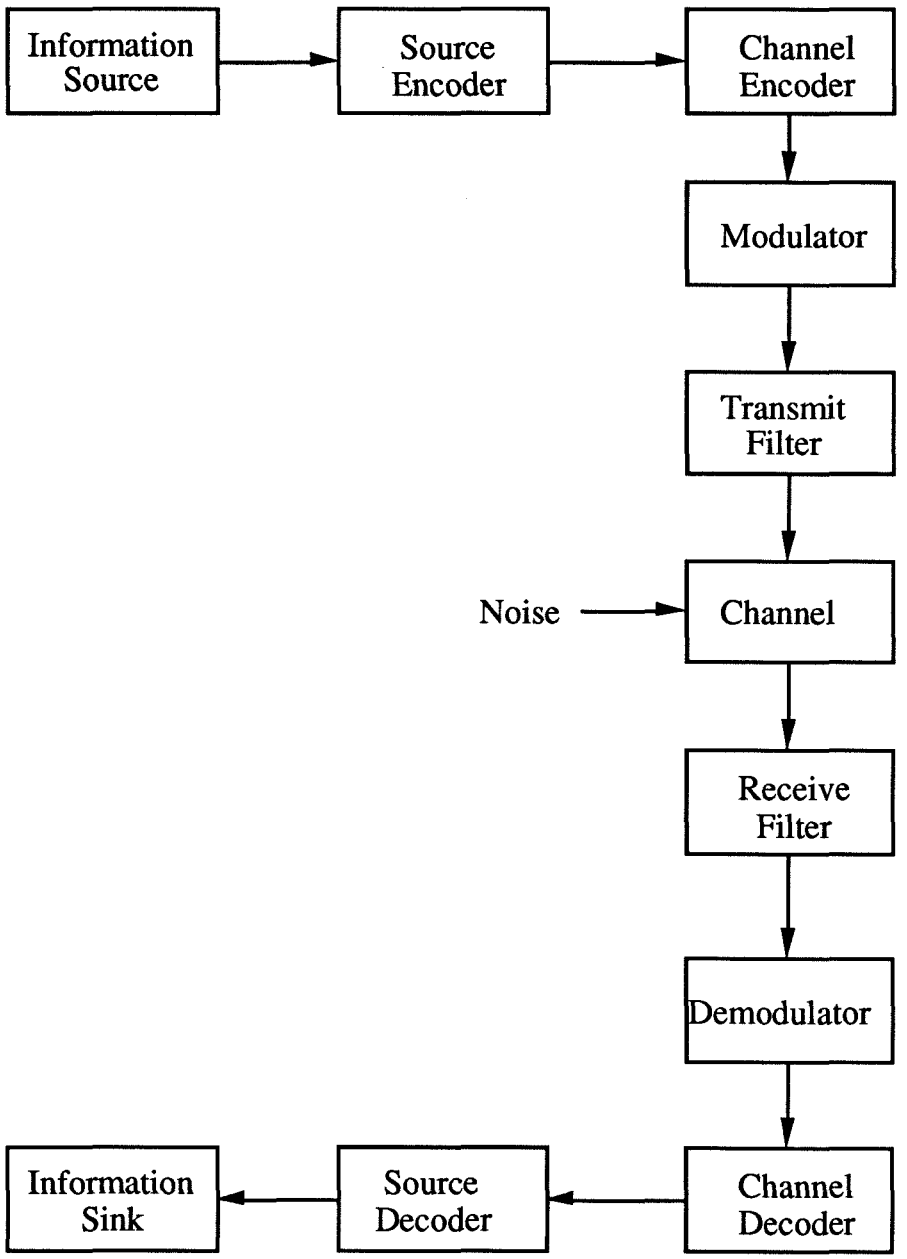

Fig. 1.1 A Digital Communication System

The source signal is passed through a *source encoder*, which essentially converts the analog source waveform into a digital, discrete-time signal. Hence, it involves the processes of sampling, quantization and any associated data compression to remove the redundancy in the signal. The output of the source encoder, which is assumed to be a bit stream, enters the *channel encoder*, which inserts controlled redundancy into the signal in order to protect the system against errors which may occur due to the non-ideality of the transmission medium. Channel encoding is the domain of the various error-correcting codes found in the literature. A basic tenet of Claude Shannon [1] is that the source encoding process, which involves the removal of redundancy, and the channel encoding process, which involves the introduction of redundancy, can be separated without any loss in information-theoretic optimality, albeit perhaps with an increase in complexity.

The encoded data is then passed through a *modulator*, which converts the bit stream into a discrete-time signal with the symbols taking maybe analog values. There is much to be gained by combining the processes of channel encoding and modulation; this is the basic idea behind trellis-coded modulation, which was proposed in 1982 by Ungerboeck [2]. The *transmit filter* shapes the discrete-time-modulated signal to give an analog waveform which is transmitted over the channel. At the receiving end, the *receive filter* converts the received analog waveform into a discrete-time signal, which is passed through the *demodulator*. Hence, we essentially have a discrete-time channel between the modulator and the demodulator.

The demodulator essentially reverses the operation of the modulator. The *channel decoder* generates an estimate of the binary data that was fed to the channel encoder and the *source decoder* attempts to reproduce the original source waveform.

The transmit and receive filter fall in the domain of the various equalization techniques found in the literature, the basic idea behind which is to account for the linear distortion introduced by the channel. In this thesis, we shall delve into the design of good transmit and receive filters for transmission over channels which introduce appreciable linear distortion. It is possible to find optimum analog filters

for the transmit and receive filters; however these are seldom realizable at affordable cost. Hence we shall partition these filters into two parts, a fixed analog part that is easily realizable and a digital part which we shall try to optimize given the channel and noise characteristics.

The basic motivation for the schemes we propose in this thesis stems from a theorem in Information Theory called the Water-Pouring Theorem [3], which is used to calculate the capacity of a channel with a non-flat frequency response. One of the basic results of this theorem is that the input waveform to a channel has to be spectrally shaped to match the channel frequency response in order to achieve capacity. We will propose a scheme where we attempt to spectrally shape the input to the channel by partitioning the signal into various frequency bands and transmitting with unequal energy over each of these bands. This scheme was motivated in part by sub-band coding [4], which is a technique that exploits the non-flat spectrum of the source signal to achieve efficient data compression. What we propose, in essence, is a complement of sub-band coding tailored toward channel-coding applications.

1.2 Outline of the Thesis

In Chapter 2, we motivate and describe the scheme to be used for data transmission over the channels of interest. We derive simplified equivalent circuits for this scheme by borrowing heavily from the theory of Multirate Signal Processing [5]. These equivalent structures give us a framework to propose some simple equalization schemes for such channels using theorems on matrices whose entries are polynomials. We describe these equalization schemes and elucidate some of their properties.

In Chapter 3, we are mainly concerned with the derivation of optimum filters for transmitting data over a channel with a non-flat frequency response and with correlated noise corrupting the output of the channel. The optimum transmission scheme leads to a set of parallel independent channels, i.e., no individual input

signal interferes at the output due to another input signal. In addition, the noise on each channel is uncorrelated with the noise on other channels. We evaluate the performance of this scheme and find that it performs much better than traditional schemes proposed towards the same objective.

In Chapter 4, we apply the filters derived in Chapter 3 to the special case of the ISDN subscriber loop channel. The aim of ISDN, or the Integrated Services Digital Network, is to give telephone users all the digital communication links they require for both voice and data communication through a single set of standardized interfaces [6]. One of the main impairments on this channel is the non-ideal frequency response of the loops. The noise is predominantly crosstalk from other wires in the same cable. The crosstalk noise depends on what is being transmitted in adjacent loops, which are assumed to be transmitting using the same scheme. Thus the problem of finding the optimum filters becomes more involved, but we were able to solve it. We present methods to model the statistical properties of the crosstalk noise in the two cases where transmission on different wires in the same bundle is synchronized, and when it is not synchronized. Using these models, we derive optimum filters for data transmission over these loops and evaluate the performance of the scheme. The main result is that transmission at the T1 rate of 1.544 Mb/s appears to be feasible over a large subset of the local loop plant. Also, we show synchronization of transmission over various wires in a bundle improves performance, but not by enough to justify the effort involved in synchronization.

We conclude the thesis in Chapter 5 by briefly summarizing our results and proposing avenues for future research. There are a host of unsolved problems that one can envision in this area. We describe some of the unsolved problems that we encountered during the course of our research.

References

[1] C. E. Shannon, "A Mathematical Theory of Communication," *Bell System Tech. Journal*, no. 27, pp. 379-423, 623-656, 1948.

[2] G. Ungerboeck, "Channel Coding with Multilevel/Phase Signals," *IEEE Trans. Info. Theory*, vol. 28, pp. 55-67, 1982.

[3] R. E. Blahut, *Principles and Practice of Information Theory*, Addison-Wesley Publishing Company, 1988.

[4] N. S. Jayant and P. Noll, *Digital Coding of Waveforms: Principles and Applications to Speech and Video*, Prentice-Hall, 1984.

[5] R. E. Crochiere and L. R. Rabiner, *Multirate Digital Signal Processing*, Prentice-Hall, 1983.

[6] Irwin Dorros, "Telephone Nets Go Digital," *IEEE Spectrum*, vol. 20, no. 4, pp. 48-53, April 1983.

Chapter 2 A Framework for Multichannel Data Transmission

A person dealing with the transmission of data over any real-life channel has to deal with quite a few impairments, a primary one being noise. Various schemes have been proposed in the past to effectively combat noise; error-control coding as envisioned by Shannon has been used for this purpose. Another impairment of great practical significance is Intersymbol Interference (ISI), which arises due to the non-ideal transfer function of the channel used. In the words of the good poet [17] (a technical one, nevertheless)—"Give me a channel without ISI and I will conquer the world." In spite of the ubiquitous nature of ISI, traditional solutions proposed to combat it, like linear equalization and decision-feedback equalization, have been quite ineffective. We have to qualify that earlier statement; of late researchers have discovered that optimum decision-feedback equalization can function efficiently if one used a prefilter to optimize the transmission bandwidth. However, the method we use to optimize the transmitted signal spectrum is quite different. It is a multichannel method motivated in part by sub-band coding applications which are used to exploit the non-uniformity of the source signal spectrum to achieve efficient transmission of the source data. The main purpose of this chapter is to motivate the framework we propose to use and to illustrate an interesting application of

this framework by making use of the framework to derive some novel equalization schemes.

2.1. Introduction

In this chapter, we consider data transmission over a discrete-time channel with intersymbol interference. The channel can be represented by its Z-transform. For example, we have the channel

$$H(z) = h_0 + h_1 z^{-1} + h_2 z^{-2} + \ldots + h_{N-1} z^{-(N-1)} \tag{2.1.1}$$

where z^{-1} denotes the delay operator and h_i (or $h(i)$) is the i th impulse response coefficient. The output $y(n)$ of this channel is related to its input $x(n)$ as follows:

$$y(n) = h_0 x(n) + h_1 x(n-1) + h_2 x(n-2) + \ldots + h_{N-1} x(n-N+1). \tag{2.1.2}$$

The channel is said to be *ISI-free* if $h_i = 0$ for $i \neq 0$. Almost all practical channels suffer from intersymbol interference.

Since we are concerned with data communication, our desire is to recover $x(n)$ at the output end of the communication system. From the form of equation (2.1.2), it is evident that some form of processing is necessary at the output end to recover $x(n)$ from $y(n)$. The traditional techniques used to combat the problem of intersymbol interference include linear and decision-feedback equalization.

Linear equalization merely attempts to invert the channel transfer function, i.e, the linear equalizer $L(z)$ tries to approximate $1/H(z)$ as closely as possible. In the absence of any kind of noise, $x(n)$ can be obtained by passing $y(n)$ through a filter with a Z-transform $1/H(z)$. When $H(z)$ has zeros outside or on the unit circle, this approach leads to problems associated with the stability of the equalizer. When the output $y(n)$ is corrupted by noise, the noise is also processed by the equalizer. Hence this technique leads to noise enhancement in spectral regions where $H(z)$ has low magnitude.

The problem of noise enhancement is tackled using a technique known as decision-feedback equalization, which is essentially an ISI-cancellation technique by knowledge of the channel impulse response and the past estimates of the transmitted symbols. The schematic of the decision feedback equalizer is shown in Fig. 2.1. A variant of this scheme, called Tomlinson Precoding [1], is used to avoid the problem of error propagation due to incorrect decisions.

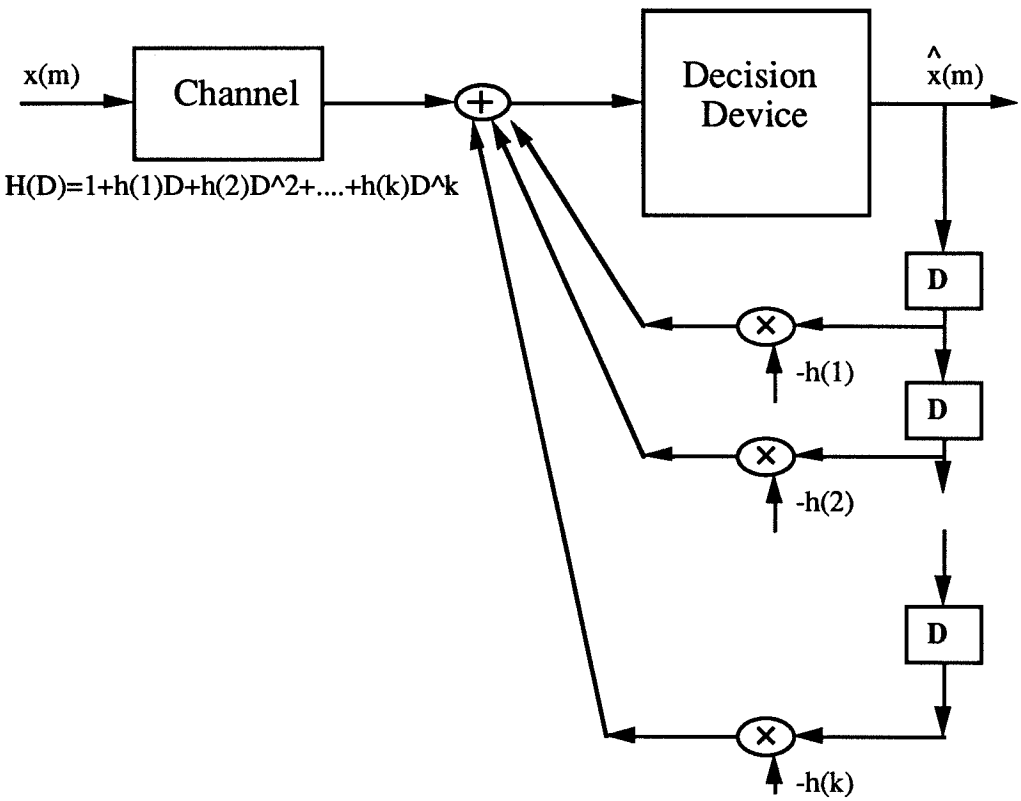

Fig 2.1. The Decision-Feedback Equalizer

While DFE sounds like a perfectly valid method to combat ISI, our negative assessment is that we are just trying to modify the channel to be a benign ISI-free channel without any attempt to tailor the transmitted signal to suit the channel characteristics. It does not make any sense to transmit data at frequencies where

the channel frequency response has zeros, since that data will be lost. Intuitively, it appears as though it is beneficial to tailor the input signal spectrum to match that of the channel in a certain sense; we want to transmit more energy where the channel has a high gain and less energy over frequency regions where the channel has low gain. The fact that DFE does not do very well can be numerically verified for a variety of channels by finding the capacity of the channel with no constraints, and the capacity of the channel when DFE is used. The methods to calculate the capacities in the two cases are elaborated on in the next paragraph for the ISI-channel and in Section 3.4 for the DFE technique. To give an example, in Fig. 2.2 we plot the capacity of the dicode channel, or the $1-D$ channel (D is functionally the same as z^{-1}), versus the capacity of the same channel with DFE. The plot clearly indicates that significant improvement must be possible over the DFE technique by using more efficient techniques.

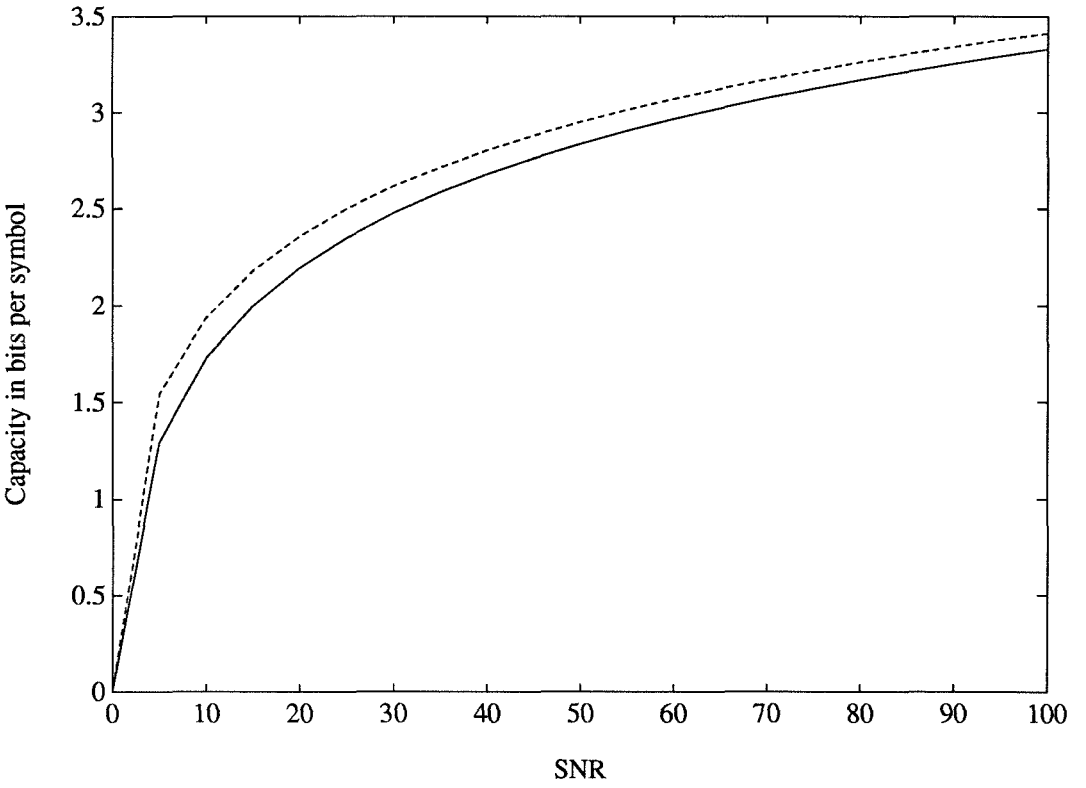

Fig. 2.2 Capacity of Dicode Channel vs Capacity with DFE
(Dotted Line - No constraints; Solid Line - DFE Used)

The intuitive idea of tailoring the input signal spectrum is given formal justification by Information Theory, by determining the capacity of a discrete-time channel with ISI. The result is known as the Water-Filling Theorem, and was first proved by Tsybakov in [13] and has been re-derived using different methods by Hirt and Massey in [12]. With the input power restricted to E_s, i.e.,

$$E[x(k)^2] \leq E_s, \tag{2.1.3}$$

the capacity of the channel $H(z)$, or equivalently $H(e^{j\omega})$ (which is the discrete-time Fourier transform of the channel or the Z-transform evaluated on the unit circle), is given by:

$$C(E_s) = \frac{1}{2\pi} \int_0^{\pi} \log[\max(\theta |H(e^{j\omega})|^2, 1)] d\omega \tag{2.1.4}$$

where θ is the solution to

$$\frac{1}{2\pi} \int_0^{\pi} \max(\theta - |H(e^{j\omega})|^{-2}, 0) \; d\omega = E_s/N_0. \tag{2.1.5}$$

The noise is assumed to be additive, white and Gaussian with variance $N_0/2$. However, what is more interesting is that the capacity-achieving inputs are correlated Gaussian random variables with mean zero and a power spectrum given by

$$S_x(\omega) = \begin{cases} \frac{N_0}{2}(\theta - |H(e^{j\omega})|^{-2}) & \text{if } \theta |H(e^{j\omega})|^2 \geq 1 \\ 0, \text{else} \end{cases} \tag{2.1.6}$$

This theorem can be illustrated in pictorial form as shown in Fig. 2.3.

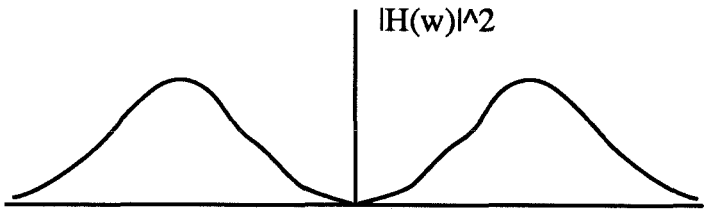

Channel Frequency Response

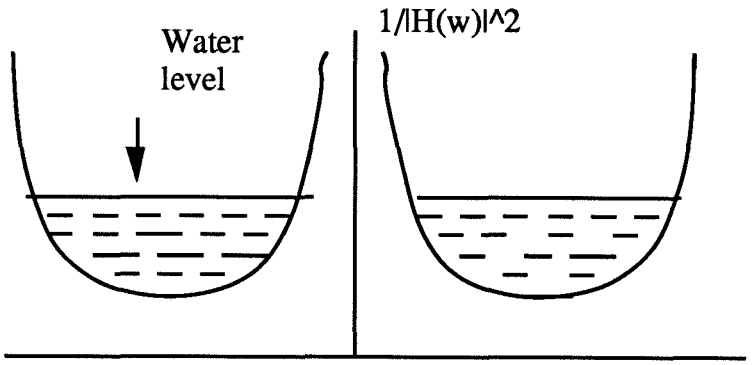

Water Filling Schematic

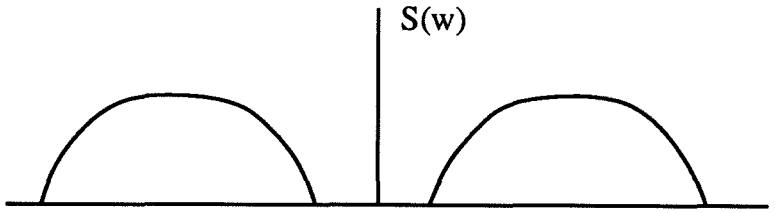

Optimum Transmitted Signal Power Spectrum

Fig. 2.3. The Water-Pouring Theorem

From this theorem, it is evident that spectral shaping of the input is quite important in achieving efficiency of transmission over ISI channels. There are various approaches that one can take to achieve the required spectral shaping. One approach is to use a single prefilter at the input to the channel. We eschew this

approach to a multichannel one: one in which we divide the input signal into several frequency bands and transmit with unequal energies in each of these frequency bands to achieve the required spectral shaping. The reason we consider this approach is that it permits us to use the exciting area of multirate signal processing in our analysis.

The multichannel approach has received a lot of interest in the last few years due to the possibility of concatenating multilevel trellis codes in order to achieve high coding gains over such channels. A host of researchers have considered this problem[2][5][14]. However, what we find lacking in their presentation is a formal and rigorous method to represent the channel under such a transmission format. The main purpose of this chapter is to do so by drawing from Multirate Signal Processing principles. Using these principles, we derive expressions for the equivalent channel model and the resultant form of the preprocessors and postprocessors. With this representation, we find ourselves in a position to derive some novel equalization schemes for ISI channels, and we do so.

The organization of this chapter is as follows: In Section 2.2, we introduce the structure to be used in the scheme, which was motivated in the previous section. Equivalent forms to the structure are obtained using well-known identities of multirate signal processing. In Section 2.3 , we consider the problem of DFE or precoding of a class of ISI channels and show how this problem can be simplified considerably by appealing to certain theorems from matrix theory. In Section 2.4, we consider some interesting properties which arise due to our decomposition, and show how some of these properties, which essentially involve a shifting of zeros and poles, can be put to use.

2.2 Description of the Scheme and Equivalent Structures

The basic structure to accomplish the multiplexing of several parallel input signals with different powers in different frequency bands is shown in Fig. 2.4.

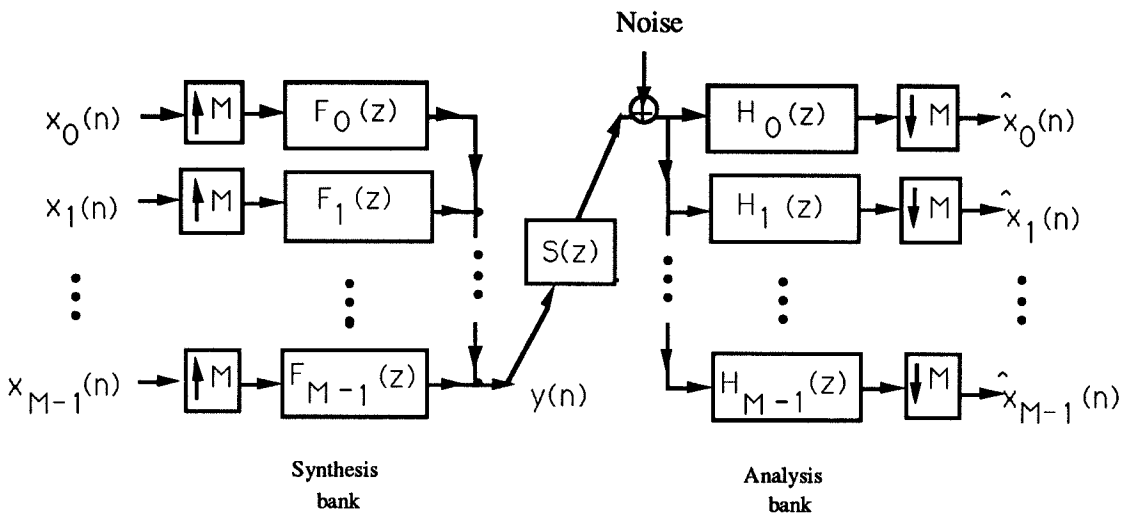

Fig 2.4. Basic System for Frequency Partitioning

The same structure has also been used for implementing transmultiplexers (e.g., see [6]). The filters $F_0(z), F_1(z), ..., F_{M-1}(z)$ are referred to as the *synthesis filters* and have their passbands non-overlapping while the combination of their passbands includes the whole frequency band. Typically, $F_0(z)$ is a lowpass filter, $F_1(z)$ through $F_{M-2}(z)$ are bandpass filters, and $F_{M-1}(z)$ is a highpass filter. The filters $H_0(z), H_1(z), ...H_{M-1}(z)$ are called the *analysis filters* and have a similar frequency structure to that of the corresponding synthesis filters.

The box with the $\boxed{\uparrow M}$ is called an *interpolator*; the relation between its input $x(n)$ and its output $y(n)$ can be described as follows:

$$y(n) = \begin{cases} x(n/M), & \text{if } n \text{ is a multiple of } M \\ 0, & \text{otherwise.} \end{cases} \tag{2.2.1}$$

In the Z-domain, we have the input-output relationship of an interpolator to be

$$Y(z) = X(z^M). \tag{2.2.2}$$

For the *decimator*, i.e., the box with the $\boxed{\downarrow M}$, the corresponding relationship is

$$y(n) = x(Mn) \tag{2.2.3}$$

which translates to

$$Y(z) = \frac{1}{M} \sum_{m=0}^{M-1} X(z^{\frac{1}{M}} e^{\frac{-j2\pi m}{M}}) \tag{2.2.4}$$

in the Z-domain. In the frequency domain, interpolation compresses the spectrum and produces images of it, while decimation expands the spectrum and might lead to aliasing. In Fig. 2.4, each synthesis filter chooses one of the images of the compressed spectrum and passes it through the channel, and at the receiving end, the corresponding analysis filter extracts the same frequency band out, with the decimator restoring the original sampling rate. The interpolator and decimator can essentially be viewed as sampling rate changers to be utilized in multiplexing operations.

The channel transfer function $S(z)$ is given by

$$S(z) = s_0 + s_1 z^{-1} + s_2 z^{-2} + ... + ... \tag{2.2.5}$$

Our initial path of research was to find suitable analysis and synthesis filters which achieve an efficient multiplexing. The criterion used to judge the efficiency of multiplexing was the crosstalk between adjacent channels and the flatness of the resultant spectrum about the band edges. Regrettably, none of the methods we tried gave us a satisfactory result to design these filters. The problem of finding efficient filters for transmultiplexing with the presence of a non-ideal channel in between remains open. However, an examination of the framework and derivation of its equivalent circuits led to quite a few interesting ideas for the data transmission problem, and we will address these in the rest of the thesis.

To simplify the analysis and synthesis filters, we use a tool known as the Polyphase Decomposition [7]. This is essentially a tool for time-division multiplexing. Depending on the numbering of the various multiplexed components, the decomposition is classified into two types, which, maybe due to a lack of a better imagination, are known as the polyphase decompositions of Type 1 and Type 2. In the Type 1 Polyphase Decomposition, a transfer function $H(z)$ is expressed as

$$H(z) = \sum_{k=0}^{M-1} z^{-k} E_k(z^M) \tag{2.2.6}$$

and the $E_k(z)$ are called the Type 1 Polyphase components of $H(z)$. For example, if $H(z) = h_0 + h_1 z^{-1} + h_2 z^{-2} + h_3 z^{-3}$ and $M = 2$, we have

$$E_0(z) = h_0 + h_2 z^{-1}$$

and

$$E_1(z) = h_1 + h_3 z^{-1}.$$

The Type 2 Polyphase Decomposition is an index-reversed version of the Type 1 decomposition. Thus, the Type 2 Polyphase decomposition of $H(z)$ is

$$H(z) = \sum_{k=0}^{M-1} z^{-(M-1-k)} R_k(z^M) \tag{2.2.7}$$

and the type 2 polyphase components of $H(z)$ are $R_k(z) = E_{M-1-k}(z)$.

Using the polyphase decompositions of Types 1 and 2, we can express the analysis and synthesis filters as

$$H_k(z) = \sum_{l=0}^{M-1} z^{-l} E_{kl}(z^M), \qquad 0 \leq k, l \leq M-1 \tag{2.2.8}$$

$$F_k(z) = \sum_{l=0}^{M-1} z^{-(M-1-l)} R_{lk}(z^M), \qquad 0 \leq k, l \leq M-1 \tag{2.2.9}$$

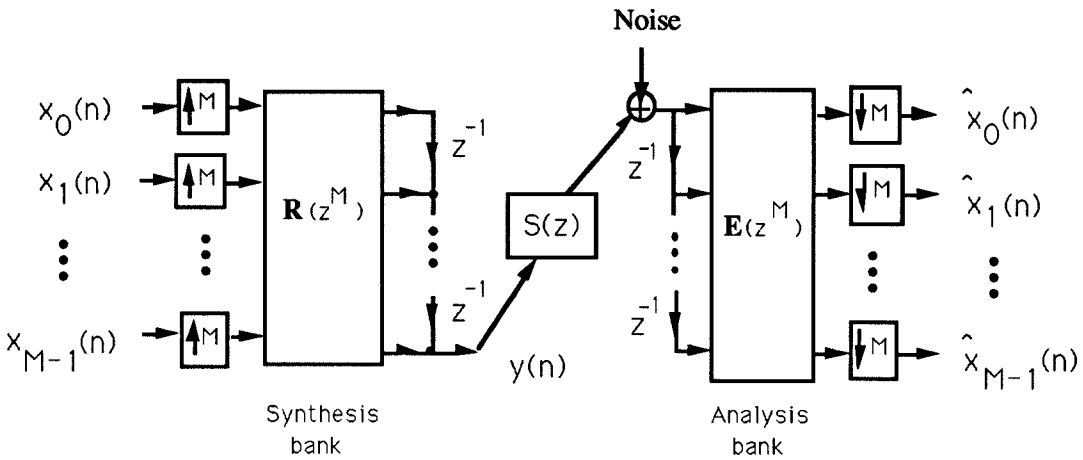

Fig 2.5. Polyphase Representation of the System in Fig 2.4.

This representation leads to Fig. 2.5 where the polyphase component matrices $\mathbf{E}(z)$ and $\mathbf{R}(z)$ are such that the $(k,l)^{\text{th}}$ element of $\mathbf{E}(z)$ is $E_{kl}(z)$ and the $(k,l)^{\text{th}}$ element of $\mathbf{R}(z)$ is $R_{lk}(z)$. We now introduce certain identities of Multirate Signal Processing, sometimes known as the 'Noble' identities. These are illustrated in Fig. 2.6. Applying these identities, the interpolators and decimators can be moved to obtain Fig. 2.7.

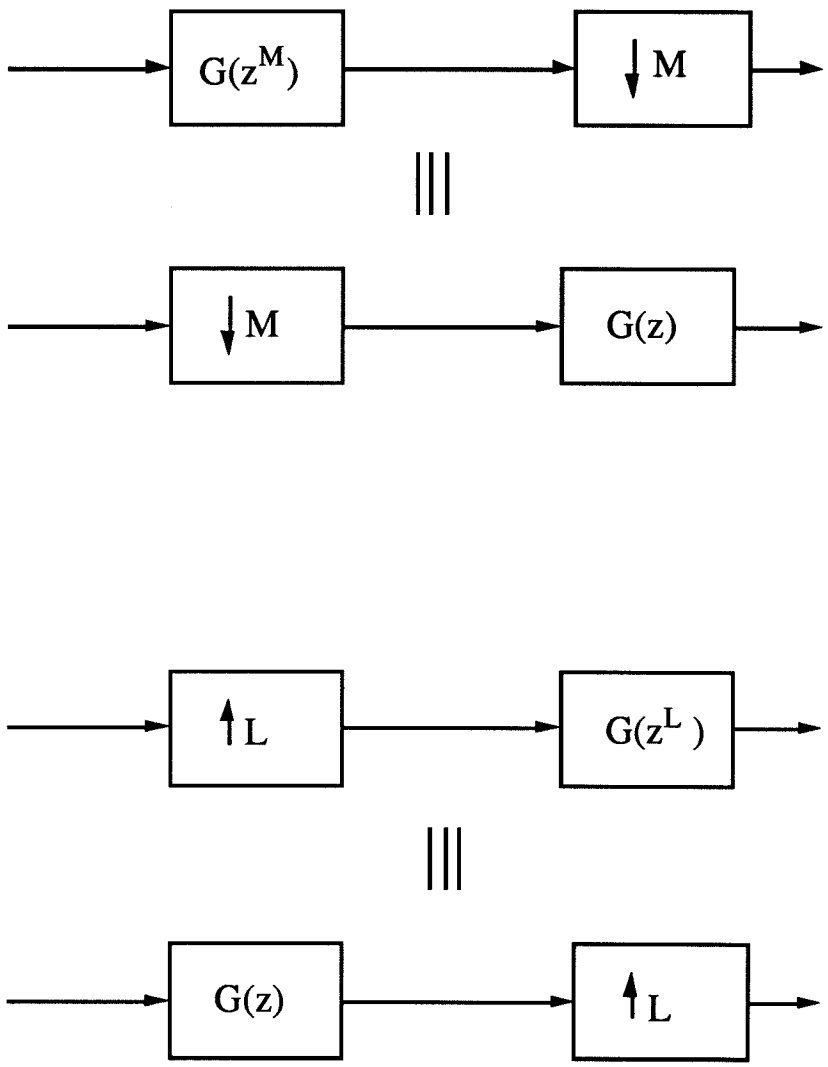

Fig 2.6. Noble Identities of Multirate Signal Processing

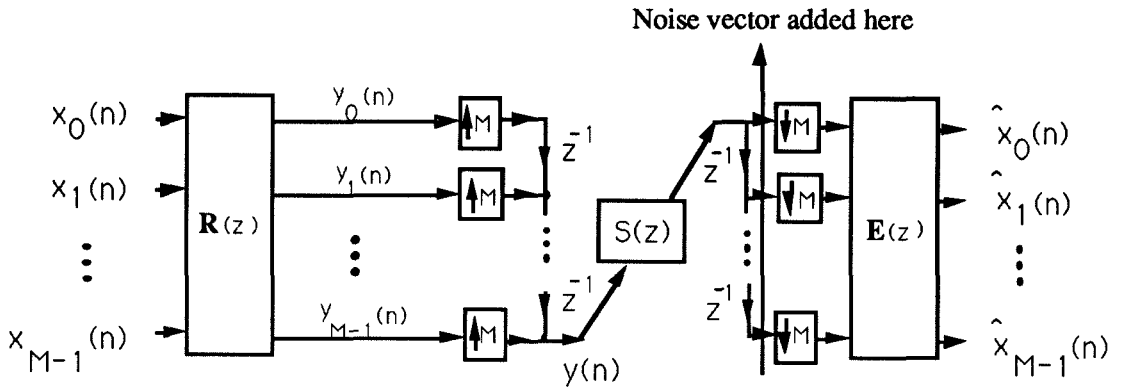

Fig 2.7. Equivalent Structure for the System in Fig 2.5.

In order to simplify this circuit, we use the following result [6]: when an input $u(n)$ is passed through an interpolator (by M), k units of delay, and a decimator (by M) (see Fig. 2.8),

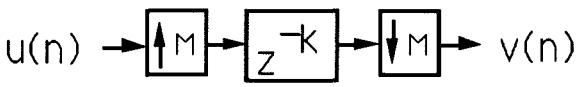

Fig 2.8. A Circuit with an Interpolator, a Delay and a Decimator

the resultant output $v(n)$ can be expressed in the Z-domain as

$$V(z) = \begin{cases} z^{-\frac{k}{M}} U(z), & \text{if } k \text{ is a multiple of } M \\ 0, & \text{if } k \text{ is not a multiple of } M \end{cases} \qquad (2.2.10).$$

Using this identity, we obtain Fig. 2.9, which is a simplified equivalent representation of our system. The analysis and synthesis filters are now represented in their polyphase forms, and are now matrix processors rather than scalar ones. We can

obtain the channel matrix $\mathbf{C}(z)$ by counting the number of delays from each input branch to each output branch and taking into account the multipliers associated wih these delays.

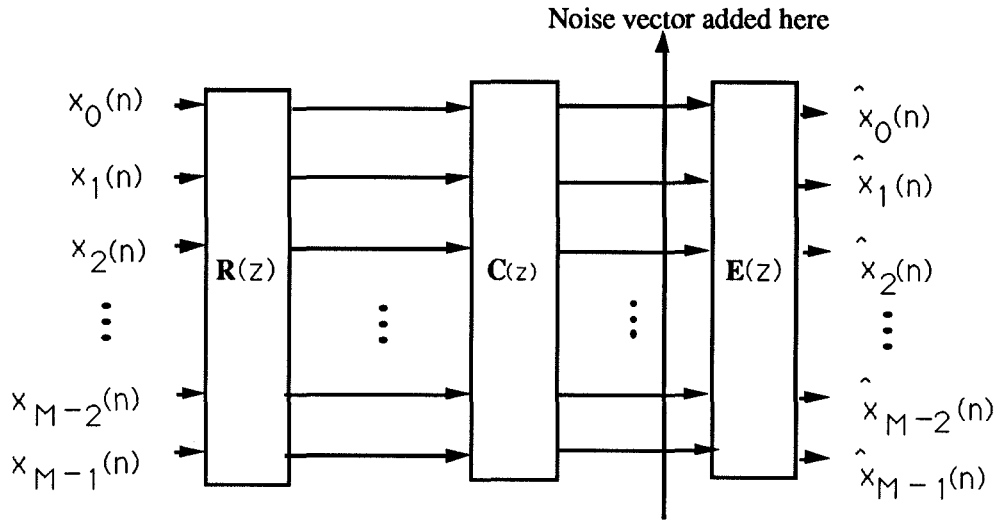

Fig 2.9. Simplified Representation of the System

The channel matrix $\mathbf{C}(z)$ for $M = 5$ is given by

$$\mathbf{C}(z) = \begin{pmatrix} S_1(z)z^{-1} & S_2(z)z^{-1} & S_3(z)z^{-1} & S_3(z)z^{-1} & S_0(z) \\ S_0(z)z^{-1} & S_1(z)z^{-1} & S_2z^{-1} & S_3(z)z^{-1} & S_4(z)z^{-1} \\ S_4(z)z^{-2} & S_0(z)z^{-1} & S_1(z)z^{-1} & S_2(z)z^{-1} & S_3(z)z^{-1} \\ S_3(z)z^{-2} & S_4(z)z^{-2} & S_0(z)z^{-1} & S_1(z)z^{-1} & S_2(z)z^{-1} \\ S_2(z)z^{-2} & S_3(z)z^{-2} & S_4(z)z^{-2} & S_0(z)z^{-1} & S_1(z)z^{-1} \end{pmatrix}$$

where the $S_k(z)$ are the Type 1 Polyphase Components of $S(z)$. $\mathbf{C}(z)$ is observed to be a *pseudo-circulant* matrix. A matrix $\mathbf{Q}(z)$ is said to be pseudo-circulant if the entries $q_{i,j}(z)$; $i, j = 0, \ldots, M-1$ satisfy

$$q_{i,j}(z) = \begin{cases} q_{0,j-i}(z), & 0 \leq i \leq j \\ z^{-1}q_{0,j-i+M}(z), & j < i < M-1 \end{cases}$$

This observation is in accordance with the results of Vaidyanathan and Mitra [9] that block implementations of digital filters lead to pseudo-circulant matrices.

In the case when the channel impulse response is of a finite length, $\mathbf{C}(z)$ is observed to be a polynomial matrix. In particular, if the length of the channel impulse response is not larger than the number of channels, then all the entries of $\mathbf{C}(z)$ are either zero or just a delay. For example, if $M = 5$, and

$$S(z) = s_0 + s_1 z^{-1} + s_2 z^{-2}$$

we have

$$\mathbf{C}(z) = \begin{pmatrix} s_1 z^{-1} & s_2 z^{-1} & 0 & 0 & s_0 \\ s_0 z^{-1} & s_1 z^{-1} & s_2 z^{-1} & 0 & 0 \\ 0 & s_0 z^{-1} & s_1 z^{-1} & s_2 z^{-1} & 0 \\ 0 & 0 & s_0 z^{-1} & s_1 z^{-1} & s_2 z^{-1} \\ s_2 z^{-2} & 0 & 0 & s_0 z^{-1} & s_1 z^{-1} \end{pmatrix}$$

By way of this derivation, we have shown that the system in Fig. 2.4 is linear and time-invariant, in spite of the presence of time-variant elements like decimators and interpolators. With this framework, we are now in a position to derive schemes to transmit data over such channels, and we shall do so in the rest of this chapter and the chapters to come.

2.3 A Novel Scheme for Block Equalization

Using the equivalent structure for our transmission scheme which was introduced in the earlier section, we now derive a scheme to perform block equalization over ISI channels. Previous schemes introduced to perform this have made use of complete block processors [3]. However, we show that the problem of block equalization can be reduced to one of scalar equalization, provided one chooses suitable processors at the input and output of the channel. We choose our pre- and postprocessors by making use of a theorem on polynomial matrices. We also illustrate some interesting properties of this decomposition.

From Fig.2.9, we can write the input-output relationship of the proposed structure:

$$\begin{pmatrix} \hat{X}_0(z) \\ \hat{X}_1(z) \\ \vdots \\ \hat{X}_{M-1}(z) \end{pmatrix} = \mathbf{E}(z)\mathbf{C}(z)\mathbf{R}(z) \begin{pmatrix} X_0(z) \\ X_1(z) \\ \vdots \\ X_{M-1}(z) \end{pmatrix} \qquad (2.3.1).$$

Since we want to convert the block equalization problem to one of scalar equalization, we are essentially looking for a decoupling of the above equation so that $\hat{X}_k(z)$ is dependent only on $X_k(z)$. We would also prefer that the dependence be ISI-free, i.e., we want $\hat{x}_k(n)$ to be a delayed version of $x_k(n)$ (in the Multirate literature, this condition is referred to as *perfect reconstruction*). In other words, we want the matrix product $\mathbf{E}(z)\mathbf{C}(z)\mathbf{R}(z)$ to be a diagonal matrix with the diagonal entries being, preferably, powers of z^{-1}. We have to choose the matrices $\mathbf{E}(z)$ and $\mathbf{R}(z)$ accordingly. Alternatively, we could choose the matrices $\mathbf{E}(z)$ and $\mathbf{R}(z)$ to obtain a diagonal matrix product and perform some kind of scalar equalization to get rid of any ISI created in this process. We examine the latter approach in this section. For implementation purposes, we would require the entries of these matrices to represent stable transfer functions. The simplicity of the entries of the prefilter and the postfilter would also be a factor in judging the implementation complexity of these processors.

The basic theorem we use to accomplish the diagonalization of the matrix product $\mathbf{E}(z)\mathbf{C}(z)\mathbf{R}(z)$ is as follows [10,11]:

Smith Form: For any $p \times m$ matrix polynomial matrix $\mathbf{P}(z)$, we can find elementary row and column operations, or corresponding unimodular matrices $\mathbf{U}(z)$ and $\mathbf{V}(z)$, such that

$$\mathbf{U}(z)\mathbf{P}(z)\mathbf{V}(z) = \mathbf{\Lambda}(z) \tag{2.3.2a}$$

where

$$\mathbf{\Lambda}(z) = \begin{pmatrix} \lambda_1(z) & 0 & \dots & 0 & 0 & \dots \\ 0 & \lambda_2(z) & \dots & 0 & 0 & \dots \\ \vdots & \vdots & \ddots & \vdots & \vdots & \vdots \\ 0 & 0 & \dots & \lambda_r(z) & 0 & \dots \\ 0 & 0 & \dots & 0 & 0 & \dots \\ \vdots & \vdots & \ddots & \vdots & \vdots & \vdots \end{pmatrix} \tag{2.3.2b}$$

Unimodular matrices are polynomial matrices having the defining property that their determinants are constant and non-zero. Here r is the (normal) rank of $P(z)$

and the $\{\lambda_i(z)\}$ are unique monic polynomials obeying a division property:

$$\lambda_i(z)|\lambda_{i+1}(z), \qquad i = 1, \ldots, r-1 \tag{2.3.2c}$$

Moreover, if we define

$$\Delta_i(z) = \text{the gcd of all } i \times i \text{ minors of} P(z) \tag{2.3.2d}$$

then we have

$$\lambda_i(z) = \frac{\Delta_i(z)}{\Delta_{i-1}(z)}, \qquad \Delta_0(z) = 1 \tag{2.3.2e}$$

The matrix $\mathbf{\Lambda}(z)$ is called the *Smith* form of $\mathbf{P}(z)$. The $\{\Delta_i(z)\}$ are called the *determinantal divisors* of $\mathbf{P}(z)$ and the $\{\lambda_i(z)\}$ the *invariant polynomials* of $\mathbf{P}(z)$. We refer the reader to [10,11] for a proof of the above theorem.

The method used to obtain the above decomposition is reproduced here from [11]. Among the elements $p_{ik}(z)$ of $\mathbf{P}(z)$ that are not identically equal to zero, we choose one which has least degree in z^{-1} and by suitable permutations of the rows and columns, we make this element $p_{11}(z)$. Then, we find the quotients and remainders of the polynomials $p_{i1}(z)$ and $p_{1k}(z)$ on division by $p_{11}(z)$:

$$\begin{aligned} p_{i1}(z) &= p_{11}(z)q_{i1}(z) + r_{i1}(z), \\ p_{1k}(z) &= p_{11}(z)q_{1k}(z) + r_{1k}(z). \end{aligned} \qquad 2 \le i \le p, 2 \le k \le m$$

If at least one of the remainders $r_{i1}(z)$, $r_{1k}(z)$, for example $r_{1k}(z)$, is not identically equal to zero, then we replace the $p_{1k}(z)$ by the remainder $r_{1k}(z)$ by subtracting the first column multiplied by $q_{1k}(z)$ from the kth column. We note that the remainder $r_{1k}(z)$ has a lower degree than the original element $p_{1k}(z)$. Then, we can again reduce the degree of the element in the top left corner of the matrix by putting in its place an element of smaller degree in z^{-1}.

However, if all the remainders $r_{i1}(z)$, $r_{1k}(z)$ are identically equal to zero, then by subtracting from the ith row the first row multiplied by $q_{i1}(z)$ and from the

k th column the first column multiplied by $q_{1k}(z)$, we reduce our polynomial matrix $\mathbf{P}(z)$ to the form:

$$\begin{pmatrix} p_{11}(z) & 0 & \dots & 0 \\ 0 & p_{22}(z) & \dots & p_{2m}(z) \\ \vdots & \vdots & \ddots & \vdots \\ 0 & p_{p2}(z) & \dots & p_{pm}(z)\dots \end{pmatrix}$$

If at least one of the elements $p_{ik}(z), (2 \leq i \leq p, 2 \leq k \leq m)$ is not divisible by $p_{11}(z)$, we add that column that contains such an element to the first column and arrive at the previous case, and can therefore replace the upper left element of the matrix by one of a lower degree. Since we cannot keep reducing the degree of this element forever, the process must terminate, giving us a matrix of the form

$$\begin{pmatrix} a_1(z) & 0 & \dots & 0 \\ 0 & b_{22}(z) & \dots & b_{2m}(z) \\ \vdots & \vdots & \ddots & \vdots \\ 0 & b_{p2}(z) & \dots & b_{pm}(z)\dots \end{pmatrix}$$

in which all the elements $b_{ik}(z)$ are divisible by $a_1(z)$. Now we apply the same process as before to the submatrix with elements $b_{ik}(z)$ and recursively arrive at the Smith form of the matrix.

By choosing the matrices $\mathbf{E}(z)$ and $\mathbf{R}(z)$ to be the appropriate unimodular matrices as per the Smith Form, we can diagonalize the matrix product $\mathbf{E}(z)\mathbf{C}(z)\mathbf{R}(z)$. We also note that if we choose $M >> N$, then most of the minors of the matrix $\mathbf{C}(z)$ will be multiples of z^{-1} and hence we can obtain perfect reconstruction of all but a few of the parallel input signals. For the channels where the $\{\lambda_i(z)\}$ are not just multiples of z^{-1}, we can attempt to perform some form of scalar equalization to eliminate the ISI.

We demonstrate the above result using the example of the $1-D$ (or, the $1-z^{-1}$) channel. For $M = 5$, we have

$$\mathbf{C}(z) = \begin{pmatrix} -z^{-1} & 0 & 0 & 0 & 1 \\ z^{-1} & -z^{-1} & 0 & 0 & 0 \\ 0 & z^{-1} & -z^{-1} & 0 & 0 \\ 0 & 0 & z^{-1} & -z^{-1} & 0 \\ 0 & 0 & 0 & z^{-1} & -z^{-1} \end{pmatrix} \qquad (2.3.3).$$

Using the Smith Form decomposition, we get

$$\mathbf{E}(z) = \begin{pmatrix} 1 & 0 & 0 & 0 & 0 \\ 0 & -1 & 0 & 0 & 0 \\ 0 & -1 & -1 & 0 & 0 \\ 0 & -1 & -1 & -1 & 0 \\ z^{-1} & 1 & 1 & 1 & 1 \end{pmatrix} \tag{2.3.4}$$

$$\mathbf{R}(z) = \begin{pmatrix} 0 & 0 & 0 & 0 & 1 \\ 0 & 1 & 0 & 0 & 1 \\ 0 & 0 & 1 & 0 & 1 \\ 0 & 0 & 0 & 1 & 1 \\ 1 & 0 & 0 & 0 & z^{-1} \end{pmatrix} \tag{2.8}$$

$$\Lambda(z) = \begin{pmatrix} 1 & 0 & 0 & 0 & 0 \\ 0 & z^{-1} & 0 & 0 & 0 \\ 0 & 0 & z^{-1} & 0 & 0 \\ 0 & 0 & 0 & z^{-1} & 0 \\ 0 & 0 & 0 & 0 & z^{-1}(1-z^{-1}) \end{pmatrix} \tag{2.3.5}.$$

Thus we have decomposed the scalar $1 - D$ channel into five channels, four of them ISI-free and the other also a $1 - D$ channel, but at a lower signalling rate. Over this channel, we could use conventional methods of equalization for such a channel, such as decision feedback equalization or precoding. Over the other channels, we can use ISI-free signalling.

We observe that the filters needed to obtain this transformation have a very low complexity as most of them involve just delays and multiplications by $+1$ or -1. Another desirable feature of this structure, from a practical point of view, is that the DFE over one of the parallel channels only has to take place at a rate which is $(1/M)$ times the signalling rate over the channel.

2.3.1 Properties of the Smith Form Decomposition

In this sub-section, we present certain properties of the Smith Form decomposition introduced in the earlier section. We try to find the number of resultant scalar channels which are ISI-free, the form of the pre- and postfilters and the effect of the filters on the noise.

To derive the properties of the system, we modify the original structure to obtain a more tractable equivalent. The modification we make is to introduce a synthetic delay in the channel so that the new channel is $z^{-1}S(z)$. With this modification, the expression for the equivalent channel matrix, e.g., for $M = 5$, becomes

$$\mathbf{C}(z) = \begin{pmatrix} S_0(z)z^{-1} & S_1(z)z^{-1} & S_2z^{-1} & S_3(z)z^{-1} & S_4(z)z^{-1} \\ S_4(z)z^{-2} & S_0(z)z^{-1} & S_1(z)z^{-1} & S_2(z)z^{-1} & S_3(z)z^{-1} \\ S_3(z)z^{-2} & S_4(z)z^{-2} & S_0(z)z^{-1} & S_1(z)z^{-1} & S_2(z)z^{-1} \\ S_2(z)z^{-2} & S_3(z)z^{-2} & S_4(z)z^{-2} & S_0(z)z^{-1} & S_1(z)z^{-1} \\ S_1(z)z^{-2} & S_2(z)z^{-2} & S_3(z)z^{-2} & S_4(z)z^{-2} & S_0(z)z^{-1} \end{pmatrix} \qquad (2.3.1.1)$$

We now consider the special case of FIR channels, the length of whose impulse response is shorter than the number of channels. As mentioned before, the equivalent channel matrix for such channels has entries which are either zeros or delays. For example, if $M = 5$, and

$$S(z) = s_0 + s_1z^{-1} + s_2z^{-2},$$

with an extra delay in the channel path, we have

$$\mathbf{C}(z) = \begin{pmatrix} s_0z^{-1} & s_1z^{-1} & s_2z^{-1} & 0 & 0 \\ 0 & s_0z^{-1} & s_1z^{-1} & s_2z^{-1} & 0 \\ 0 & 0 & s_0z^{-1} & s_1z^{-1} & s_2z^{-1} \\ s_2z^{-2} & 0 & 0 & s_0z^{-1} & s_1z^{-1} \\ s_1z^{-2} & s_2z^{-2} & 0 & 0 & s_0z^{-1} \end{pmatrix} \qquad (2.3.1.2)$$

The Smith Form decomposition gives us M scalar channels. We consider the number of resultant channels which are ISI-free. While the exact number of such channels depends on M and on N, the length of the channel impulse response, and on the actual impulse response coefficients, a sharp lower bound on this number is easily obtained.

Property 2.1 : The number of resultant channels in the Smith Form decomposition with no ISI is at least $M - N + 1$.

Proof: We observe that the top left $(M - N + 1) \times (M - N + 1)$ submatrix of the channel matrix is upper triangular, with the diagonal elements being s_0z^{-1}. We

denote the g.c.d. of the $k \times k$ minors of $\mathbf{C}(z)$ as $\Delta_k(z)$. With $\Delta_0(z)$ defined to be 1, we know that the resultant diagonal elements in the Smith form are given by

$$\lambda_k(z) = \frac{\Delta_k(z)}{\Delta_{k-1}(z)}. \tag{2.3.1.2}$$

We also know that the division property $\lambda_k(z)|\lambda_{k+1}(z)$ holds.

It follows that $\lambda_1(z)$ is just a multiple of z^{-1}, because of the fact that all the 1×1 minors of $\mathbf{C}(z)$ are zero or delays. We claim that $\lambda_k(z)$ is just a multiple of z^{-1} for $2 \leq k \leq M - N + 1$ too. We prove this claim by induction. For such k, we have a minor of size k which is just a scalar multiple of z^{-k}, which is the determinant of the top left $k \times k$ submatrix of $\mathbf{C}(z)$. We make the induction assumption by assuming that the result is true for all $k < l$. Then, it follows that $\Delta_k(z) = \kappa_k z^{-k}$ for such k by recursion starting from $k = 1$, where κ_k is a constant. Now $\Delta_l(z)$ has degree at least l in z^{-1}. Otherwise, $\lambda_l(z) = \Delta_l(z)/\Delta_{l-1}(z)$ would have degree less than 1, i.e., it is a constant or may even imply negative delays. Yet $\lambda_{l-1}(z)$ is a scalar multiple of z^{-1}, and hence the division property in the Smith Form, i.e., $\lambda_{i-1}(z)|\lambda_i(z)$, would be violated. Since we already have a minor of size l which is just a multiple of z^{-l}, it follows that $\Delta_l(z) = \kappa_l z^{-l}$. This implies that $\lambda_l(z)$ is a multiple of z^{-1}, and the proof is complete.

The number of resultant channels with no ISI is thus lowerbounded by $M - N + 1$. This bound was observed to be an equality for most channels. However, we did find some cases where more ISI-free channels could be obtained.

Property 2.2: The top left $(M - N + 1) \times (M - N + 1)$ submatrices of both the preprocessor $\mathbf{R}(z)$ and the postprocessor $\mathbf{E}(z)$ are constants, i.e., they have no dependence on z^{-1}.

Proof: The proof of this claim follows from the method described earlier to derive the Smith Form and the structure of the equivalent channel matrix $\mathbf{C}(z)$. In the decomposition, we take care of a row first and then a column. We observe that for the first $M - N + 1$ columns, higher degree elements occur only below the $(M - N + 1)$th row. Hence the pre-multiplying matrix, which has to cancel these

elements, has polynomial elements only in these rows for the first $M-N+1$ columns, which proves the claim for the pre-multiplying matrix. The same argument can be applied to the postmultiplying matrix to obtain the result.

This property has its implications in using methods like vector coding [2] over ISI channels. We could conceivably use a $(M-N+1)\times(M-N+1)$ unitary matrix as a prefilter to our preprocessor to control the input power in a multidimensional lattice, and obtain improvements in coding gain. The rest of the channels could be used to transmit unmodified lattice points, which, due to their regular spacing, can facilitate synchronization. We have not explored this avenue further, and leave it as a suggestion for further research.

Property 2.3: The postfilter $\mathbf{E}(z)$ colors the noise.

Proof: In order that the output noise not be colored by the postfilter, we require the postfilter to be lossless [15], i.e.,

$$\tilde{\mathbf{E}}(z)\mathbf{E}(z) = \mathbf{I}$$

where $\tilde{\mathbf{E}}(z)$ is defined as

$$\tilde{\mathbf{E}}(z) = \mathbf{E}^T(z^{-1}).$$

A general theorem about lossless matrices is that the degree of the system, which is the number of delays needed to implement the system, is the same as the degree of the determinant of the matrix [15]. In our case, we know that $\mathbf{E}(z)$ is unimodular, hence its determinant is a constant, independent of z^{-1}. However, the presence of delays in the matrix indicates that we need at least one delay to implement it, i.e., the degree of the system is at least one. Hence $\mathbf{E}(z)$ cannot be lossless, which means the noise at the output will be colored.

This property is one which restricts the use of the proposed decomposition in a practical environment, where it is easier to deal with white noise than with colored noise. However, in the next chapter, we will derive an optimum scheme to transmit over such channels, in which we will find that the optimum filters have far more desirable properties.

2.3.2 Effects of the Block Framework on the System

We find that the block framework we use to transmit data over the channel produces interesting modifications to the poles and zeros of the system. In particular, poles are shifted away from the unit circle (we consider only stable systems, with all poles inside the unit circle). The position of the zeros of the channel which lie on the unit circle are shifted depending on the number of parallel channels used for transmission. We demonstrate the reasons for these transformations, and the Smith Form gives us a method to verify that these indeed hold. The properties presented in this subsection do not depend on the length of the impulse response, specifically on whether it is shorter than the number of channels used. Indeed, if we consider a channel with poles, the impulse response is of infinite length and no amount of parallel decomposition can achieve a situation where the channel impulse response is shorter than the number of parallel channels used.

Property 2.4: If the original channel has a pole at ρ, the resultant channels have a pole at ρ^M.

Proof: This is a result of the fact that the elements of the equivalent channel matrix are the polyphase components of the original channel impulse response. For, if the Z-transform of the original channel had a component of the form

$$\sum_{m=0}^{\infty} \rho^m z^{-m},$$

then a polyphase component has a component of the form

$$\sum_{m=0}^{\infty} (\rho^M)^m z^{-m},$$

which translates to a pole at ρ^M. The method to obtain the Smith Form of a rational matrix is basically the same as that for a polynomial matrix; we just convert the problem to that of decomposing a polynomial matrix by factoring out the least common multiple of the denominators of all the elements in the matrix (see [10]). Thus the resultant elements of the Smith Form decomposition will have the poles

of the polyphase elements in the denominator, which implies that they have a pole at ρ^M.

The more interesting property of this block format is how the zeros of the channel move on the unit circle depending on the size of the blocks used. Property 2.5 elucidates this phenomenon.

Property 2.5: If the original channel has a zero on the unit circle at $\omega = \theta$, then the block channel has a zero at $\omega = M\theta \bmod 2\pi$.

Proof: Since the original channel has a zero at $\omega = \theta$, an input sequence $\{e^{jn\theta}\}$ will produce an output of zero. The corresponding input to the block channel will be of the form

$$\mathbf{u}(n) = \begin{pmatrix} e^{jMn\theta} \\ e^{-j\theta}e^{jMn\theta} \\ \vdots \\ e^{-j(M-1)\theta}e^{jMn\theta} \end{pmatrix}$$

Since each of the individual terms in the input vector has a harmonic component at the frequency $\omega = M\theta$, or equivalently at $\omega = M\theta \bmod 2\pi$ due to the periodicity of the discrete-time Fourier transform. Thus an input with a harmonic component at $\omega = M\theta \bmod 2\pi$ produces a zero output from the block system, which proves that the block system has a zero at this frequency.

As an example, we show how a parallel decomposition of the $1+D$ channel leads to several ISI-free channels and an additional channel which, when M is even, is a $1-D$ channel. The phenomenon by which the zero of the block channel shifts can be explained as follows: The $1+z^{-1}$ channel has a zero at $z=-1$. Thus an input sequence $\{(-1)^n\}$, which has a period of two, leads to a zero output. However, in the case of the block channel, the corresponding input sequence to produce a zero output is a vector sequence of the form (for $M=4$)

$$\ldots, \begin{pmatrix} 1 \\ -1 \\ 1 \\ -1 \end{pmatrix}, \begin{pmatrix} 1 \\ -1 \\ 1 \\ -1 \end{pmatrix}, \begin{pmatrix} 1 \\ -1 \\ 1 \\ -1 \end{pmatrix}, \begin{pmatrix} 1 \\ -1 \\ 1 \\ -1 \end{pmatrix}, \ldots$$

This sequence has a period of unity and hence the zero of the block channel is at $z=1$ and thus the block channel, when decomposed, gives rise to a $1-z^{-1}$ channel

as one of its parallel channels. When M is odd, the input sequence producing a zero output has a period of two and thus the zero of the block channel remains at $z = -1$.

A verification of the above phenomenon can be seen using the Smith Form Decomposition for the $1 + z^{-1}$ channel for $M = 4$. We have

$$\mathbf{C}(z) = \begin{pmatrix} z^{-1} & 0 & 0 & 1 \\ z^{-1} & z^{-1} & 0 & 0 \\ 0 & z^{-1} & z^{-1} & 0 \\ 0 & z^{-1} & z^{-1} & 0 \\ 0 & 0 & z^{-1} & z^{-1} \end{pmatrix} \tag{2.3.2.1}$$

$$\mathbf{E}(z) = \begin{pmatrix} 1 & 0 & 0 & 0 \\ 0 & 1 & 0 & 0 \\ 0 & -1 & 1 & 0 \\ -z^{-1} & 1 & -1 & 1 \end{pmatrix} \tag{2.3.2.2}$$

$$\mathbf{R}(z) = \begin{pmatrix} 0 & 0 & 0 & 1 \\ 0 & 1 & 0 & -1 \\ 0 & 0 & 1 & 1 \\ 1 & 0 & 0 & -z^{-1} \end{pmatrix} \tag{2.3.2.3}$$

$$\Lambda(z) = \begin{pmatrix} 1 & 0 & 0 & 0 \\ 0 & z^{-1} & 0 & 0 \\ 0 & 0 & z^{-1} & 0 \\ 0 & 0 & 0 & z^{-1}(1 - z^{-1}) \end{pmatrix} \tag{2.3.2.4}$$

The importance of this result lies in the fact that it gives us a method to use codes designed for one ISI channel over another ISI channel. In line coding, a method of interleaving is commonly used to modify codes having a zero at one frequency so that the resultant code has a zero at another frequency [16]. We have essentially found the channel coding analog of this result. In the example of the $1 + D$ channel presented above, we can use codes designed for the ISI-free channel and codes designed for the $1 - D$ channel by making use of the Smith Form decomposition.

2.4 Conclusions

The main purpose of this chapter was to motivate and present a multirate signal processing framework for data transmission over ISI channels. Using results from the Multirate Signal Processing literature, we derived simplified equivalent circuits for the scheme presented. Using this equivalent, we were able to derive a novel method for equalization of such channels using results from the theory of polynomial matrices. We presented various properties of this decomposition, and showed how this decomposition could be used to modify channel zeros, which facilitates coding over such channels. We will find the framework derived in this chapter to be invaluable in later chapters in deriving a different set of filters and equalizers for transmission over channels with ISI and colored noise.

References

[1] M. Tomlinson,"New Automatic Equalizers Employing Modulo Arithmetic," *Electronics Letters*, vol.7, no. 3, pp. 138-139, March 1971.

[2] S. Kasturia, J. T. Aslanis and J. M. Cioffi, " Vector Coding for Partial Response Channels," *IEEE Trans. Info. Theory*, vol. 36, no. 4, pp. 741-762, 1990.

[3] S. Kasturia and J.M. Cioffi, "Vector Coding with Decision Feedback Equalization for Partial Response Channels," *Proceedings Globecom' 88,* vol. 60, pp. 1497–1514, Dec. 1988.

[4] G.D. Forney Jr. and A.R. Calderbank, "Coset Codes for Partial Response Channels; or, Coset Codes with Spectral Nulls," *IEEE Trans. Info. Theory,* vol. 35, no. 5, pp. 925-943, sept. 1989.

[5] J. W. Lechleider, "The Optimum Combination of Block Codes and Receivers for Arbitrary Channels," *IEEE Trans. Commun.*, vol. 38, no. 5, pp. 615-621, 1990.

[6] R.D. Koilpillai, T.Q. Nguyen and P.P. Vaidyanathan, "Theory and Design of Perfect Reconstruction Transmultiplexers and their Relation to Perfect Reconstruction QMF Banks," Conference Record, *Twenty-third Asilomar Conference on Signals, Systems and Computers*, pp. 247-251, Oct.-Nov. 1989.

[7] P.P. Vaidyanathan, "Theory and Design of M-Channel Maximally Decimated Quadrature Mirror Filters with Arbitrary M, Having the Perfect Reconstruction Property," *IEEE Trans. on Acoustics, Speech and Signal Processing,* vol. ASSP-35, no. 4, pp. 476-492, April 1987.

[8] P.P. Vaidyanathan, "Quadrature Mirror Filter Banks, M-Band Extensions and Perfect Reconstruction Techniques'," *IEEE ASSP Magazine,* vol. 4, pp. 4-20, July 1987.

[9] P.P. Vaidyanathan and S.K. Mitra, "Polyphase Networks, Block Digital Filtering, LPTV Systems, and Alias-Free QMF Banks: A Unified Approach Based on Pseudocirculants," *IEEE Trans. on Acoustics, Speech and Signal Processing,* vol. 36, no. 3, pp. 381-391, March 1988.

[10] Thomas Kailath, "Linear Systems," Prentice Hall Inc., Englewood Cliffs, NJ 07632, Chapter 6, 1980.

[11] F.R. Gantmacher, "The Theory of Matrices," Chelsea Publishing Co., New York, NY, vol. 1, Chapter 6, 1959.

[12] Walter Hirt and J. L. Massey, " Capacity of the Discrete-Time Gaussian Channel with Intersymbol Interference," *IEEE Trans. Info. Theory*, vol. 34, no. 3, pp. 380-388, May 1988.

[13] B. S. Tsybakov, " Capacity of a Discrete-time Gaussian Channel with a filter," *Probl. Peredach. Inform.* , vol. 6, pp. 78-82, 1970.

[14] John A. C. Bingham, "Multicarrier Modulation for Data Transmission : An Idea Whose Time Has Come," *IEEE Communications Magazine*, vol. 28, no. 5, pp. 5-14, May 1990.

[15] P. P. Vaidyanathan, *Multirate Systems and Filter Banks*, book in preparation.

[16] J. Pierce, "Some Practical Aspects of Digital Transmission," *IEEE Spectrum*, vol. 5, pp. 63-70, Nov. 1968.

[17] R. Ramésh, private communication.

Chapter 3 Optimum Filters for Multichannel Data Transmission

In the previous chapter, we proposed a framework for multichannel data transmission over a channel with ISI. In this chapter, we consider the problem of finding the best prefilter and postfilter possible under certain restrictions, to achieve the least possible error between the input and the output. We choose our filters to be reasonably low in complexity, and try to find the optimum filters to transmit block symbols using the multichannel format. The prefilter and postfilter take care of the ISI encountered by a single block of data, and the residual ISI is cancelled using a Block Decision Feedback Equalizer. This is just a generalization of the DFE introduced in earlier chapters, with the modification that the decision feedback coefficients are matrices rather than scalars. It turns out that using these optimum filters leads to significant performance gains over scalar schemes, and we illustrate this by analysis and examples.

3.1 Introduction

As mentioned in the previous chapter, our original plan of research was to find good analysis and synthesis filters to transmit data over the ISI channel; good filters would suppress adjacent channel interference while maintaining a rather well-behaved self frequency response. We were unable to solve this problem, which still remains open. However, our next train of thought was that we were, in a sense, capturing more of the channel using a block input than we were while using a scalar input and DFE. So we might be able to do better using this format by choosing filters to take care of the ISI within a block, and use a DFE to attend to the ISI outside the block. This train of thought led us to propose the structure shown in Figure 3.1. Note that this is essentially the same as the scheme shown in Fig. 2.4, except for the addition of the Block Decision Feedback Equalizer. We also note the presence of the extra synthetic delay added in the channel path.

The inputs to the channel are from a zero-mean PAM set and signal values in the same block may be correlated, but we assume uncorrelated blocks. Mathematically, this is expressed as

$$E[\mathbf{x}(n)\mathbf{x}^T(l)] = \mathbf{R}_{xx}\delta_{nl} \tag{3.1.1}$$

where $E[\ ]$ denotes statistical expectation, and δ_{nl} is the Kronecker delta function, which is zero unless $n = l$, when it is 1. The vector $\mathbf{x}(n)$ is composed of $x_0(n), x_1(n), \ldots x_{M-1}(n)$, which are scalar components. By virtue of being a correlation matrix, $\mathbf{R}_{xx}$ is positive semidefinite. The noise $w(n)$ is assumed to be uncorrelated to the signal.

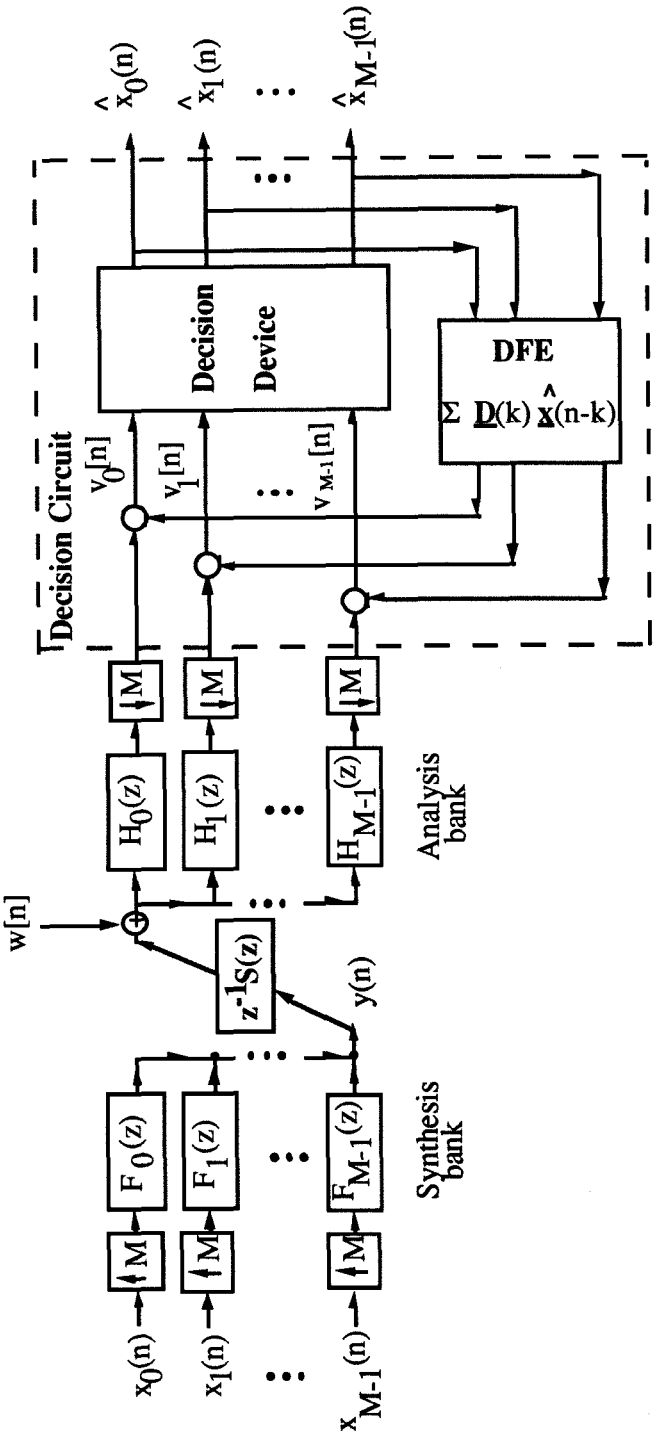

Fig. 3.1 Basic Scheme Used to Transmit Block Data with Block Decision Feedback Equalization

The analysis which was performed in the earlier chapter to derive the equivalent circuit for the structure in Fig 2.4 using Multirate Signal Processing can be carried out again to get the Equivalent Circuit shown in Fig. 3.2. The channel matrix $\mathbf{C}(z)$ for $M = 5$ is given by

$$\mathbf{C}(z) = \begin{pmatrix} S_0(z)z^{-1} & S_1(z)z^{-1} & S_2z^{-1} & S_3(z)z^{-1} & S_4(z)z^{-1} \\ S_4(z)z^{-2} & S_0(z)z^{-1} & S_1(z)z^{-1} & S_2(z)z^{-1} & S_3(z)z^{-1} \\ S_3(z)z^{-2} & S_4(z)z^{-2} & S_0(z)z^{-1} & S_1(z)z^{-1} & S_2(z)z^{-1} \\ S_2(z)z^{-2} & S_3(z)z^{-2} & S_4(z)z^{-2} & S_0(z)z^{-1} & S_1(z)z^{-1} \\ S_1(z)z^{-2} & S_2(z)z^{-2} & S_3(z)z^{-2} & S_4(z)z^{-2} & S_0(z)z^{-1} \end{pmatrix} \tag{3.1.2}$$

where $S_k(z)$ are the Type 1 polyphase components of $S(z)$. We observe that $\mathbf{C}(z)$ can be written in the form

$$\mathbf{C}(z) = \mathbf{C_1}z^{-1} + \mathbf{C_2}z^{-2} + \mathbf{C_3}z^{-3} + \ldots \tag{3.1.3}$$

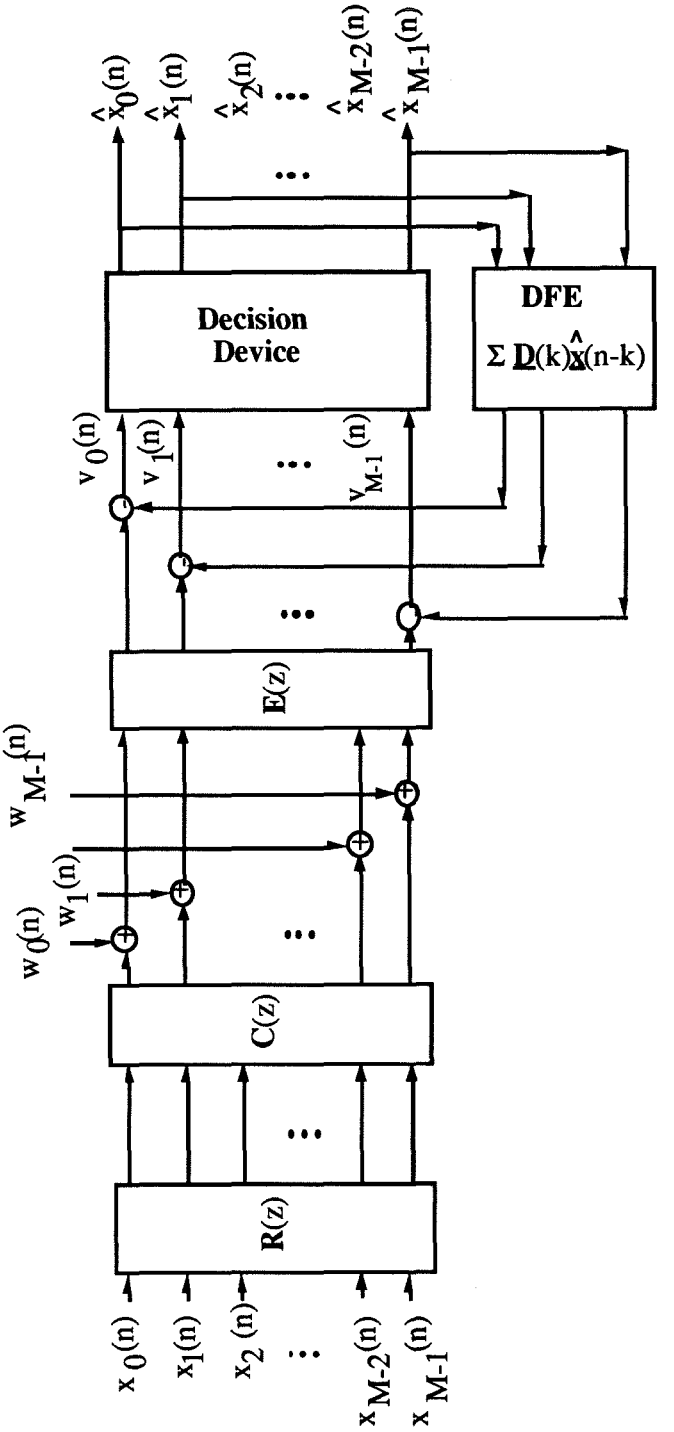

Fig 3.2. Simplified Representation of the System in Fig.3.1

Using this equivalent circuit with the second order statistics of the input and the noise, we derive the optimum filters (or rather, their polyphase forms) and the optimum BDFE that minimize the mean-squared error between the input and the output.

A similar problem has been tackled by Kasturia et al. in [1] and by Lechleider in [2]. Kasturia et al. make use of a zero-forcing optimality criterion and an orthogonal postprocessor in order to avoid coloring the noise. Lechleider considers the problem of maximization of the signal-to-noise ratios on each of the individual subchannels created by a biorthogonal set of transmitters and receivers with respect to the channel. In this chapter, we find the optimum filters to minimize the mean-squared error between the input and the output, with no restrictive assumptions on these filters. Our results also include the possibility of the input signals being correlated.

The organization of the chapter is as follows: In Section 3.2, the necessary preprocessors and postprocessors are found by minimizing the mean-squared error between the input and output. In Section 3.3, we investigate the implications of using the optimum filters in the special case of uncorrelated inputs. In this case, we find that the optimal pre- and postprocessors give rise to a set of parallel independent channels, with the optimal postprocessor being a whitening filter for the noise. The implication of this result is that normal trellis codes, which have been designed to combat white noise, can be used efficiently over channels with ISI and colored noise, just by using optimal pre- and postprocessors. In Section 3.4, we analyze the performance of the scheme with the optimal pre- and postprocessors and compare its performance to that of a DFE. In Section 3.5, we consider an example channel and demonstrate the performance of the scheme and present some physical reasoning for the improved performance. We conclude the chapter with a brief summary in Section 3.6.

3.2 Derivation of the Optimum Filters

In this section, we derive the finite-length analysis and synthesis filters that minimize the mean-squared error between the input and the output. The Block DFE is chosen to minimize the ISI outside the block in a least squared error sense. We restrict ourselves to the case where $\mathbf{E}(z)$ and $\mathbf{R}(z)$ cease to be functions of z, i.e., they are just scalar matrices $\mathbf{B}$ and $\mathbf{A}$ respectively. This implies that the analysis and synthesis filters are of length M, which is the same as the number of parallel channels being used.

From Fig. 3.2, we can write the expression for the input $\mathbf{v}(n)$ to the decision device in terms of $\mathbf{x}(n)$, $\hat{\mathbf{x}}(n)$, and the various circuit elements. We have

$$\mathbf{v}(n) = \mathbf{B}\mathbf{C_1}\mathbf{A}\ \mathbf{x}(n-1) + \sum_{k=2}^{\infty} \mathbf{B}\mathbf{C_k}\mathbf{A}\ \mathbf{x}(n-k) + \mathbf{B}\mathbf{w}(n) + \sum_{k=2}^{\infty} \mathbf{D_k}\hat{\mathbf{x}}(n-k). \quad (3.2.1)$$

The term $\mathbf{B}\mathbf{C_1}\mathbf{A}\ \mathbf{x}(n-1)$ in the above equation represents the desired signal at the output of the channel and the rest of the terms represent the undesirable interference. In Fig. 3.2, we note that the demultiplexing has transformed the noise sequence $w(n)$ into a noise vector sequence $\mathbf{w}(n)$ at the output of the channel matrix. This noise vector is given by

$$\begin{aligned}\mathbf{w}(n) &= [w(Mn), w(Mn-1), \ldots, w(Mn-M+1)]^T \\ &= [w_0(n), w_1(n), \ldots, w_{M-1}(n)]^T\end{aligned}$$

and its autocorrelation matrix for zero lag is given by

$$\begin{aligned}&E[\mathbf{w}(n)\mathbf{w}^T(n)] = \mathbf{R_{ww}}(0) = \mathbf{R}_w \\ &= \begin{pmatrix} E[w_0(n)w_0(n)] & \cdots & E[w_0(n)w_{M-1}(n)] \\ E[w_1(n)w_0(n)] & E[w_1(n)w_1(n)] & \cdots \\ \vdots & \ddots & \vdots \\ E[w_{M-1}(n)w_0(n)] & \cdots & E[w_{m-1}(n)w_{M-1}(n)] \end{pmatrix}. \quad (3.2.2)\end{aligned}$$

where the matrix $\mathbf{R}_w$ is symmetric and positive semi-definite. We assume that the matrix $\mathbf{R}_w$ is non-singular. In the case when the noise sequence $w(n)$ is wide-sense stationary, the matrix $\mathbf{R}_w$ turns out to be a symmetric Toeplitz matrix; a matrix is

said to be Toeplitz if it has equal elements along the major and each minor diagonal. If the noise is WSS, then $\mathbf{R}_w$ is singular only if $w(n)$ is a harmonic process, i.e., it consists only of a finite number of sinusoids [5]. Thus the singularity of $\mathbf{R}_w$ is not a very restrictive assumption. In case it is singular, we shall transcend the problem by adding a modicum of white noise to the singular noise already present.

Due to the non-linear relationship between $\mathbf{v}(n)$ and $\hat{\mathbf{x}}(n)$ (which arises due to the decision device), a rigorous mathematical analysis of equation (3.2.1) is intractable. However, under the assumption of perfect decisions, i.e., $\hat{\mathbf{x}}(n) = \mathbf{x}(n)$, we shall proceed and derive an expression for the mean-squared error. This will, of course, be a rigorous lower bound to the mean-squared error attainable. This bound could actually be achieved by using a block precoder [11] at the input to the channel instead of the block DFE at the output of the channel. The block precoder gets rid of the problem of error propagation, which is the main reason for the non-ideal decisions of the DFE.

The mean-squared error E between $\mathbf{v}(n)$ and $\mathbf{x}(n-1)$ is given by

$$\begin{aligned} \mathcal{E} &= E[(\mathbf{v}(n) - \mathbf{x}(n-1))^T(\mathbf{v}(n) - \mathbf{x}(n-1))] \\ &= E\big[Tr[(\mathbf{v}(n) - \mathbf{x}(n-1))(\mathbf{v}(n) - \mathbf{x}(n-1))^T]\big] \end{aligned} \tag{3.2.3}$$

where $Tr[\ ]$ denotes the trace of a matrix. Using equations (3.1.1) and (3.2.2), we get

$$\begin{aligned} \mathcal{E} = Tr[&(\mathbf{BC_1A} - \mathbf{I})\mathbf{R}_{xx}(\mathbf{BC_1A} - \mathbf{I})^T + \mathbf{BR}_w\mathbf{B}^T + \\ &\sum_{k=2}^{\infty}(\mathbf{BC_kA} - \mathbf{D_k})\mathbf{R}_{xx}(\mathbf{BC_kA} - \mathbf{D_k})^T]. \end{aligned} \tag{3.2.4}$$

Since the contributions due to the individual terms in the above expression are additive (the trace is additive), we can set

$$\mathbf{BC_kA} = \mathbf{D}_k\ ; \qquad k \geq 2,$$

and cancel the contributions of these terms altogether, thereby contributing the minimum possible amount to the mean-squared error. This gives us

$$\mathcal{E} = Tr[(\mathbf{BC_1A} - \mathbf{I})\mathbf{R}_{xx}(\mathbf{BC_1A} - \mathbf{I})^T + \mathbf{BR}_w\mathbf{B}^T]. \tag{3.2.5}$$

We first find the optimum $\mathbf{B}$, assuming $\mathbf{A}$ given. This problem can be solved by completing the square, a standard approach in estimation theory. We observe that the matrix whose trace is being taken in equation (3.2.5) can be written in the form

$$(\mathbf{B}-\mathbf{Q})\mathbf{P}(\mathbf{B}-\mathbf{Q})^T+\mathbf{M}$$

where $\mathbf{P}$ is positive definite and $\mathbf{M}$ is independent of $\mathbf{B}$. Thus, to minimize $\mathcal{E}$, we set $\mathbf{B}=\mathbf{Q}$, which gives us the optimum $\mathbf{B}_0$:

$$\mathbf{B}_0=\mathbf{R}_{xx}\mathbf{A}^T\mathbf{C}_1^T(\mathbf{R}_w+\mathbf{C}_1\mathbf{A}\mathbf{R}_{xx}\mathbf{A}^T\mathbf{C}_1^T)^{-1} \tag{3.2.6}$$

and a corresponding mean-squared error of

$$\mathcal{E}=Tr[\mathbf{R}_{xx}-\mathbf{R}_{xx}\mathbf{A}^T\mathbf{C}_1^T(\mathbf{R}_w+\mathbf{C}_1\mathbf{A}\mathbf{R}_{xx}\mathbf{A}^T\mathbf{C}_1^T)^{-1}\mathbf{C}_1\mathbf{A}\mathbf{R}_{xx}]. \tag{3.2.7}$$

We now want to find the prefilter $\mathbf{A}$ so that this $\mathcal{E}$ is minimized. However, for this problem to be useful or even to make sense, a power constraint must be considered at the input to the channel. Otherwise, we could choose the elements of $\mathbf{A}$ to be very large and the elements of $\mathbf{B}$ to be essentially zero, thus cancelling the effect of the noise altogether. All practical channels have restrictions on the power that can be transmitted. For example, on a telephone line, the phone company restricts the power used for transmission in order to operate longer on batteries during power outages, although this is not an overriding consideration.

The power constraint we consider is an average power constraint:

$$E[(\mathbf{A}\mathbf{x}(n))^T(\mathbf{A}\mathbf{x}(n))]=E[Tr[(\mathbf{A}\mathbf{x}(n))(\mathbf{A}\mathbf{x}(n))^T]]=Tr[\mathbf{A}\mathbf{R}_{xx}\mathbf{A}^T]=P. \tag{3.2.8}$$

In order to minimize $\mathcal{E}$ under the constraint in (3.2.8), we follow an approach similar to the one in [3]. We make the substitution

$$\mathbf{A}=\mathbf{G}\mathbf{U} \tag{3.2.9}$$

where $\mathbf{U}$ is the unitary matrix that diagonalizes $\mathbf{R}_{xx}$. In other words,

$$\mathbf{U}\mathbf{R}_{xx}\mathbf{U}^T=\mathbf{\Lambda}=\text{diag}\{\lambda_1,\lambda_2,\ldots\lambda_M\},\quad \lambda_1\geq\lambda_2\geq\ldots\geq\lambda_M. \tag{3.2.10}$$

The matrix $\mathbf{G}$ in equation (3.2.9) is the one to be found in order to minimize the mean-squared error. We note that since $\mathbf{U}$ is non-singular, then for any $\mathbf{A}$, there exists a matrix $\mathbf{G}$ so that (3.2.9) holds. Using (3.2.9) in (3.2.7), we get

$$\mathcal{E} = Tr[\mathbf{R}_{xx} - \mathbf{R}_{xx}\mathbf{U}^T\mathbf{G}^T\mathbf{C}_1^T(\mathbf{R}_w + \mathbf{C}_1\mathbf{G}\mathbf{\Lambda}\mathbf{G}^T\mathbf{C}_1^T)^{-1}\mathbf{C}_1\mathbf{G}\mathbf{U}\mathbf{R}_{xx}]. \tag{3.2.11}$$

Using the fact that the trace is invariant to cyclic permutations together with equation (3.2.10), we obtain

$$\mathcal{E} = Tr[\mathbf{R}_{xx} - \mathbf{\Lambda}^2\mathbf{G}^T\mathbf{C}_1^T(\mathbf{R}_w + \mathbf{C}_1\mathbf{G}\mathbf{\Lambda}\mathbf{G}^T\mathbf{C}_1^T)^{-1}\mathbf{C}_1\mathbf{G}]. \tag{3.2.12}$$

In Appendix 3.A.1, we show that this equation can be rewritten as

$$\mathcal{E} = Tr[\mathbf{R}_{xx} - \mathbf{\Lambda}] + Tr[(\mathbf{I} + \mathbf{\Lambda}^{1/2}\mathbf{G}^T\mathbf{C}_1^T\mathbf{R}_w^{-1}\mathbf{C}_1\mathbf{G}\mathbf{\Lambda}^{1/2})^{-1}\mathbf{\Lambda}]. \tag{3.2.13}$$

Since the trace is invariant to cyclic permutations, it follows that

$$Tr[\mathbf{\Lambda}] = Tr[\mathbf{U}\mathbf{R}_{xx}\mathbf{U}^T] = Tr[\mathbf{R}_{xx}\mathbf{U}^T\mathbf{U}] = Tr[\mathbf{R}_{xx}].$$

Hence we have

$$\mathcal{E} = Tr[(\mathbf{I} + \mathbf{\Lambda}^{1/2}\mathbf{G}^T\mathbf{C}_1^T\mathbf{R}_w^{-1}\mathbf{C}_1\mathbf{G}\mathbf{\Lambda}^{1/2})^{-1}\mathbf{\Lambda}]. \tag{3.2.14}$$

Thus, we now have to find $\mathbf{G}$ to minimize $Tr[\mathbf{W}^{-1}\mathbf{\Lambda}]$ where

$$\mathbf{W} = \mathbf{I} + \mathbf{\Lambda}^{1/2}\mathbf{G}^T\mathbf{C}_1^T\mathbf{R}_w^{-1}\mathbf{C}_1\mathbf{G}\mathbf{\Lambda}^{1/2}. \tag{3.2.15}$$

In other words, we have to find $\mathbf{G}$ to minimize $\sum_{i=1}^{M}[\mathbf{W}^{-1}]_{ii}\lambda_i$. Since the λ_i are non-negative, we essentially have to minimize the individual diagonal elements of $\mathbf{W}^{-1}$.

We note that $\mathbf{W}$ is positive definite. For such a matrix, it can be shown that

$$\{\mathbf{W}^{-1}\}_{ii} \geq w_{ii}^{-1} \tag{3.2.16}$$

with equality only if $\mathbf{W}$ is diagonal. One proof of the above inequality is given in Appendix 3.A.2; an alternative proof of this inequality can be found in [9]. Thus it follows that in order to minimize $\mathcal{E}$, we need $\mathbf{\Lambda}^{1/2}\mathbf{G}^T\mathbf{C}_1^T\mathbf{R}_w^{-1}\mathbf{C}_1\mathbf{G}\mathbf{\Lambda}^{1/2}$ to be diagonal, which implies that $\mathbf{G}^T\mathbf{C}_1^T\mathbf{R}_w^{-1}\mathbf{C}_1\mathbf{G}$ be diagonal. Denoting the columns of $\mathbf{G}$ by $\mathbf{g}_i$, this condition can be expressed as

$$\mathbf{g}_i^T\mathbf{C}_1^T\mathbf{R}_w^{-1}\mathbf{C}_1\mathbf{g}_j = \kappa_i\delta_{ij}. \tag{3.2.17}$$

The optimal solution we now derive will be consistent with the above condition.

Assuming $\mathbf{G}^T\mathbf{C}_1^T\mathbf{R}_w^{-1}\mathbf{C}_1\mathbf{G}$ is diagonal, the quantity to be minimized is

$$\mathcal{E} = \sum_{i=1}^{M}\left(1+\lambda_i\mathbf{g}_i^T\mathbf{C}_1^T\mathbf{R}_w^{-1}\mathbf{C}_1\mathbf{g}_i\right)^{-1}\lambda_i. \tag{3.2.18}$$

Since $\mathbf{A} = \mathbf{GU}$, the power constraint can be rewritten as

$$P = Tr[\mathbf{A}\mathbf{R}_{xx}\mathbf{A}^T] = Tr[\mathbf{G}\mathbf{\Lambda}\mathbf{G}^T].$$

As the trace is invariant to cyclic permutations, we obtain

$$P = Tr[\mathbf{\Lambda}\mathbf{G}^T\mathbf{G}] = \sum_{i=1}^{M}\lambda_i\mathbf{g}_i^T\mathbf{g}_i. \tag{3.2.19}$$

Using a Lagrange multiplier, we can now routinely minimize the mean-squared error. The result is

$$\lambda_k\mathbf{C}_1^T\mathbf{R}_{ww}^{-1}\mathbf{C}_1\mathbf{g}_k = \mu\left(1+\lambda_k\mathbf{g}_k^T\mathbf{C}_1^T\mathbf{R}_{ww}^{-1}\mathbf{C}_1\mathbf{g}_k\right)^2\mathbf{g}_k. \tag{3.2.20}$$

Thus the optimal $\mathbf{g}_k$'s are eigenvectors of the matrix $\mathbf{C}_1^T\mathbf{R}_{ww}^{-1}\mathbf{C}_1$. Since this matrix is symmetric, we can find enough orthogonal eigenvectors to satisfy the diagonality constraint (3.2.17). As usual, μ is a Lagrange multiplier to be determined so that the power constraint is satisfied.

The astute reader might note the fact that the imposition of the diagonality constraint in equation (3.2.17) seems independent of the constraint (3.2.19) on $\mathbf{G}$,

and thus may not necessarily result in the optimal constrained solution. We put any aspersions to rest by pointing out that premultiplying $\mathbf{G}$ by a unitary matrix does not change the constraint, but would be sufficient to achieve the diagonality condition.

Having determined the optimal $\mathbf{G}$, the corresponding $\mathbf{A}$,$\mathbf{B}$ and the decision feedback coefficients $\mathbf{D}_k$ can easily be found. Though equation (3.2.6) involves the inversion of a matrix in determining the optimal $\mathbf{B}$, we can modify this matrix inversion problem into one of inverting a diagonal matrix by use of the so-called matrix inversion lemma [4]. Details are given in Appendix 3.A.3.

3.3 Implications of the Optimum Filters

In this case we consider the special case when the input symbols on each channel are uncorrelated. In this case $\mathbf{R}_{xx}$ is a diagonal matrix $\mathbf{\Lambda}$ and $\mathbf{U}$ is the identity matrix. In this case, the optimal matrix $\mathbf{B}$ has the form

$$\mathbf{B} = \mathbf{\Lambda}(\mathbf{I} - \mathbf{\Lambda}_1\mathbf{\Lambda}_2\mathbf{\Lambda})\mathbf{A}^T\mathbf{C}_1^T\mathbf{R}_{ww}^{-1} \tag{3.3.1}$$

while the matrix product $\mathbf{BC}_1\mathbf{A}$ is obtained as

$$\mathbf{BC}_1\mathbf{A} = \mathbf{\Lambda}(\mathbf{I} - \mathbf{\Lambda}_1\mathbf{\Lambda}_2\mathbf{\Lambda})\mathbf{\Lambda}_1, \tag{3.3.2}$$

where the matrices $\mathbf{\Lambda}_1$ and $\mathbf{\Lambda}_2$ are as defined in Appendix 3.A.3. We find a surprising result while considering the autocorrelation function at zero lag of the noise passed through the optimal postprocessor $\mathbf{B}_0$. This autocorrelation is given by

$$\begin{aligned} E[\mathbf{B}_0\mathbf{w}(n)\mathbf{w}^T(n)\mathbf{B}_0^T &= \mathbf{B}_0\mathbf{R}_{ww}\mathbf{B}_0^T \\ &= \mathbf{\Lambda}(\mathbf{I} - \mathbf{\Lambda}_1\mathbf{\Lambda}_2\mathbf{\Lambda})\mathbf{A}^T\mathbf{C}_1^T\mathbf{R}_{ww}^{-1}\mathbf{R}_{ww}\mathbf{R}_{ww}^{-1}\mathbf{C}_1\mathbf{A}(\mathbf{I} - \mathbf{\Lambda}_1\mathbf{\Lambda}_2\mathbf{\Lambda})\mathbf{\Lambda} \\ &= \mathbf{\Lambda}^2(\mathbf{I} - \mathbf{\Lambda}_1\mathbf{\Lambda}_2\mathbf{\Lambda})^2\mathbf{\Lambda}_1 \end{aligned} \tag{3.3.3}$$

which is a diagonal matrix. In other words, the optimal postprocessor, in the case of independent inputs in each subchannel, is, in a sense, a whitening filter for the noise. The implication of this result is that normal trellis codes [6], which have

been designed for detection in white noise, can be used efficiently over channels with colored noise (e.g., the ISDN subscriber loop, where the primary impairment is crosstalk from adjacent channels [7]) by making use of the optimum pre- and postprocessors.

In the case of white noise, we observe that the columns of $\mathbf{B}$ are orthogonal and the matrix product $\mathbf{BC_1A}$ is diagonal. Both these are assumptions made in [1] by Kasturia et al. We also observe that $\mathbf{B}$ is, in a sense, a matched filter to $\mathbf{C_1A}$, except for a premultiplying diagonal matrix. In his paper, Lechleider [2] has given a physical argument that $\mathbf{BC_1A}$ be diagonal for optimality. We have been able to mathematically arrive at the same condition, albeit for a slightly different problem.

3.4 Performance Evaluation

We have derived an optimum scheme for the transmission of blocked data. The motivation for this scheme was that we could find a scheme which would perform better than a scalar transmission scheme with decision feedback equalization. Hence, in this section, we evaluate the performance of the proposed scheme by determining its capacity under the constraint that the input power is limited. We then compare the performance of this scheme to scalar transmission with decision feedback equalization and demonstrate that gains can be obtained by using the proposed scheme.

We will evaluate the capacity of the two schemes under the following assumptions. We assume the noise to be additive white Gaussian with variance σ^2. The total power in each block input to the channel, blocks being of size M, is constrained to be equal to P. Correspondingly, the input power of each symbol when using scalar transmission with DFE is restricted to be equal to P/M. In the block case, the noise correlation matrix $\mathbf{R}_w$ is now given by

$$\mathbf{R}_w = \sigma^2\mathbf{I}. \tag{3.4.1}$$

The columns of the prefilter are the eigenvectors of the matrix $\mathbf{C}_1^T\mathbf{C}_1$, and we denote

the eigenvalues of this matrix as α_i. In other words,

$$\mathbf{C}_1^T \mathbf{C}_1 \mathbf{a}_i = \alpha_i \mathbf{a}_i. \tag{3.4.2}$$

We note that the eigenvalues are positive since the matrix in question is non-singular.

The basic theorem of Shannon we will use to evaluate the capacity of the two transmission schemes is as follows [8]: A discrete-time memoryless channel (i.e., a channel with no ISI) with additive gaussian noise of variance σ^2 and a gain a, with the input power restricted to λ is given by

$$C(\lambda) = \frac{1}{2} \log(1 + \frac{a^2 \lambda}{\sigma^2}). \tag{3.4.3}$$

In the case of scalar transmission with DFE, the resultant channel is one with no ISI since the ISI is ideally cancelled by the decision feedback equalizer. We thus have a channel of gain s_0, with additive noise variance σ^2, and with an input power constraint of P/M. Thus the capacity of scalar transmission with DFE, expressed per block of M symbols, is given by

$$C_s = \frac{M}{2} \log(1 + \frac{s_0^2 P}{M\sigma^2}). \tag{3.4.4}$$

For the block case, when the parallel input symbols are independent, the resultant is a parallel set of independent channels, each of which is ISI-free, due to the ideality of the Block DFE. The capacity of the block scheme is thus the sum of the capacities of the individual parallel channels under the constraint that the total block input power is constrained to be P. We have

$$\mathbf{C}_1^T \mathbf{C}_1 \mathbf{a}_i = \alpha_i \mathbf{a}_i$$

and assume that the energies of the columns are β_i^2. In other words,

$$\mathbf{a}_i^T \mathbf{a}_i = \beta_i^2. \tag{3.4.5}$$

With the input correlation matrix being Λ, which is diagonal with elements λ_i, the input power constraint to the channel can be expressed as

$$\begin{aligned} P &= \sum_{i=1}^{M} \lambda_i \mathbf{a}_i^T \mathbf{a}_i \\ &= \sum_{i=1}^{M} \lambda_i \beta_i^2. \end{aligned} \tag{3.4.6}$$

It is evident that we can set $\beta_i^2 = 1$ and optimize the λ_i's to maximize the capacity of the scheme. We shall do so , and thus the power constraint translates to

$$P = \sum_{i=1}^{M} \lambda_i. \tag{3.4.7}$$

Using equations (3.3.2) and (3.3.3), we obtain the gains of the individual channels to be

$$a_i = \frac{\lambda_i \alpha_i}{(\sigma^2 + \lambda_i \alpha_i)} \tag{3.4.8}$$

and the noise variances at the outputs of the individual channels to be

$$\sigma_i^2 = \frac{\lambda_i^2 \alpha_i \sigma^2}{(\sigma^2 + \lambda_i \alpha_i)^2}. \tag{3.4.9}$$

The input powers to each of the channels is given by λ_i. Using equation (3.4.3), we thus obtain the total capacity (per block) of the proposed scheme to be

$$C = \sum_{i=1}^{M} \frac{1}{2} \log(1 + \frac{\lambda_k \alpha_k}{\sigma^2}). \tag{3.4.10}$$

This is to be maximized with respect to the λ_i under the constraint given in equation (3.4.7). The λ_i, being input powers, are non-negative.

It can be shown that the function to be maximized is a concave function. Thus we can use the Kuhn-Tucker conditions [10] to find the maximum. The conditions turn out to be

$$\frac{\alpha_i}{\sigma^2 + \lambda_i \alpha_i} + \mu \leq 0 \tag{3.4.11}$$

with equality if λ_i is non-zero. Here μ is a Lagrange multiplier, and is chosen so that the power constraint is satisfied. Let A be the set of indices for which λ_i is non-zero. Then we have

$$\lambda_i = \frac{1}{|A|}(P + \sigma^2 \sum_{i \in A} \frac{1}{\alpha_i}) - \frac{\sigma^2}{\alpha_i} \tag{3.4.12}$$

and the capacity is given by

$$C = \frac{1}{2} \sum_{i \in A} \log[\frac{\alpha_i}{|A|}(P/\sigma^2 + \sum_{i \in A} \frac{1}{\alpha_i})]. \tag{3.4.13}$$

This can be rewritten as

$$C = \frac{|A|}{2} \log\left[\frac{1}{|A|}(P/\sigma^2 + \sum_{i \in A} \frac{1}{\alpha_i})\right] + \frac{1}{2} \log \prod_{i \in A} \alpha_i. \tag{3.4.14}$$

If the input power P is large enough, then $A = 1, 2, \ldots M$ and $|A| = M$. In this case, we have

$$C = \frac{M}{2} \log(\frac{P}{M\sigma^2} + Tr[(\mathbf{C}_1^T \mathbf{C}_1)^{-1}]/M) + \frac{1}{2} \log[\det(\mathbf{C}_1^T \mathbf{C}_1)]. \tag{3.4.15}$$

From the form of $\mathbf{C}_1$, it is evident that

$$\det(\mathbf{C}_1^T \mathbf{C}_1) = s_0^{2M} \tag{3.4.16}$$

which gives us

$$C = \frac{M}{2} \log(\frac{s_0^2 P}{M\sigma^2} + s_0^2 Tr[(\mathbf{C}_1^T \mathbf{C}_1)^{-1}]/M). \tag{3.4.17}$$

We compare this with the capacity obtained when using scalar transmission with DFE, which is given by equation (3.4.4):

$$C_s = \frac{M}{2} \log(\frac{s_0^2 P}{M\sigma^2} + 1).$$

It can be shown that $s_0^2 Tr[(\mathbf{C}_1^T \mathbf{C}_1)^{-1}]/M$ has a minimum value of 1, which implies that the optimized block transmission scheme always outperforms scalar transmission with DFE. The minimum value occurs when the matrix $\mathbf{C}_1$ is a scalar multiple

of the identity matrix, which implies that there is no ISI within the block, hence the scheme is ineffective in taking care of ISI within the block; thus we must obtain no performance improvement over the DFE technique.

3.5 An Example Channel

In this section, we present numerical results for data transmission using both the scalar DFE scheme and the optimum block scheme for the special case of the "dicode" channel and white noise. The dicode channel has a Z-transform which is given by

$$H(z) = 1 - z^{-1}. \tag{3.5.1}$$

The frequency response of this channel is plotted in Fig. 3.3. We observe that the channel has a spectral null at zero frequency.

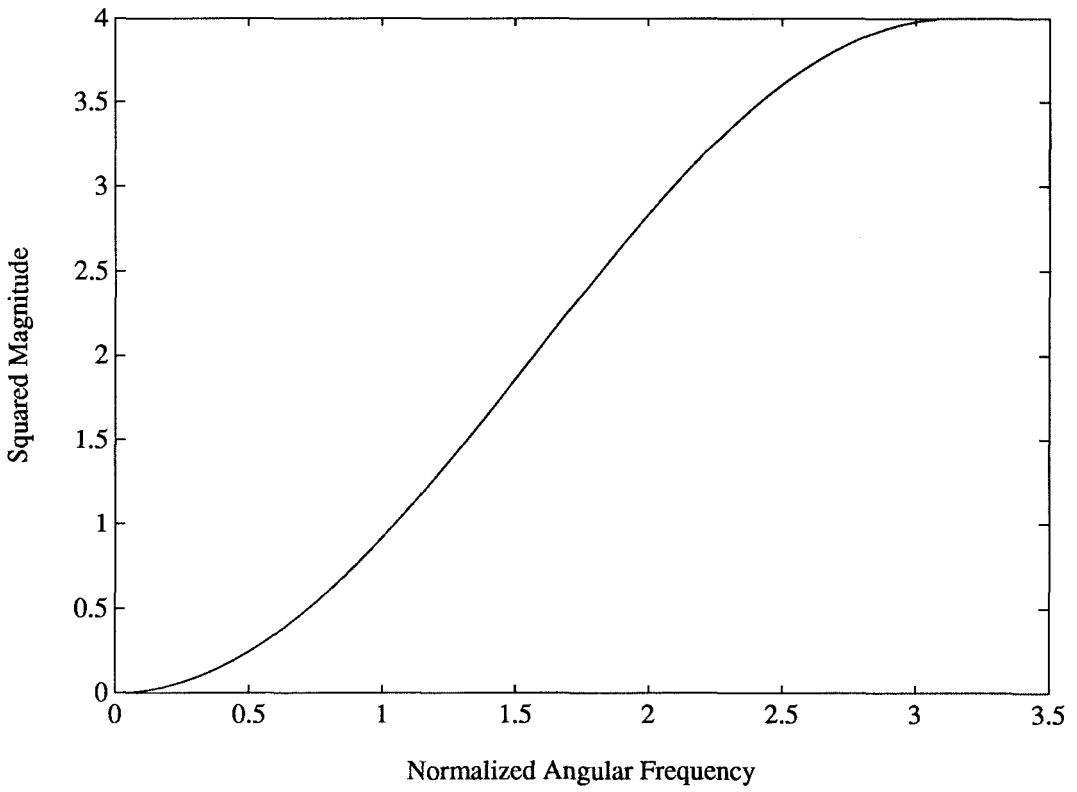

Fig. 3.3 Frequency Response of Dicode Channel

The columns of the optimum prefilter, as discussed before, are the eigenvectors of the matrix $\mathbf{C}_1^T\mathbf{C}_1$. For a given signal to noise ratio, the input power to each of the individual parallel channels is chosen as per the procedure outlined in the Section. 3.4. We plot the capacity of scalar transmission with DFE over this channel and compare it with transmission using the block scheme with input powers optimized. The results are shown in Fig. 3.4, and clearly demonstrate the superior performance of the block scheme.

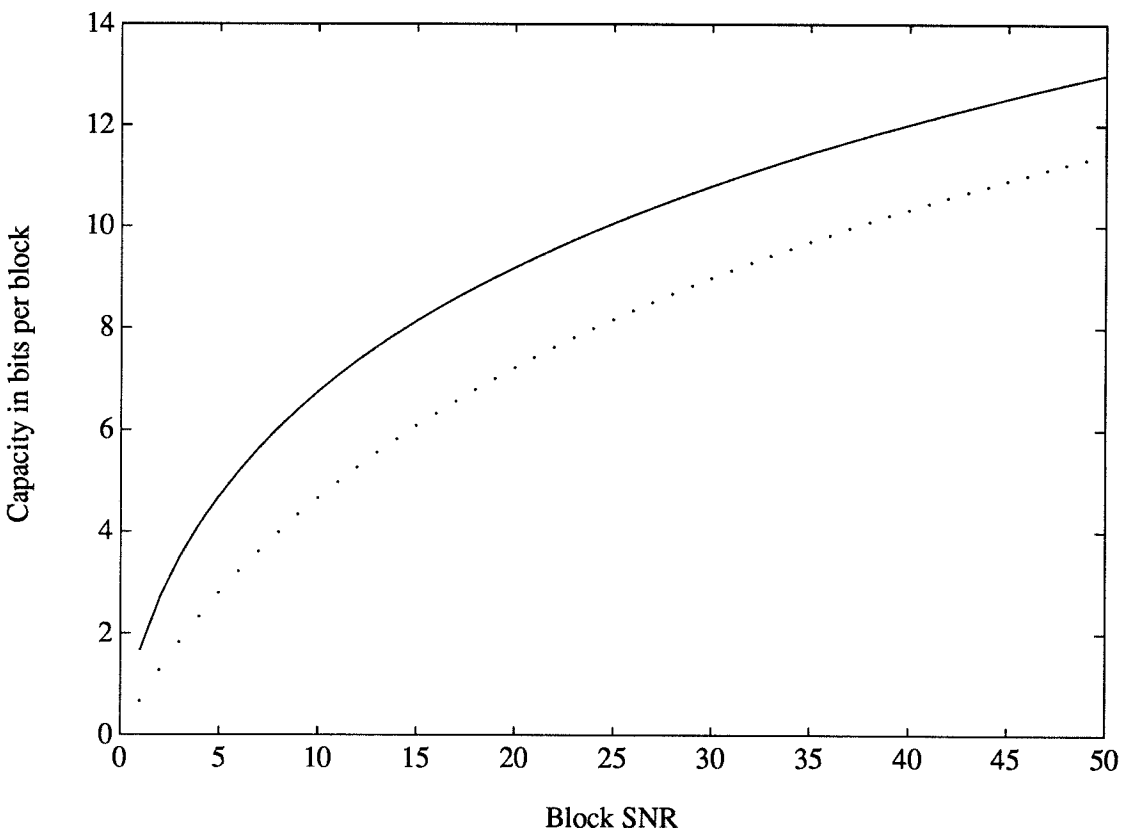

Fig. 3.4 Capacities of Scalar DFE and Block Schemes- Dicode Channel
(Solid Line - Block Scheme; Dotted Line - Scalar DFE)

We now address the question of why the block scheme appears to perform so well. To obtain the answer, we need look only as far as the frequency domain. We note that all our optimization was done in the time domain; however, the optimum filters we obtained have desirable properties in the frequency domain too. We plot the frequency responses of the synthesis filters at the input to the channel in Fig. 3.5. We observe that these filters have the property of splitting the spectrum into various frequency bands, though not with a whole lot of attenuation between adjacent bands. Thus, the block scheme, in a way, achieves what we had set out to do initially, but failed in the process.

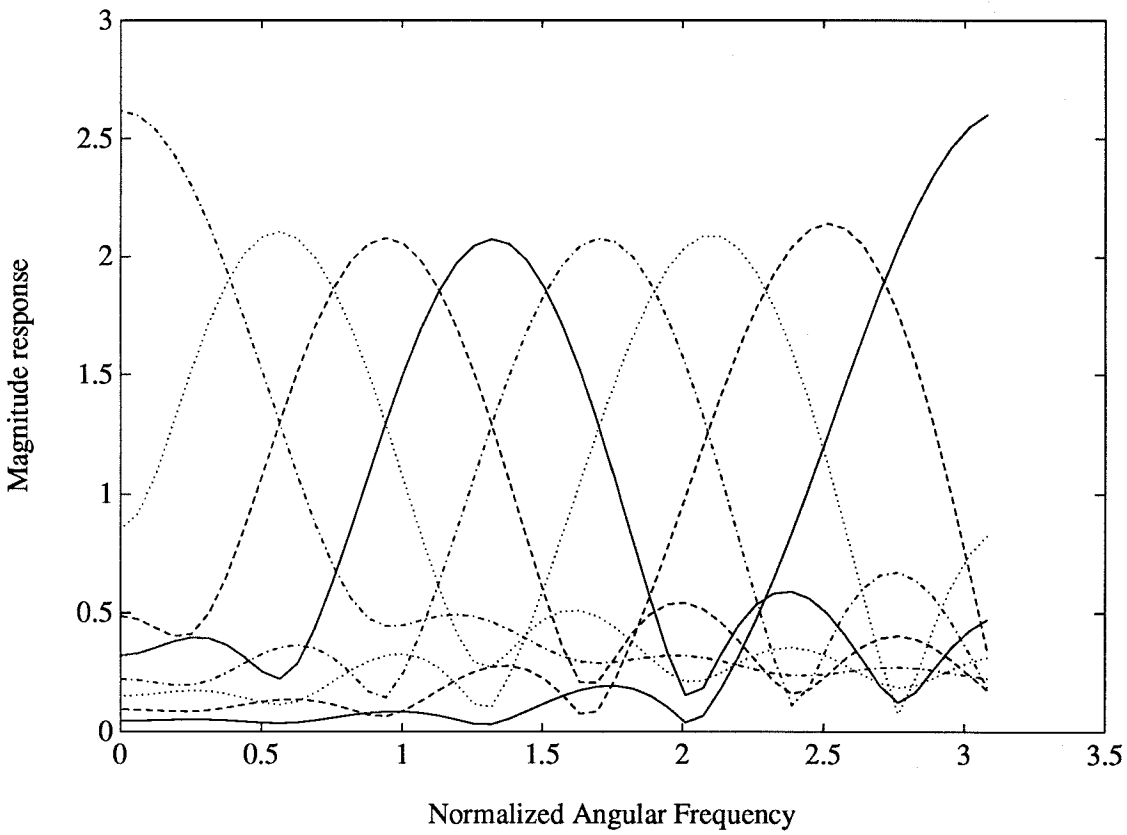

Fig. 3.5 Frequency Responses of Synthesis Filters

To obtain some further insight, we also look at the spectral properties of the signal at the input to the channel. This signal is characterized best as a cyclostationary signal [12] and does not have a power spectrum in the true sense of the word. However, we plot a pseudo power spectrum, which is the average of the power spectra of the signals on each of the individual subchannels, in Fig. 3.6. We observe that this power spectrum is quite similar to the one dictated by the waterpouring theorem for the input signal achieving capacity. Thus, we find that the block scheme succeeds in the desired spectral shaping of the input, and we believe this is the main reason for its superior performance.

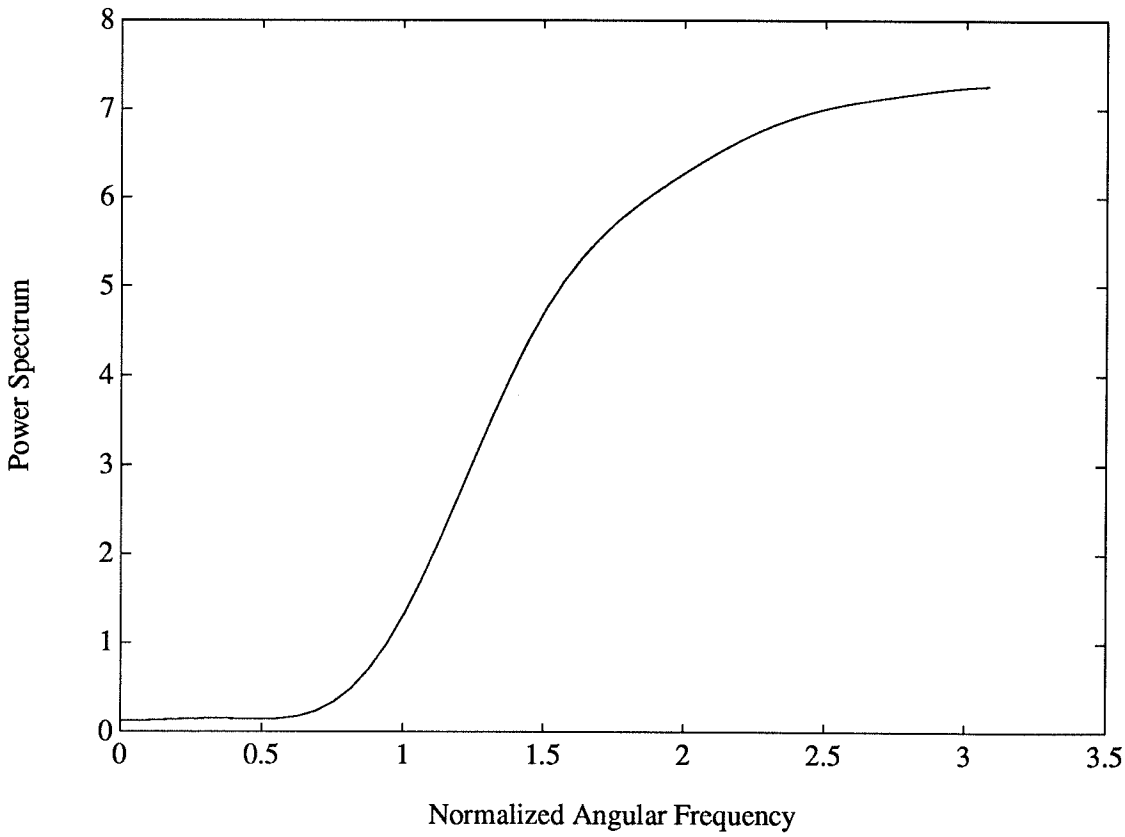

Fig. 3.6 Pseudo Power Spectrum of Optimum Input -- Dicode Channel

3.6 Conclusions

In this chapter, we derived the optimum finite-length prefilters and postfilters that minimized the mean-squared error between the input and the output of a channel with ISI, where decision-feedback equalization was used to counter the ISI present outside the block. The optimum prefilter was found to be a matrix of the eigenvectors of the correlation matrix of the channel impulse response and noise combined; hence, in a sense, it represents the Karhunen-Loeve transform [13] of the channel and noise. For the case of uncorrelated input symbols, the technique gave us a set of parallel independent channels, with the postfilter whitening the noise the best it could. Thus we obtained an efficient technique to transmit existing trellis codes over channels with ISI and colored noise.

We also evaluated the capacity of the proposed scheme and compared it to the capacity of the channel when using DFE. We found that substantial improvements could be obtained by using the block transmission scheme. We also observed that the block transmission scheme, along with an optimized input distribution, attempts to mimic the optimum input power spectrum as dictated by the water-pouring theorem, thus giving us a physical explanation for its superior performance.

3.A.1 Appendix: Using the Matrix Inversion Lemma

In this section, we show the following relationship:

$$Tr[\mathbf{\Lambda}^2\mathbf{M}^T(\mathbf{M}\mathbf{\Lambda}\mathbf{M}^T+\mathbf{P})^{-1}\mathbf{M} = Tr[\mathbf{\Lambda}-(\mathbf{I}+\mathbf{\Lambda}^{1/2}\mathbf{M}^T\mathbf{P}^{-1}\mathbf{M}\mathbf{\Lambda}^{1/2})^{-1}\mathbf{\Lambda}]. \quad (3A1.1)$$

In order to show this we make use of the matrix inversion lemma[4]:

$$\begin{aligned} &\text{If } \mathbf{A} = \mathbf{B}+\mathbf{C}\mathbf{D}^{-1}\mathbf{C}^T \\ &\text{then } \mathbf{A}^{-1} = \mathbf{B}^{-1}-\mathbf{B}^{-1}\mathbf{C}(\mathbf{C}^T\mathbf{B}^{-1}\mathbf{C}+\mathbf{D})^{-1}\mathbf{C}^T\mathbf{B}^{-1}. \end{aligned} \quad (3A1.2)$$

Applying this lemma to the R.H.S. of (3A1.1) (where $\mathbf{D}$ is replaced by $\mathbf{P}$) gives us

$$Tr[\mathbf{\Lambda}-(\mathbf{I}-\mathbf{\Lambda}^{1/2}\mathbf{M}^T(\mathbf{P}+\mathbf{M}\mathbf{\Lambda}^{1/2}\mathbf{\Lambda}^{1/2}\mathbf{M}^T)^{-1}\mathbf{M}\mathbf{\Lambda}^{1/2})\mathbf{\Lambda}]$$

which can be seen to be equal to the L.H.S. of (3A1.1), using the fact that the trace is invariant to a cyclic permutation.

3.A.2 Appendix: A Property of Positive Definite Matrices

In this section we show that for a positive definite matrix $\mathbf{W}$,

$$[\mathbf{W}^{-1}]_{ii} \geq [w_{ii}]^{-1} \tag{3A2.1}$$

with equality only if $\mathbf{W}$ is diagonal. Since $\mathbf{W}$ is positive definite, it can be written as

$$\mathbf{W} = \mathbf{V}^T \mathbf{\Gamma} \mathbf{V} \tag{3A2.2}$$

where

$$\mathbf{V}^T \mathbf{V} = \mathbf{I}$$

and

$$\mathbf{\Gamma} = \text{diag}\{\gamma_1, \gamma_2, \ldots, \gamma_M\}, \quad \gamma_i > 0, i = 1, 2, \ldots, M.$$

We note that

$$\mathbf{W}^{-1} = \mathbf{V}^T \mathbf{\Gamma}^{-1} \mathbf{V}. \tag{3A2.3}$$

Thus, we have

$$w_{kk} = \sum_{i=1}^{M} \gamma_i v_{ik}^2 \tag{3A2.4}$$

and

$$[\mathbf{W}^{-1}]_{kk} = \sum_{j=1}^{M} \frac{1}{\gamma_j} v_{jk}^2. \tag{3A2.5}$$

Hence, it follows that

$$\begin{aligned} [\mathbf{W}^{-1}]_{kk} w_{kk} &= \sum_{i=1}^{M} \sum_{j=1}^{M} \frac{\gamma_i}{\gamma_j} v_{ik}^2 v_{jk}^2 \\ &= \frac{1}{2} \sum_{i=1}^{M} \sum_{j=1}^{M} \left(\frac{\gamma_i}{\gamma_j} + \frac{\gamma_j}{\gamma_i}\right) v_{ik}^2 v_{jk}^2 \end{aligned} \tag{3A2.6}$$

where the last step follows due to symmetry.

Using the fact that $(x + 1/x)$ has a minimum value of 2 for positive x (this minimum occurs when $x = 1$), we obtain

$$[\mathbf{W}^{-1}]_{kk} w_{kk} \geq \sum_{i=1}^{M} \sum_{j=1}^{M} v_{ik}^2 v_{jk}^2.$$

From the unitary property of $\mathbf{V}$, it follows that the right-hand side of the above inequality is unity, from which the inequality (3A2.1) follows.

To prove that equality occurs in (3A2.1) only if $\mathbf{W}$ is diagonal, we write

$$\frac{\gamma_i}{\gamma_j} + \frac{\gamma_j}{\gamma_i} = 2 + \epsilon_{ij} \quad , \epsilon_{ij} \geq 0 \tag{3A2.7}$$

where ϵ_{ij} is zero if $i = j$. We thus have

$$[\mathbf{W}^{-1}]_{kk} w_{kk} = 1 + \frac{1}{2} \sum_{i=1}^{M} \sum_{j=1}^{M} \epsilon_{ij} v_{ik}^2 v_{jk}^2. \tag{3A2.8}$$

For the case when all eigenvalues of $\mathbf{W}$ are distinct, ϵ_{ij} is positive for $i \neq j$; therefore, for equality in (3A2.1) we must have

$$v_{ik} v_{jk} = 0 \qquad \text{for } i \neq j.$$

This implies that there can be only one non-zero element in each column of $\mathbf{V}$ and this element has to be unity due to the fact that $\mathbf{V}$ is unitary. In other words, $\mathbf{V}$ is a permutation matrix and it follows that $\mathbf{W}$ is a diagonal matrix.

For the case when the eigenvalues are not distinct, the proof is more involved. In this case, $\gamma_i = \gamma_j$, i.e. $\epsilon_{ij} = 0$ for $i \neq j$. For such i, j, we assume, without loss of generality, that $v_{ik} v_{jk} \neq 0$ for all k. Let S be the set of indices for which the eigenvalues are equal. Then, it follows that

$$v_{qk} v_{lk} = 0$$

where $q \in S$ and $l \notin S$. This implies that, for all k, $v_{lk} = 0$ for $l \notin S$. From equation (3A2.2), we obtain

$$w_{kl} = \sum_{i=1}^{M} \gamma_i v_{ik} v_{il}. \tag{3A2.9}$$

In the case of equality in (3A2.1), the arguments above indicate that this is equivalent to

$$w_{kl} = \sum_{i \in S} \gamma_i v_{ik} v_{il}. \tag{3A2.10}$$

From the definition of the set S, it follows that

$$w_{kl} = \gamma \sum_{i \in S} v_{ik} v_{il} = \gamma \sum_{i=1}^{M} v_{ik} v_{il}. \qquad (3A2.11)$$

The last step follows since $v_{lk} = 0$ for $l \notin S$. Due to the unitary nature of V, we have

$$\sum_{i=1}^{M} v_{ik} v_{il} = 0 \quad \text{for } k \neq l \qquad (3A2.12)$$

which proves that the off-diagonal elements are zero.

3.A.3 Appendix: Simplifying the Postfilter

In this appendix, we use the matrix inversion lemma to simplify the form of the optimal postfilter, which, as a function of the prefilter $\mathbf{A}$, is given by equation (3.2.6):

$$\mathbf{B}_0 = \mathbf{R}_{xx}\mathbf{A}^T\mathbf{C}_1^T(\mathbf{R}_w + \mathbf{C}_1\mathbf{A}\mathbf{R}_{xx}\mathbf{A}^T\mathbf{C}_1^T)^{-1}. \qquad (3A3.1)$$

Using equation (3.2.9) this can be rewritten as

$$\mathbf{B}_0 = \mathbf{R}_{xx}\mathbf{U}^T\mathbf{G}^T\mathbf{C}_1^T(\mathbf{R}_w + \mathbf{C}_1\mathbf{G}\mathbf{\Lambda}\mathbf{G}^T\mathbf{C}_1^T)^{-1}. \qquad (3A3.2)$$

Application of the matrix inversion lemma in equation (3A1.2) to equation (3A3.2) results in

$$\mathbf{B}_0 = \mathbf{R}_{xx}\mathbf{U}^T\mathbf{G}^T\mathbf{C}_1^T\Big(\mathbf{R}_w^{-1} - \mathbf{R}_w^{-1}\mathbf{C}_1\mathbf{G}\mathbf{\Lambda}^{1/2}(\mathbf{\Lambda}^{1/2}\mathbf{G}^T\mathbf{C}_1^T\mathbf{R}_w^{-1}\mathbf{C}_1\mathbf{G}\mathbf{\Lambda}^{1/2} + \mathbf{I})^{-1}\mathbf{\Lambda}^{1/2}\mathbf{G}^T\mathbf{C}_1^T\mathbf{R}_w^{-1}\Big). \qquad (3A3.3)$$

We note that $\mathbf{G}^T\mathbf{C}_1^T\mathbf{R}_w^{-1}\mathbf{C}_1\mathbf{G}$ is a diagonal matrix due to (3.3.17). We denote this matrix $\mathbf{\Lambda}_1$. Since the inverse of a diagonal matrix is a diagonal matrix, it follows that the matrix $(\mathbf{\Lambda}^{1/2}\mathbf{G}^T\mathbf{C}_1^T\mathbf{R}_w^{-1}\mathbf{C}_1\mathbf{G}\mathbf{\Lambda}^{1/2} + \mathbf{I})^{-1}$ is diagonal, and we denote this matrix $\mathbf{\Lambda}_2$. Thus we obtain

$$\begin{aligned}\mathbf{B}_0 &= \mathbf{R}_{xx}\mathbf{U}^T\mathbf{G}^T\mathbf{C}_1^T\mathbf{R}_w^{-1} - \mathbf{R}_{xx}\mathbf{U}^T\mathbf{\Lambda}_1\mathbf{\Lambda}^{1/2}\mathbf{\Lambda}_2\mathbf{\Lambda}^{1/2}\mathbf{G}^T\mathbf{C}_1^T\mathbf{R}_w^{-1} \\ &= \mathbf{R}_{xx}\mathbf{U}^T(\mathbf{I} - \mathbf{\Lambda}_1\mathbf{\Lambda}_2\mathbf{\Lambda})\mathbf{G}^T\mathbf{C}_1^T\mathbf{R}_w^{-1}.\end{aligned} \qquad (3A3.4)$$

where we have conveniently used the fact that multiplication of diagonal matrices is commutative.

References

[1] S. Kasturia, J. Aslanis and J.M. Cioffi, "Vector Coding for Partial Response Channels," *IEEE Trans. Info. Theory*, vol. 36, no. 4, pp. 726-740, July 1990.

[2] J.W. Lechleider, "The Optimum Combination of Block Codes and Receivers for Arbitrary Channels," *IEEE Trans. Commun.*, vol. 38, no. 5, pp. 615-621, May 1990.

[3] H.S. Malvar and D.H. Staelin, "Optimal Pre- and Postfilters for Multichannel Signal Processing," *IEEE Trans. on Acoustics, Speech and Signal Processing*, vol. 36, no. 2, pp. 287-289, Feb. 1988.

[4] Simon Haykin, *Adaptive Filter Theory*, Prentice Hall Inc., Englewood Cliffs, NJ 07632, p. 385, 1986.

[5] S. Kay, *Modern Spectrum Estimation: Theory and Application*, Prentice Hall Inc., Englewood Cliffs, NJ 07632, p. 422, 1988.

[6] G. D. Forney Jr., "Coset Codes- Part I: Introduction and Geometrical Classification," *IEEE Trans. on Info. Theory,* vol. 34, no. 5, pp. 1123-1151, Sept.1988.

[7] D. G. Messerschmitt, "Design Issues in the ISDN U-Interface Transceiver," *IEEE JSAC,* vol. SAC-4, no. 8, pp. 1281-1293, Nov. 1986.

[8] Richard E. Blahut, *Principles and Practice of Information Theory*, Addison-Wesley Publishing Company, 1987.

[9] J. Salz, "Digital Transmission over Cross-Coupled Linear Channels," *AT&T Technical Journal*, vol. 64, no. 6, pp. 1147-1159, July-August 1985.

[10] Joel Franklin, *Methods of Mathematical Economics : Linear and Non-linear Programming, Fixed-Point Theorems*, Springer-Verlag New York Inc., 1980.

[11] S. Kasturia and J. M. Cioffi, "Vector Coding with Decision Feedback Equalization for Partial Response Channels," *Proceedings Globecom' 88* , vol. 60, pp. 1497-1514, Dec. 1988.

[12] Vinay Sathe and P. P. Vaidyanathan, " Effects of Multirate Systems on the Statistical Properties of Random Inputs," presented at the *IEEE ICASSP'91*, Toronto, Canada, May 1991.

[13] N. S. Jayant and P. Noll, *Digital Coding of Waveforms*, Prentice-Hall, 1984.

Chapter 4 The ISDN Digital Subscriber Loop

In the next few decades, one expects the Integrated Services Digital Network to revolutionize the communications industry. Obtaining services like voice, video, digital television, fax, etc. over the telephone lines is of great interest both to subscribers and the telephone companies. The use of telephone lines to provide imaging services necessitates the transmission of data at very high rates over these lines. While one can envision fiber optic lines being brought to the desktop in the next few decades, there is a wealth of infrastructure already present in the form of the twisted-pair copper loop. We investigate the possiblity of using the local loops already available to provide data rates as high as the T1 rate, i.e., 1.544 Mb/s. While this research may have the side effect of delaying the advent of fiber to the home, it nevertheless gives us a stopgap arrangement for the use of ISDN before an all-fiber local loop is installed. Thus it may really hasten fiber-to-the-home (FTTH). In this chapter, we will investigate multichannel transmission over the ISDN digital subscriber loop. The principal impairments on this channel are intersymbol interference and noise. The noise is predominantly crosstalk, which depends on the transmitted signals from neighboring loops assumed to be using the same scheme for transmission. Hence the noise on the channel depends on the transmitted signal, and this complicates the problem of finding the optimum filters. However, we have been able to obtain a solution to this problem. We will evaluate

the performance of this method over some representative loops using models for the loop and the crosstalk and demonstrate the possibility of T1 transmission over a large subset of the local loop plant available.

4.1 Introduction

In this chapter, we investigate the application of the multichannel method derived in the previous chapter to the special case of the ISDN subscriber loop. Though both market forces and current technology have contributed to limit rates on the local loop to about 160 kB/s, we believe that T1 transmission on a large subset of the loops used is feasible. In our analysis, we are able to present a method to include crosstalk models explicitly in the calculation of the optimum filters to be used. This is an area where previous researchers have found little success.

The main impairments on the local loop are intersymbol interference and crosstalk from adjacent loops in the same bundle [6]. We will provide plots of typical impulse responses of some loops. The impulse responses of the loops were obtained from Bell Communications Research. We use these impulse responses to generate the impulse responses of the resultant channels at the required signalling rates.

The noise on the local loop is predominantly crossalk from adjacent loops in the same binder group. We also present models for the crosstalk noise. This is a particularly interesting case of noise since the noise depends on the signals being transmitted in adjacent loops, which, we assume, are transmitting using the same scheme. Hence, finding the optimum input power allocation and the filters to achieve the minimum mean-squared error is a difficult problem, but we have been able to obtain a method to solve it. With synchronized transmission between loops in a bundle, the crosstalk noise is accurately modeled as cyclostationary. If there is a lack of synchronization between loops, the crosstalk noise is wide-sense stationary. We present methods to consider both these cases and observe that the performance is not too different in the two cases. We will find the optimum filters to maximize

the throughput, given a certain probability of error and a restriction on the input power to be used.

The organization of this chapter is as follows: In Section 4.2, we present some physical characteristics of the local loop plant and its classification depending on length and physical structure. In Section 4.3, we present models for the transfer characteristics of some of the loops over which we perform our simulations. In Section 4.4, we present models for the crosstalk transfer functions involved. In Section 4.5, we determine expressions for the correlation of the crosstalk noise as a function of the input correlation and the crosstalk transfer function. We do so for two cases; cyclostationary crosstalk and wide-sense stationary crosstalk. In Section 4.6, we demonstrate how to determine the optimum filters and the optimum input power distribution over these channels for both cases of crosstalk noise. In Section 4.7, we present some experimental results applicable to much of the local loop plant. We conclude the chapter in Section 4.8 by briefly summarizing our findings.

4.2 Loop Characteristics and Classification

A single pair of copper wires is used to provide plain old telephone service (POTS). This pair serves three purposes: provision of DC power for the instrument, a path for the 20Hz signal used to ring the phone and an analog voice frequency link typically used in the range of 300 to 3600 Hz. At the end office, pairs are bundled together at the exit from the main distribution frame. Usually 50 pairs are placed together in a single casing known as the *binder group*. The wire is covered with insulation; usually polyvinyl, and sometimes paper. Pairs are twisted to provide some degree of interference rejection from other pairs. Nevertheless, crosstalk from other pairs is a major impairment on the local loop.

The size of the wire is of particular importance in determining the performance of transmission systems, since the losses on the wire vary according to its size. The size of the individual wires in the group varies from 22 gauge down to 26 gauge. The binder group may have both splice and gauge changes. Frequently, a pair may

be tapped at more than one location, thereby resulting in several terminations. The unterminated end of the tap leads to reflections towards the binder group and distorts the signal received, both in magnitude and phase. At voiceband frequencies, the bridged taps have little effect on the performance of the system, since the length of the bridged taps is only a small fraction of the wavelength. But as we transmit at higher rates, e.g., T1, we use significantly higher bandwidth, and the effect of these taps will be highly detrimental. We shall, however, not work with a transmission line model for the loops. Instead, we will use simple models for the frequency response (or equivalently the impulse response) and use this to evaluate the performance on these loops.

In order to provide some degree of loop classification, the Bell System, prior to divestiture, created an administrative division of loops known as the Carrier Serving Area (CSA) in the early 1970's. The CSA consists of all loops meeting the following restrictions. The maximum length of a loop is restricted to 12000 feet. No wire smaller than 26 gauge may be present. If 26 gauge is present, then the length of the loop, along with all the bridged taps, may not exceed 9000 feet. The total length of all bridged taps may not exceed 2500 feet and no one tap may be longer than 2000 feet. These restrictions serve to bound the total amount of attenuation due to losses in the copper and the possible degradation due to bridged taps.

4.3 Loop Responses

We need models for the impulse responses of the loops to assess the performance of the proposed transmission schemes on them. The modeling of the loops was done at Bell Communications Research. The Bellcore research staff generated the pulse response of the loops using a square pulse with a duration of 62.5 ns. We plot the pulse response of a representative loop, which consists of 12 kft of 24 gauge wire, in Fig. 4.1. We acknowledge the help of Dr. Kamran Sistanizadeh of Bellcore in obtaining these loop responses.

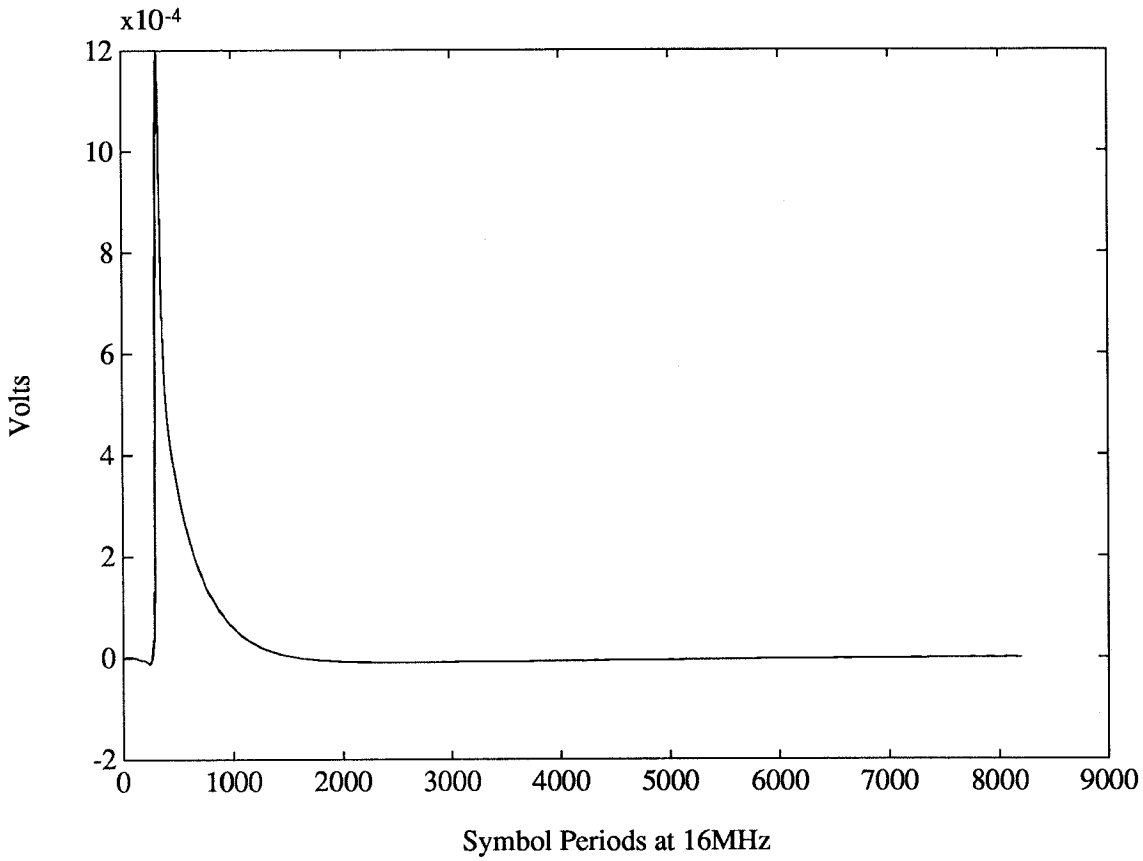

Fig. 4.1 Pulse Response of a Representative Loop

When using the local loop for transmission, we append certain filters at the transmitting and receiving ends. These are called the *hybrids* associated with the loop. We assume transmission at 640 kHz in this discussion. At the transmitting end, we have a rectangular pulse of duration 1.5625 μs to modulate the discrete-time input signal, a lowpass filter which has a 3dB cutoff frequency of 320 kHz, and a transformer to filter out d.c. We model the transformer as an RC filter, with

a single zero at d.c. and a 3dB cutoff frequency of 300 Hz. At the receiving end, the signal is passed through a transformer and a lowpass filter which has the same characteristics as the one used at the transmitting end. We assume that the lowpass filters are 4th order Butterworth filters. The resulting signal at the output of the hybrids at the receiving end is then sampled to obtain a discrete-time output signal which is then demultiplexed and passed through the postfilter.

The overall channel we have is a discrete-time channel, whose impulse response is obtained by sampling the continuous-time impulse response of the loop with the associated hybrids. We plot this response for the same loop mentioned previously in Fig. 4.2.

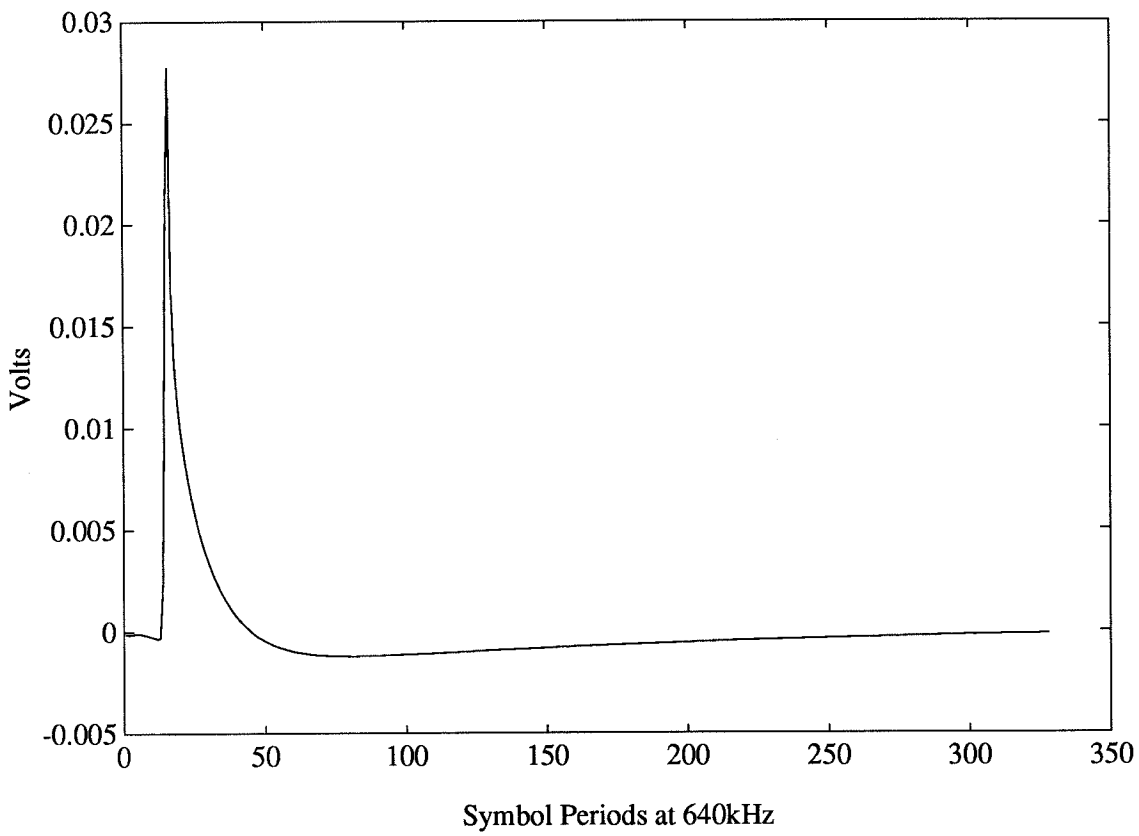

Fig. 4.2 Impulse Response of Loop with Associated Hybrids

We note that the long tails of the channel impulse response suggest the use of a pole-zero model to represent the channel. This may be used to simplify the form of the block decision feedback equalizer by using a pole-zero decision feedback equalizer as has been done in [1]. We have not investigated this aspect further and propose it as a suggestion for further research. In this thesis, we use the estimates of the channel impulse response to assess the performance of the block transmission scheme over the local loop, while assuming a perfect decision feedback equalizer.

4.4 Crosstalk

The most important impairments in a cable system are thermal noise due to random motion of the electrons in conductors, impulse noise caused due to switching elements, and crosstalk noise. The thermal noise is almost always Gaussian, and is uncorrelated to the transmitted signal. It is typically modeled as additive white Gaussian noise. The characteristics of impulse noise are not as well known. In order to ensure that impulse noise is suppressed, and to account for losses due to timing recovery, performance margins are commonly specified for any transmission system used.

Since the dominant impairment on the loops is crosstalk, we can include these performance margins in our analysis by increasing the magnitude of the crosstalk noise. Crosstalk noise is a result of the proximity of the wire-pairs within the binder group. The twisting of the wire-pairs is able to reject some of the interference, but the residual interference is a considerable impairment.

There are two crosstalk mechanisms which are modeled differently. *Near-end crosstalk* is due to other transmitters located at the same end of the cable as the receiver in question. The interference due to the transmitter on the same cable pair is called the *echo* and is cancelled to facilitate full-duplex transmission. In this work, we assume that the echo has been cancelled, and that any residual distortion can be accounted for by performance margins. *Far-end crosstalk* is due to transmitters located at the far end of the cable. This excludes the transmitter at the far end on

the same wire pair since this transmits the signal we want to receive. We illustrate the crosstalk and echo mechanisms in Fig. 4.3.

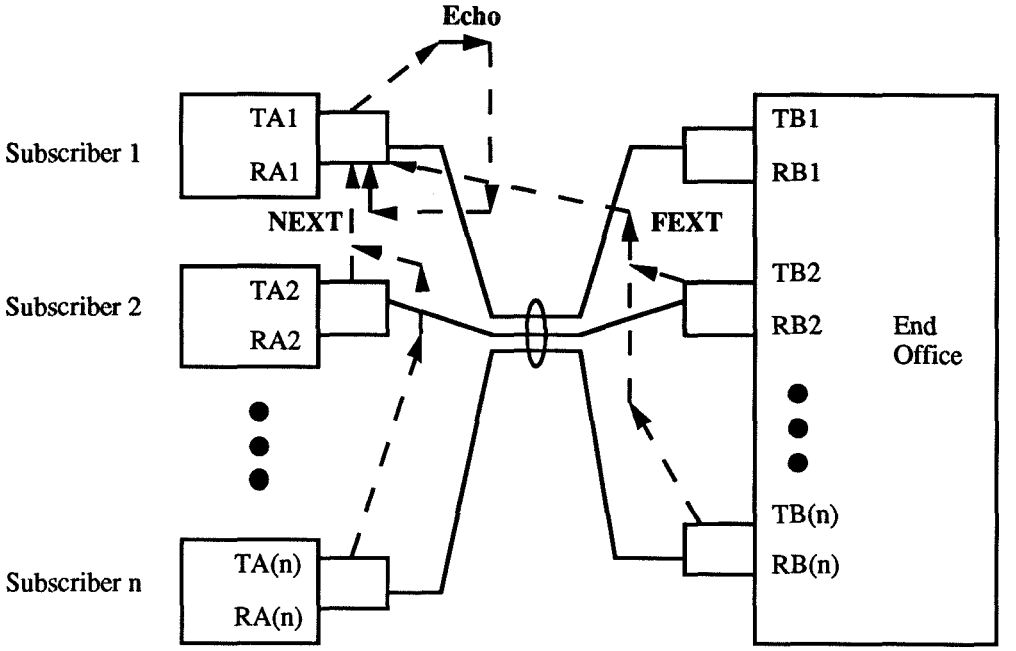

Fig. 4.3. Crosstalk Mechanisms in the Local Loop

The near-end crosstalk can be modeled as the input signal passing through a transfer function of the form [2]

$$H_{NEXT}(\omega) = j\omega \int_0^l e^{-2\Gamma(\omega)x} c(x)dx \tag{4.4.1}$$

where l is the length of the wire, $c(x)$ is representative of the capacitive coupling between wires as a function of length, and $\Gamma(\omega)$ is the characteristic impedance of the wire as a function of frequency. We have

$$\Gamma(\omega) = \sqrt{(R + j\omega L)(G + j\omega C)} \tag{4.4.2}$$

where R, L, C and G are, respectively, the resistance, inductance, capacitance and conductance of the wire per unit length. Other transfer function models for the

crosstalk exist, a simple one is of the form [3]

$$|H_{NEXT}(f)|^2 = K_{NEXT} f^{3/2} \tag{4.4.3}$$

where K_{NEXT} is a coupling constant, which has been empirically determined to be of the order of 10^{-13}. We note that this model lacks phase information, which is vital to the modeling of the crosstalk as a cyclostationary process. However, we shall use it to obtain the performance of the scheme under the assumption that the crosstalk noise is wide-sense stationary. The model in equation (4.4.1) does not agree very well with the measured crosstalk frequency responses given by equation (4.4.2), hence we shall not use it to estimate the performance of our scheme over the local loop. We shall, however, use it to compare the performance of the scheme under the disparate assumptions of wide-sense stationary and cyclostationary crosstalk.

Far-end crosstalk is modeled by the transfer function

$$|H_{FEXT}(f)|^2 = K_{FEXT} |C(f)|^2 f^2 \tag{4.4.4}$$

with K_{FEXT} being a coupling constant and $C(f)$ is the frequency response of the wire. We neglect far-end crosstalk noise in comparison to near-end crosstalk noise since it is attenuated by the length of the wire.

We will derive the optimum filters to transmit data in the presence of near-end crosstalk. In order to do this, we need accurate statistical models for the crosstalk noise. In the next section, we will characterize the crosstalk noise and present expressions for its correlation matrix.

4.5 Statistical Modeling of Crosstalk Noise

In Fig. 4.4, we present the scheme used for transmission over the local loop. The discrete-time input signal is passed through a shaping filter and fed to the loop, which is padded with transformers at either end to filter out d.c. The output from the channel is passed through a receive filter and then sampled to obtain a discrete-time output signal, which is then passed through the postfilter and equalizer. As shown, the crosstalk noise is modeled as being added at the output of the loop, hence the discrete-time noise sequence at the postfilter input is a filtered and sampled version of this signal.

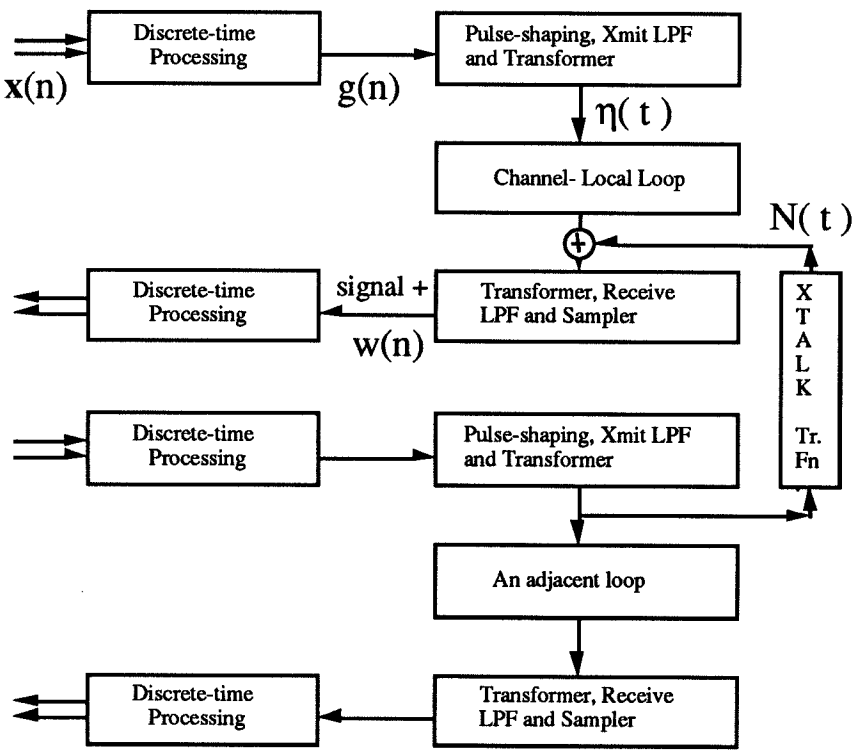

Fig. 4.4. Crosstalk- The Whole Picture

The statistical model for the crosstalk noise is obtained by passing the input signal through the crosstalk transfer function, as shown in the figure. We now present a way to model the crosstalk noise statistically, so that we can use the

expression for the correlation matrix of the crosstalk noise to obtain the optimum pre- and postfilters. But first, just to add to the suspense, we shall finally formally define a cyclostationary process.

Definition: A discrete-time signal $g(n)$ is said to be *cyclostationary with period M* [4] if

$$E[g(n+kM)] = E[g(n)] \quad \text{for all } k, n$$

and

$$E[g(n+kM)g(l+kM)] = E[g(n)g(l)] \quad \text{for all } k, n, l.$$

Analogously, a signal $g(t)$ in continuous time is said to be *cyclostationary with period* T if

$$E(g(t)] = E[g(t+kT)] \quad \text{for all } t \text{ and integer } k$$

and

$$E[g(t_1+kT)g(t_2+kT)] = E[g(t_1)g(t_2)] \quad \text{for all } t_1, t_2, \text{ and integer } k.$$

The discrete-time input vector signal $\mathbf{x}(n)$ has been assumed to be a wide-sense stationary (WSS) vector process, correlated only within blocks, with the individual $x_i(n), \quad i = 0, \ldots M-1$ being uncorrelated. The correlation matrix of $\mathbf{x}(n)$ is $\mathbf{\Lambda}$, a diagonal matrix, with the diagonal elements being non-negative. This is passed through the matrix $\mathbf{A}$, which is a linear-time invariant vector system; hence the output $\mathbf{g}(n) = \mathbf{A}\mathbf{x}(n)$ is a WSS vector process. We assume that $\mathbf{x}(n)$ is zero mean, which implies that $\mathbf{g}(n)$ is zero-mean. The vector signal $\mathbf{g}(n)$ is then multiplexed to give a scalar signal which given by

$$g(Mn+M-1-i) = g_i(n). \tag{4.5.1}$$

Given an index n_1, we can always express it as $n_1 = Ml + M - 1 - i$ for some l and i, where $0 \leq i \leq M-1$. Thus we have

$$\begin{aligned} E[g(n_1+kM) &= E[g_i(l+k)] \\ &= E[g_i(l)] \\ &= E[g(n_1)]. \end{aligned} \tag{4.5.2}$$

where we have used the fact that the mean of the WSS process $\mathbf{g}(n)$ is independent of the position n. Thus

$$E[g(n)] = E[g(n + kM)]. \tag{4.5.3}$$

We similarly have

$$\begin{aligned} E[g(n_1 + kM)g(l_1 + kM)] = E[g_i(p + k)g_j(q + k)] = \\ = E[g_i(p)g_j(q)] \end{aligned} \tag{4.5.4}$$

where $n_1 = Mp + M - 1 - i$ and $l_1 = Mq + M - 1 - j$ with $0 \leq i, j \leq M - 1$. We also find

$$E[g(n_1)g(l_1)] = E[g_i(p)g_j(q)]. \tag{4.5.5}$$

Thus

$$E[g(n)g(l)] = E[g(n + kM)g(l + kM)]. \tag{4.5.6}$$

Since $g(n)$ satisfies equations (4.5.3) and (4.5.6), which define a discrete-time wide-sense cyclostationary process of period M, we have

Fact 1: The multiplexed output $g(n)$ of the synthesis bank is wide-sense cyclostationary with period M.

The crosstalk noise added at the output of the loop is obtained by passing the input process to the loop through the crosstalk transfer function. The input to the loop is a continuous time signal which is obtained by passing the discrete-time signal $g(n)$ through a transmit filter with impulse response $p(t)$. In our case, Fig. 4.4 shows that the transmit filter is a cascade of the pulse shaping filter and the transformer. We can now characterize the input to the channel statistically.

Fact 2: The input to the channel $\eta(t)$ is a wide-sense cyclostationary process in continuous time with period MT, where T is the symbol duration.

Proof:

The signal $\eta(t)$ is given by

$$\eta(t) = \sum_{n=-\infty}^{\infty} g(n)p(t - nT). \tag{4.5.7}$$

Hence we have

$$\begin{aligned} E[\eta(t+kMT)] &= \sum_{n=-\infty}^{\infty} E[g(n)p(t-nT+kMT)] \\ &= \sum_{m=-\infty}^{\infty} E[g(m+kM)p(t-mT)] \\ &= \sum_{m=-\infty}^{\infty} E[g(m)p(t-mT)] \\ &= E[\eta(t)] \end{aligned} \tag{4.5.8}$$

where we have used the wide-sense cyclostationary property of $g(n)$ in discrete time. We also have

$$\begin{aligned} &E[\eta(t_1+kMT)\eta(t_2+kMT)] = \\ &\qquad \sum_{n=-\infty}^{\infty}\sum_{m=-\infty}^{\infty} E[g(n)g(m)p(t_1-nT+kMT)p(t_2-mT+kMT)] \\ &\qquad = \sum_{i=-\infty}^{\infty}\sum_{j=-\infty}^{\infty} E[g(i+kM)g(j+kM)]p(t_1-iT)p(t_2-jT) \\ &\qquad = \sum_{i=-\infty}^{\infty}\sum_{j=-\infty}^{\infty} E[g(i)g(j)]p(t_1-iT)p(t_2-jT) \\ &\qquad = E[\eta(t_1)\eta(t_2)] \end{aligned} \tag{4.5.9}$$

where we have again used the wide-sense cyclostationarity of $g(n)$. The result follows.

We have two cases to consider. The first case is when we assume that transmission on all the wires is fairly well synchronized. In this case, we shall see that the crosstalk noise turns out to be cyclostationary. However, if we assume a lack of synchronization between different wires, then our time origin is random, and we assume it can occur anywhere between 0 and MT with a uniform probability distribution, thus rendering the crosstalk noise to be a wide-sense stationary process. We shall analyze these two cases separately, and in each case, derive an expression for the noise correlation matrix at the input to the polyphase matrix of the analysis bank, i.e., the postfilter.

4.5.1 Cyclostationary Crosstalk Noise

When transmission on the loops in a binder group is synchronized to a fair degree, the noise that is added at the output of the loop is well modeled as $\eta(t)$ passed through the crosstalk transfer function. This noise $N(t)$ can be viewed as being obtained by passing the discrete-time wide-sense cyclostationary process $g(n)$ through a transmit filter which is a cascade of the shaping filter, the transformer and the crosstalk transfer function. Hence $N(t)$ is wide-sense cyclostationary with period MT. $N(t)$ is passed through the receive filter; the output of this filter $W(t)$ is also wide-sense cyclostationary with the same period. It is then sampled (and maybe delayed) to obtain the discrete-time noise sequence $w(n)$.

We have

$$w(n) = W(nT) \tag{4.5.1.1}$$

where $W(t)$ is wide-sense cyclostationary with period MT. We note that

$$\begin{aligned} E[w(n+kM)] &= E[W(nT+kMT)] \\ &= E[W(nT)] \\ &= E[w(n)] \end{aligned} \tag{4.5.1.2}$$

and

$$\begin{aligned} E[w(n_1+kM)w(n_2+kM)] &= E[W(n_1T+kMT)W(n_2T+kMT)] \\ &= E[W(n_1T)W(n_2T)] \\ &= E[w(n_1)w(n_2)] \end{aligned} \tag{4.5.1.3}$$

where we have used the wide-sense cyclostationary property of $W(t)$. Equations (4.5.1.2) and (4.5.1.3) show that $w(n)$ is a discrete-time wide-sense cyclostationary process with period M.

The input to the postfilter $\mathbf{B}$ is a blocked version of $w(n)$. It can be expressed as

$$\mathbf{w}(n) = [w(Mn), w(Mn-1), \ldots, w(Mn-M+1)]^T. \tag{4.5.1.4}$$

We wish to find the correlation matrix, at zero lag, of $\mathbf{w}(n)$, since this is essential to find the optimum filters $\mathbf{A}$ and $\mathbf{B}$, as we found in the previous chapter. We have

$$W(t) = \sum_{n=-\infty}^{\infty} g(n)h(t - nT) \tag{4.5.1.5}$$

where $h(t)$ is the impulse response of the cascade of the transmit filters, the crosstalk transfer function and the receive filters. Thus

$$w(m) = \sum_{n=-\infty}^{\infty} g(n)h(mT - nT), \tag{4.5.1.6}$$

which is a convolution of $g(n)$ with the sampled version of $h(t)$, which we shall denote $h(n)$.

Between $\mathbf{g}(n)$ and $\mathbf{w}(n)$, we recognize that we have the same structure we had analyzed before in Chapter 4. Hence we have $\mathbf{w}(n)$ as the output of the filter $\mathbf{H}(z)$ to the input $\mathbf{g}(\mathbf{n})$, where $\mathbf{H}(z)$, for $M = 5$, is given by

$$\mathbf{H}(z) = \begin{pmatrix} H_1(z)z^{-1} & H_2(z)z^{-1} & H_3(z)z^{-1} & H_3(z)z^{-1} & H_0(z) \\ H_0(z)z^{-1} & H_1(z)z^{-1} & H_2z^{-1} & H_3(z)z^{-1} & H_4(z)z^{-1} \\ H_4(z)z^{-2} & H_0(z)z^{-1} & H_1(z)z^{-1} & H_2(z)z^{-1} & H_3(z)z^{-1} \\ H_3(z)z^{-2} & H_4(z)z^{-2} & H_0(z)z^{-1} & H_1(z)z^{-1} & H_2(z)z^{-1} \\ H_2(z)z^{-2} & H_3(z)z^{-2} & H_4(z)z^{-2} & H_0(z)z^{-1} & H_1(z)z^{-1} \end{pmatrix} \tag{4.5.1.7}$$

Here the $H_k(z)$ are the Type 1 polyphase components of $H(z)$, which is the Z-transform of $h(n)$.

We wish to find the correlation matrix at zero lag of $\mathbf{w}(n)$. This can easily be found since $\mathbf{w}(n)$ is the output of the linear system $\mathbf{H}(z)$ to the input $\mathbf{g}(n)$, whose statistics we know. Recall that $\mathbf{g}(n)$ was obtained by passing $\mathbf{x}(n)$ through the prefilter $\mathbf{A}$. We now state a fact that enables us to find the necessary correlation matrices.

Fact 4.5.1.1: Let $\mathbf{x}(n)$ be an $N \times 1$ vector WSS input to an $M \times N$ transfer matrix $\mathbf{H}(z)$, or equivalently to $\mathbf{H}(e^{j\omega})$. The power spectral density of the output $M \times 1$ WSS vector process $\mathbf{y}(n)$ is given by [5]

$$\mathbf{S_{yy}}(e^{j\omega}) = \mathbf{H}(e^{j\omega})\mathbf{S_{xx}}(e^{j\omega})\mathbf{H}^{\dagger}(e^{j\omega}) \tag{4.5.1.8}$$

where $\mathbf{H}^{\dagger}(e^{j\omega})$ is obtained by transposing the matrix in which the elements are the conjugates of those in $\mathbf{H}(e^{j\omega})$.

This can easily be proved by using the convolution expression for $\mathbf{y}(n)$ and the definition of the power spectral density. Details are omitted.

We know that the autocorrelation of $\mathbf{x}(n)$ is given by

$$\mathbf{R_{xx}}(n) = \mathbf{\Lambda}\delta(n) \qquad (4.5.1.9).$$

Thus the power spectral density of $\mathbf{x}(n)$ is given by

$$\mathbf{S_{xx}}(e^{j\omega}) = \mathbf{\Lambda} \qquad (4.5.1.10)$$

We obtain $\mathbf{g}(n)$ by passing $\mathbf{x}(n)$ through a linear filter with impulse response $\mathbf{A}\delta(n)$ or equivalently, a frequency response of $\mathbf{A}$. Thus we have

$$\mathbf{S_{gg}}(e^{j\omega}) = \mathbf{A\Lambda A}^{T}. \qquad (4.5.1.11)$$

The power spectral density of $\mathbf{w}(n)$ is given by

$$\mathbf{S_{ww}}(e^{j\omega}) = \mathbf{H}(e^{j\omega})\mathbf{A\Lambda A}^{T}\mathbf{H}^{\dagger}(e^{j\omega}) \qquad (4.5.1.12)$$

Thus, the correlation matrix at zero lag of $\mathbf{w}(n)$ is obtained as

$$\mathbf{R_w} = \mathbf{R_{ww}}(0) = \frac{1}{2\pi}\int_{-\pi}^{\pi} \mathbf{H}(e^{j\omega})\mathbf{A\Lambda A}^{T}\mathbf{H}^{\dagger}(e^{j\omega})d\omega. \qquad (4.5.1.13)$$

In order to guarantee that this matrix is non-singular, we assume a modicum of white noise with a power spectral density of σ^2 to be present along with the crosstalk noise at the output of the loop. At the input to the postfilter $\mathbf{B}$, the contribution of this white noise is a colored noise component which is obtained by passing the white noise through the receive filters and sampling the result. We denote the correlation matrix of this noise for a white noise power spectral density of unity to be $\mathbf{R}$. Since $\mathbf{R}$ is the correlation matrix of a real wide-sense stationary process, it is symmetric,

Toeplitz and, in general, non-singular. This gives us an equivalent noise correlation matrix of

$$\mathbf{R_w} = \frac{1}{2\pi}\int_{-\pi}^{\pi} \mathbf{H}(e^{j\omega})\mathbf{A}\mathbf{\Lambda}\mathbf{A}^T\mathbf{H}^\dagger(e^{j\omega})d\omega + \sigma^2\mathbf{R}. \qquad (4.5.1.14)$$

We observe that the noise correlation matrix depends on the prefilter $\mathbf{A}$ and the input correlation matrix $\mathbf{\Lambda}$. In later sections, we shall see how to find the optimum filter and the optimum input powers to satisfy a certain criterion.

4.5.2 Wide-Sense Stationary Crossstalk

When there is a lack of synchronization between loops in a binder group, the crosstalk noise is no longer cyclostationary. In this case we make the assumption that the phases of the block inputs from the interfering transmitters are randomized and that the randomization is so that the interfering process can be represented as $\hat{\eta}(t) = \eta(t-\theta)$ where θ is a random variable with a uniform probability density in $(0, MT)$. Since $\eta(t)$ is cyclostationary with period MT, it follows that $\hat{\eta}(t)$ is a wide-sense stationary process. A proof of this well-known result can be found in [4].

We now attempt to find the correlation matrix of the crosstalk noise $\mathbf{w}(n)$ in this case. In the derivation, we shall freely assume that integrations and summations can be interchanged at any point, without worrying about the mathematics behind such interchanges. First, we find the power spectral density of the process $\hat{\eta}(t)$. From [4], we have

$$R_{\hat{\eta}\hat{\eta}}(\tau) = \frac{1}{MT}\int_0^{MT} E[\eta(t)\eta(t+\tau)]dt \qquad (4.5.2.1)$$

By the definition of $\eta(t)$, we have

$$R_{\hat{\eta}\hat{\eta}}(\tau) = \frac{1}{MT}\int_0^{MT} E\Big[\sum_{m=-\infty}^{\infty}\sum_{n=-\infty}^{\infty} g(n)g(m)p(t-nT)p(t+\tau-mT)\Big]dt \qquad (4.5.2.2)$$

We set $m = n+q$ and $t - nT = v$ to get

$$R_{\hat{\eta}\hat{\eta}}(\tau) = \frac{1}{MT}\sum_{n=-\infty}^{\infty}\int_{v=-nT}^{(M-n)T}\sum_{q=-\infty}^{\infty} E\big[g(n)g(n+q)\big]p(v)p(v+\tau-qT)dv. \qquad (4.5.2.3)$$

We now rewrite n as $mM + l$ where $0 \leq l \leq M-1$. Thus the summation over n becomes a double summation over m and l. We thus have

$$R_{\hat{\eta}\hat{\eta}}(\tau) = \frac{1}{MT} \sum_{l=0}^{M-1} \sum_{m=-\infty}^{\infty} \int_{-mM-l}^{M-mM-l} \sum_{q=-\infty}^{\infty} \Big(E\big[g(mM+l)g(mM+l+q)\big] p(v)p(v+\tau-qT) \Big) dv. \tag{4.5.2.4}$$

Using the wide-sense cyclostationary property of $g(n)$, we obtain

$$R_{\hat{\eta}\hat{\eta}}(\tau) = \frac{1}{MT} \sum_{l=0}^{M-1} \sum_{m=-\infty}^{\infty} \int_{-mM-l}^{M-mM-l} \sum_{q=-\infty}^{\infty} E\big[g(l)g(l+q)\big] p(v)p(v+\tau-qT) dv \tag{4.5.2.5}$$

which can be expressed as

$$R_{\hat{\eta}\hat{\eta}}(\tau) = \frac{1}{MT} \sum_{l=0}^{M-1} \int_{-\infty}^{\infty} \sum_{q=-\infty}^{\infty} E\big[g(l)g(l+q)\big] p(v)p(v+\tau-qT) dv \tag{4.5.2.6}$$

Equivalently, we have

$$R_{\hat{\eta}\hat{\eta}}(\tau) = \sum_{q=-\infty}^{\infty} \left[\frac{1}{M} \sum_{l=0}^{M-1} E\big[g(l)g(l+q)\big] \right] \frac{1}{T} \int_{-\infty}^{\infty} p(v)p(v+\tau-qT) dv. \tag{4.5.2.7}$$

We note that this expression depends only on τ, which is indicative of the process being wide-sense stationary.

By the same argument, we have, for the crosstalk noise at the sampler,

$$R_{WW}(\tau) = \sum_{q=-\infty}^{\infty} \left[\frac{1}{M} \sum_{l=0}^{M-1} E\big[g(l)g(l+q)\big] \right] \frac{1}{T} \int_{-\infty}^{\infty} h(v)h(v+\tau-qT) dt \tag{4.5.2.8}$$

where, as stated before, $h(t)$ is the impulse response of the cascade of the transmit filters, the crosstalk transfer function and the receive filters. The sampled version of $W(t)$ is $w(n)$, which is multiplexed to obtain the noise vector $\mathbf{w}(n)$ at the input of the postfilter $\mathbf{B}$. We now state, without proof, that the sampled version of a

continuous time WSS process is wide-sense stationary in discrete time. For a proof, we refer the reader to [4]. The autocorrelation function of $w(n)$ is given by

$$R_{ww}(n) = \sum_{q=-\infty}^{\infty} \left[\frac{1}{M} \sum_{l=0}^{M-1} E[g(l)g(l+q)] \right] R_h(n-q) \tag{4.5.2.9}$$

where

$$R_h(m) = \frac{1}{T} \int_{-\infty}^{\infty} h(v)h(v+mT)dt \tag{4.5.2.10}$$

We note that $w(n)$ is obtained by passing a discrete-time WSS process $\hat{g}(n)$ with autocorrelation function

$$R_{\hat{g}\hat{g}}(n) = \left[\frac{1}{M} \sum_{l=0}^{M-1} E[g(l)g(l+n)] \right]$$

through a transfer function $\hat{h}(n)$ which is the impulse response corresponding to a spectral factor [4] of

$$S_{\hat{h}}(e^{j\omega}) = \sum_{n=-\infty}^{\infty} R_{\hat{h}}(n)e^{-j\omega n}.$$

The vector process $\mathbf{w}(n)$ which is given by

$$\mathbf{w}(n) = [w(Mn), w(Mn-1), \ldots, w(Mn-M+1)]^T \tag{4.5.2.11}$$

is the noise input to the postfilter $\mathbf{B}$. $\mathbf{w}(n)$ can be equivalently obtained by passing the vector process

$$\hat{\mathbf{g}}(n) = [\hat{g}(Mn), \hat{g}(Mn-1), \ldots, \hat{g}(Mn-M+1)]^T$$

through the transfer matrix [6]

$$\hat{\mathbf{H}}(z) = \begin{pmatrix} \hat{H}_0(z) & \hat{H}_1(z) & \ldots & \ldots & \hat{H}_{M-1}(z) \\ z^{-1}\hat{H}_{M-1}(z) & \hat{H}_0(z) & \hat{H}_1(z) & \ldots & \hat{H}_{M-2}(z) \\ \vdots & \vdots & \ddots & \ddots & \vdots \\ z^{-1}\hat{H}_1(z) & z^{-1}\hat{H}_2(z) & \ldots & \ldots & \hat{H}_0(z) \end{pmatrix} \tag{4.5.2.12}$$

The correlation matrix at zero lag of the noise vector $\mathbf{w}(n)$ is given by

$$\mathbf{R}_{\mathbf{w}} = \frac{1}{2\pi} \int_{-\pi}^{\pi} \hat{\mathbf{H}}(e^{j\omega})\mathbf{S}_{\hat{\mathbf{g}}}(e^{j\omega})\hat{\mathbf{H}}^{\dagger}(e^{j\omega})d\omega. \tag{4.5.2.13}$$

The power spectral density matrix $\mathbf{S}_{\hat{\mathbf{g}}}(e^{j\omega})$ of the vector process $\hat{\mathbf{g}}(n)$ is the discrete-time Fourier transform of its autocorrelation matrix sequence, which is given by

$$\mathbf{R}_{\hat{\mathbf{g}}}(n) = E\big[\hat{\mathbf{g}}(m)\hat{\mathbf{g}}^T(m+n)\big]. \tag{4.5.2.14}$$

Expressing this in terms of the autocorrelation sequence of the scalar process $\hat{g}(n)$, we have

$$\mathbf{R}_{\hat{\mathbf{g}}}(n) = \begin{pmatrix} R_{\hat{g}\hat{g}}(Mn) & R_{\hat{g}\hat{g}}(Mn+1) & \dots & R_{\hat{g}\hat{g}}(Mn+M-1) \\ R_{\hat{g}\hat{g}}(Mn-1) & R_{\hat{g}\hat{g}}(Mn) & \dots & R_{\hat{g}\hat{g}}(Mn+M-2) \\ \vdots & \vdots & \ddots & \vdots \\ R_{\hat{g}\hat{g}}(Mn-M+1) & R_{\hat{g}\hat{g}}(Mn-M+2) & \dots & R_{\hat{g}\hat{g}}(Mn) \end{pmatrix} \tag{4.5.2.15}$$

which is a Toeplitz matrix.

In our case, we have

$$R_{\hat{g}\hat{g}}(n) = \left[\frac{1}{M}\sum_{l=0}^{M-1} E[g(l)g(l+n)]\right]. \tag{4.5.2.16}$$

We also know that $E[g(l)g(l+n)]$ is non-zero only if both l and $l+n$ are in $[0, M-1]$, since $g(n)$ is correlated only within blocks. Thus $R_{\hat{g}\hat{g}}(n)$ is non-zero only for $-(M-1) \leq n \leq M-1$. Hence, the autocorrelation matrix sequence of the vector process $\hat{\mathbf{g}}(n)$ has only three terms, those corresponding to $n = -1, 0, 1$. These matrices are given by

$$\mathbf{R}_{\hat{\mathbf{g}}}(0) = \frac{1}{M}\begin{pmatrix} r(0) & r(1) & r(2) & \dots & r(M-1) \\ r(1) & r(0) & r(1) & \dots & r(M-2) \\ \vdots & \vdots & \vdots & \ddots & \vdots \\ r(M-1) & r(M-2) & r(M-3) & \dots & r(0) \end{pmatrix} \tag{4.5.2.17}$$

and

$$\mathbf{R}_{\hat{\mathbf{g}}}(1) = \frac{1}{M}\begin{pmatrix} 0 & 0 & 0 & \dots & 0 \\ r(M-1) & 0 & 0 & \dots & 0 \\ r(M-2) & r(M-1) & 0 & \dots & 0 \\ r(M-3) & r(M-2) & r(M-1) & \dots & 0 \\ \vdots & \vdots & \vdots & \ddots & \vdots \\ r(1) & r(2) & r(3) & \dots & 0 \end{pmatrix}, \tag{4.5.2.18}$$

where

$$r(k) = \sum_{i=0}^{M-1-k} E[g_i(n)g_{i+k}(n)]. \tag{4.5.2.19}$$

The other autocorrelation matrix coefficient is given by

$$\mathbf{R}_{\hat{\mathbf{g}}}(-1) = \mathbf{R}_{\hat{\mathbf{g}}}{}^T(1). \tag{4.5.2.20}$$

We have the autocorrelation matrix of $\mathbf{g}(n)$ to be given by

$$\begin{aligned}\mathbf{R}_{\mathbf{g}} &= \mathbf{A}\mathbf{\Lambda}\mathbf{A}^T \\ &= \begin{pmatrix} E[g_0^2(n)] & E[g_0g_1(n)] & \dots & E[g_0(n)g_{M-1}(n)] \\ E[g_0g_1(n)] & E[g_1^2(n)] & \dots & E[g_1(n)g_{M-1}(n)] \\ \vdots & \vdots & \ddots & \vdots \\ E[g_0(n)g_{M-1}(n)] & E[g_1(n)g_{M-1}(n)] & \dots & E[g_{M-1}^2(n)] \end{pmatrix}.\end{aligned} \tag{4.5.2.21}$$

We want to express the autocorrelation matrix coefficients of $\hat{\mathbf{g}}(n)$ in terms of $\mathbf{R}_{\mathbf{g}}$. This can be done as follows:

$$\mathbf{R}_{\hat{\mathbf{g}}}(0) = \frac{1}{M}\left[\mathbf{R}_{\mathbf{g}} + \sum_{k=1}^{M-1} \mathbf{P}_k\mathbf{R}_{\mathbf{g}}\mathbf{P}_k^T + \sum_{k=1}^{M-1} \mathbf{P}_k^T\mathbf{R}_{\mathbf{g}}\mathbf{P}_k\right] \tag{4.5.2.22}$$

where $\mathbf{P}_k$ is defined such that

$$\begin{aligned}(\mathbf{P}_k)_{i,i+k} &= 1 \qquad 0 \le i \le M-1-k \\ (\mathbf{P}_k)_{i,j} &= 0 \quad \text{otherwise.}\end{aligned} \tag{4.5.2.23}$$

We also have

$$\mathbf{R}_{\hat{\mathbf{g}}}(1) = \frac{1}{M}\sum_{k=1}^{M-1} \mathbf{U}_k\mathbf{R}_{\mathbf{g}}\mathbf{V}_k \tag{4.5.2.24}$$

where, for $0 \le i, j \le M-1$,

$$\begin{aligned}(\mathbf{V}_k)_{i,j} &= 1 \qquad \text{if } i+j = k-1 \\ &= 0 \qquad \text{otherwise}\end{aligned} \tag{4.5.2.25}$$

and

$$\begin{aligned}(\mathbf{U}_k)_{i,j} &= 1 \qquad \text{if } i+j = M+k-1 \\ &= 0 \qquad \text{otherwise.}\end{aligned} \tag{4.5.2.26}$$

Equations (4.5.2.22) and (4.5.2.24) can be proved simply by direct substitution and we shall not go into the proofs. The interested reader may convince himself of these identities by trying some simple examples.

The power spectral density matrix $\mathbf{S}_{\hat{\mathbf{g}}}(e^{j\omega})$ of the vector process $\hat{\mathbf{g}}(n)$ is thus given by

$$\mathbf{S}_{\hat{\mathbf{g}}}(e^{j\omega}) = \mathbf{R}_{\hat{\mathbf{g}}}(0) + e^{-j\omega}\mathbf{R}_{\hat{\mathbf{g}}}(1) + e^{j\omega}\mathbf{R}_{\hat{\mathbf{g}}}{}^{T}(1). \tag{4.5.2.27}$$

The correlation matrix at lag zero of the noise process at the input to the postfilter $\mathbf{B}$ is given by

$$\mathbf{R}_{\mathbf{w}} = \frac{1}{2\pi}\int_{-\pi}^{\pi}\Big[\hat{\mathbf{H}}(e^{j\omega})\mathbf{R}_{\hat{\mathbf{g}}}(0)\hat{\mathbf{H}}^{\dagger}(e^{j\omega}) + e^{-j\omega}\hat{\mathbf{H}}(e^{j\omega})\mathbf{R}_{\hat{\mathbf{g}}}(1)\hat{\mathbf{H}}^{\dagger}(e^{j\omega}) + \hat{\mathbf{H}}(e^{j\omega})\mathbf{R}_{\hat{\mathbf{g}}}{}^{T}(1)\hat{\mathbf{H}}^{\dagger}(e^{j\omega})e^{j\omega}\Big]d\omega. \tag{4.5.2.28}$$

Hence we have

$$\mathbf{R}_{\mathbf{w}} = \frac{1}{M}\frac{1}{2\pi}\int_{-\pi}^{\pi}\Big[\hat{\mathbf{H}}(e^{j\omega})\big[\mathbf{A}\mathbf{\Lambda}\mathbf{A}^{T} + \sum_{k=1}^{M-1}\mathbf{P}_k\mathbf{A}\mathbf{\Lambda}\mathbf{A}^{T}\mathbf{P}_k^{T} + \mathbf{P}_k^{T}\mathbf{A}\mathbf{\Lambda}\mathbf{A}^{T}\mathbf{P}_k + e^{-j\omega}\mathbf{U}_k\mathbf{A}\mathbf{\Lambda}\mathbf{A}^{T}\mathbf{V}_k + e^{j\omega}\mathbf{V}_k\mathbf{A}\mathbf{\Lambda}\mathbf{A}^{T}\mathbf{U}_k\big]\hat{\mathbf{H}}^{\dagger}(e^{j\omega})\Big]d\omega. \tag{4.5.2.29}$$

Thus we have an expression for $\mathbf{R}_{\mathbf{w}}$ in terms of $\mathbf{A}$ and $\mathbf{\Lambda}$. We shall use this expression in a later section to find the optimum prefilter $\mathbf{A}$, which, as we know, is a matrix of the eigenvectors of the matrix $\mathbf{C}_1\mathbf{R}_{\mathbf{w}}{}^{-1}\mathbf{C}_1$. In this case too, we assume the presence of white noise at the output of the loop in addition to the crosstalk noise.

4.6 Derivation of the Optimum Filters

In this section, we shall derive the optimum filters to be used for block data transmission over the local loop, with the main impairment being crosstalk. We shall derive the results in detail for the cyclostationary crosstalk case; the extension to the wide-sense stationary crosstalk case is straightforward.

The criterion we use to define the optimality of the system is the throughput of the system or the data rate, given a constant probability of error and a constraint on the input power. Stated differently, we want to restrict the input power to P and maintain a constant probability of error P_e on all channels, while maximizing the total number of bits transmitted per block of symbols.

For a given signal set, the minimum distance of the signal set and the noise variance at the output of the channel have to satisfy

$$20\log_{10}\left(\frac{d_{\min}}{2\sigma}\right) \geq 13.5\text{dB} \tag{4.6.1}$$

in order to achieve a probability of error of less than 10^{-6}. Hence, in order to maintain a probability of error lower than 10^{-6}, we require

$$\frac{d^2}{4\sigma^2} = 10^{1.35} = K. \tag{4.6.2}$$

If we use a PAM signal set, the average energy of the symbols can be expressed in terms of the number of levels used, m, and the distance between the levels, d. The relationship is

$$E = \frac{(m^2-1)d^2}{12}. \tag{4.6.3}$$

Coded modulation schemes or trellis codes increase the distance between the transmitted levels, but the price to be paid is the higher number of levels being used. For example, a 4-dimensional 16 state code [7] increases the squared minimum distance by a factor of 4, while doubling the number of levels in the constellation. Thus, d^2 is replaced by $4d^2$ and m by $2^{1/4}m$ for this code, in the expression for energy in terms of minimum distance and the number of levels. While using a trellis code, there is

an additional contribution to the probability of error due to an increased number of nearest neighbors, but we neglect this contribution to a first order approximation at low error rates.

While using the aforementioned trellis code over a channel with output energy E_i and an output noise variance of σ_i^2, we require, as a consequence of equation (4.6.3),

$$\frac{4d_i^2}{4\sigma^2} = \frac{12E_i}{\sigma_i^2(2^{1/2}m_i^2 - 1)} = K. \tag{4.6.4}$$

Here, we see that the number of levels at the output of the channel per dimension is $2^{1/4}m_i$ and the minimum distance has been increased by a factor of 2. Thus the number of signal points m_i is given by

$$m_i^2 = 2^{-1/2}\left(1 + \frac{12E_i}{K\sigma_i^2}\right). \tag{4.6.5}$$

Therefore, the number of bits which can be transmitted per symbol over this channel, while maintaining a probability of error of 10^{-6}, is given by

$$b_i = \log_2 m_i = \frac{1}{2}\log_2\left(1 + \frac{12E_i}{K\sigma_i^2}\right) - 1/4. \tag{4.6.6}$$

In the previous chapter, we derived the gains and the noise variances of the subchannels formed by the block transmission technique described in that chapter. These are repeated here. With the eigenvalues of the matrix $\mathbf{C_1}^T\mathbf{R_w}^{-1}\mathbf{C_1}$ being denoted by γ_i, and the input powers to the corresponding channels being λ_i, the gains of the channels are given by

$$g_i = \frac{\lambda_i\gamma_i}{(1 + \lambda_i\gamma_i)} \tag{4.6.7}$$

and

$$\sigma_i^2 = \frac{\lambda_i^2\gamma_i}{(1 + \lambda_i\gamma_i)^2}. \tag{4.6.8}$$

Thus, over such a channel, the number of bits that can be transmitted with a probability of error of 10^{-6} using the 4-d 16-state trellis code is given by

$$b_i = \frac{1}{2}\log_2\left(1 + \frac{12\lambda_i\gamma_i}{K}\right) - 1/4 \tag{4.6.9}$$

which we rewrite as

$$b_i = \frac{1}{2}\log_2\left(1 + \frac{\lambda_i \gamma_i}{K_1}\right) - 1/4. \tag{4.6.9}$$

This formula for the throughput assumes that the noise is Gaussian, which may not seem to be a very valid assumption for crosstalk noise; however, we can assume that the crosstalk noise is Gaussian by appealing to the central limit theorem. The crosstalk noise is obtained by passing a set of random variables through various linear filters, thereby involving numerous summations of the random variables; the resultant random variables are close to Gaussian.

Since the subchannels formed by the block transmission scheme are independent, the total throughput of a block is simply the sum of the throughputs of the individual subchannels, and is given by

$$\begin{aligned} R_{total} &= \sum_{i=1}^{M} b_i \\ &= \sum_{i=1}^{M} \left[\frac{1}{2}\log_2\left(1 + \frac{\lambda_i \gamma_i}{K_1}\right) - 1/4\right] \end{aligned} \tag{4.6.10}$$

We note that if the input power to a certain subchannel is zero, then no bits are transmitted over it, thereby transcending the need to double the number of levels required in the trellis code. In this case, the extra 1/4 bits of redundancy will not figure in the throughput. We want to maximize this throughput under the condition that the input energy be constrained to some P. We had solved essentially the same problem earlier in Section 3.4 while finding the capacity of the block transmission scheme over an ISI channel with white noise. Using the same techniques, we obtain

$$\frac{\gamma_i}{K_1 + \lambda_i \gamma_i} + \mu \leq 0 \tag{4.6.11}$$

with equality if λ_i is non-zero. Here μ is a Lagrange multiplier, and is chosen so that the power constraint is satisfied. Let U be the set of indices for which λ_i is non-zero. Then we have, for these indices,

$$\lambda_i = \frac{1}{|U|}(P + K_1 \sum_{l \in U} \frac{1}{\gamma_l}) - \frac{K_1}{\gamma_i}. \tag{4.6.12}$$

We note that for a real transmission system, the number of bits transmitted per PAM symbol will have to be a quarter-integer (while using a 4-d code), hence the optimization has to be over quarter-integer values, which makes the problem computationally quite complex. Hence, we shall find a real solution and perform round-off operations to obtain sub-optimum integer solutions.

In the last section, we had derived the correlation matrix $\mathbf{R_w}$ of the noise at the input of the postfilter. With the crosstalk noise being cyclostationary, this matrix was given by

$$\mathbf{R_w} = \frac{1}{2\pi}\int_{-\pi}^{\pi} \mathbf{H}(e^{j\omega})\mathbf{A}\mathbf{\Lambda}\mathbf{A}^T\mathbf{H}^\dagger(e^{j\omega})d\omega + \sigma^2\mathbf{R} \tag{4.6.13}$$

Using Parseval's theorem, this expression can be rewritten as

$$\mathbf{R_w} = \sum_{n=0}^{\infty} \mathbf{h}(n)\mathbf{A}\mathbf{\Lambda}\mathbf{A}^T\mathbf{h}^T(n) + \sigma^2\mathbf{R} \tag{4.6.14}$$

where $\mathbf{h}(n)$ is the matrix impulse response sequence corresponding to the matrix transfer function $\mathbf{H}(e^{j\omega})$, and is assumed to be causal, i.e., it is zero for negative n. We require the prefilter $\mathbf{A}$ to be the orthogonal matrix that diagonalizes $\mathbf{C}_1^T{\mathbf{R_w}}^{-1}\mathbf{C}_1$. In other words, we want

$$\mathbf{A}^T\mathbf{C}_1^T\left(\sum_{n=0}^{\infty} \mathbf{h}(n)\mathbf{A}\mathbf{\Lambda}\mathbf{A}^T\mathbf{h}^T(n) + \sigma^2\mathbf{R}\right)^{-1}\mathbf{C}_1\mathbf{A} = \mathbf{\Gamma} \tag{4.6.15}$$

where we require the λ_i's and the γ_i's to satisfy equation (4.6.12). By taking the inverse of both sides in equation (4.6.15), we obtain

$$\sum_{n=0}^{\infty} \mathbf{h}(n)\mathbf{A}\mathbf{\Lambda}\mathbf{A}^T\mathbf{h}^T(n) + \sigma^2\mathbf{I} = \mathbf{C}_1\mathbf{A}\mathbf{\Gamma}^{-1}\mathbf{A}^T\mathbf{C}_1^T \tag{4.6.16}$$

We note that $\mathbf{\Gamma}^{-1}$ exists due to the fact that $\mathbf{R_w}$ is non-singular.

We first consider the special case when the set of indices U with $\lambda_i > 0$ is the whole set $i = 1, 2, \ldots M$. In this case, we have

$$\lambda_i = \frac{1}{M}(P + K_1\sum_{l=1}^{M}\frac{1}{\gamma_l}) - \frac{K_1}{\gamma_i} \tag{4.6.17}$$

and thus

$$\mathbf{\Lambda} = \frac{1}{M}(P + K_1 Tr[\mathbf{\Gamma}^{-1}])\mathbf{I} - \mathbf{\Gamma}^{-1}. \tag{4.6.18}$$

If we denote

$$\mathbf{Q} = \mathbf{A}\mathbf{\Gamma}^{-1}\mathbf{A}^T \tag{4.6.19},$$

we find that equation (4.6.16) can be rewritten as

$$\sum_{n=0}^{\infty} \mathbf{h}(n)\left(\frac{1}{M}(P + K_1 Tr[\mathbf{Q}])\mathbf{I} - K_1\mathbf{Q}\right)\mathbf{h}^T(n) + \sigma^2\mathbf{R} = \mathbf{C}_1\mathbf{Q}\mathbf{C}_1^T, \tag{4.6.20}$$

where we have used the invariance of the trace of a matrix product to cyclic permutations to obtain

$$\begin{aligned} Tr[\mathbf{Q}] &= Tr[\mathbf{A}\mathbf{\Gamma}^{-1}\mathbf{A}^T] \\ &= Tr[\mathbf{\Gamma}^{-1}\mathbf{A}^T\mathbf{A}]. \\ &= Tr[\mathbf{\Gamma}^{-1}] \end{aligned}$$

By the definition of the trace of a matrix, we have

$$Tr[\mathbf{Q}] = \sum_{i=1}^{M} q_{ii}. \tag{4.6.21}$$

Hence, it is evident that equation (4.6.16) gives us a set of linear equations in the elements of $\mathbf{Q}$, which can be solved in a straightforward manner to obtain $\mathbf{Q}$. Once $\mathbf{Q}$ is obtained, finding the prefilter $\mathbf{A}$ and the λ_i boils down to a simple matter of calculating the eigenvalues and the eigenvectors of $\mathbf{Q}$.

When the optimality conditions force some of the λ_i's to be zero, however, the problem becomes much more involved. We do not have an exact solution for this case, but we present an algorithm to determine the solution. We do not have a definitive proof of the convergence of this algorithm, but it did converge in a wide variety of examples. We do present an incomplete proof of the existence of a solution.

The proposed algorithm to determine the optimum $\mathbf{A}$ and the λ_i is as follows:

Initialization: Determine $\mathbf{Q}$ using equation (6.6.16). Let

$$\mathbf{Q} = \mathbf{V}\mathbf{\Gamma}^{-1}\mathbf{V}^T$$

where γ_i^{-1} are the eigenvalues of $\mathbf{Q}$ and $\mathbf{V}$ is a unitary matrix of the eigenvectors of $\mathbf{Q}$. Calculate

$$\mathbf{Q}_1 = \frac{1}{M}(P + K_1 Tr[\mathbf{Q}])\mathbf{I} - K_1\mathbf{Q}$$

We have

$$\mathbf{Q}_1 = \mathbf{V}\mathbf{\Lambda}\mathbf{V}^T$$

where

$$\lambda_i = \frac{1}{M}(P + K_1 \sum_{l=1}^{M} \gamma_l^{-1}) - K_1\gamma_i^{-1}.$$

If $\lambda_i \geq 0$ for all I, then we have a solution, hence we terminate the process. Otherwise, we define $\mathbf{Q}_2 = (P/M)\mathbf{I}$.

Step 2: Set $\mathbf{Q}_1 = \mathbf{Q}_2$. Determine $\mathbf{Q}$ using

$$\sum_{n=0}^{\infty} \mathbf{h}(n)\mathbf{Q}_2\mathbf{h}^T(n) + \sigma^2\mathbf{R} = \mathbf{C}_1\mathbf{Q}\mathbf{C}_1^T.$$

Step 3: Find the eigenvalues γ_i^{-1} and the unitary diagonalizing matrix $\mathbf{V}$ of $\mathbf{Q}$.

Step 4: find λ_i using

$$\frac{\gamma_i}{K_1 + \lambda_i\gamma_i} + \mu \leq 0$$

with equality if λ_i is non-zero. For $i \in U$, the set of indices where λ_i is non-zero,

$$\lambda_i = \frac{1}{|U|}(P + K_1 \sum_{l \in U} \frac{1}{\gamma_l}) - \frac{K_1}{\gamma_i}$$

Step 4 : Determine

$$\mathbf{Q}_2 = \mathbf{V}\mathbf{\Lambda}\mathbf{V}^T$$

If

$$\text{norm}(\mathbf{Q}_2 - \mathbf{Q}_1) < \text{some } \epsilon,$$

Stop. Otherwise, go back to Step 2.

An incomplete, pseudo-proof of the existence of a solution using the above algorithm can be presented as follows. We note that at any stage, $\mathbf{Q}_1$ and $\mathbf{Q}_2$ are

both positive semi-definite matrices with a trace equal to P. Steps 2 through 4 of the algorithm present a mapping $\mathbf{Q}_2 \rightarrow \mathbf{Q}_1$, i.e., a mapping from the set of positive semi-definite matrices with trace P to itself. This set can be shown to be closed, convex and bounded. The mapping $\mathbf{Q}_2 \rightarrow \mathbf{Q}_1$ can be shown to be continuous if the eigenvalues of $\mathbf{Q}$ are distinct at any stage; this implies, in most cases, that both the eigenvalues and eigenvectors of $\mathbf{Q}$ are continuous functions of a perturbation [8]. Thus we can apply a variant of the Brouwer fixed point theorem [9], which states that a continuous mapping from a closed, bounded convex set to itself has a fixed point. This theorem implies that there exists a $\mathbf{Q}_1$ equal to its $\mathbf{Q}_2$, which implies that we have a solution to our problem.

For the wide-sense stationary crosstalk case, we have a very analogous situation, except that the expression for the noise correlation matrix as a function of the input correlation matrix $\mathbf{A}\Lambda\mathbf{A}^T$ is far more complicated. Nevertheless, the same techniques and the same algorithm as described above apply to the wide-sense stationary crosstalk case too.

4.7 Numerical Results

We numerically obtained the performance of the optimum block transmission methods over some of the loops, data on whose impulse responses was provided by Bellcore. As stated before, the loop was padded with a transformer, a Butterworth lowpass filter to 320kHz and a rectangular pulse shaper of duration 1.5625 μs at the transmitter side. At the receiver side, we have a transformer and a Butterworth lowpass filter.

From the plot of the impulse response of the loop in Fig. 6.2, it can be seen that the impulse response is low up to a certain time whereafter it is quite high. It would certainly be preferable to have an impulse response coefficient matrix whose entries are high so as to obtain maximum signal power at the output. Hence we have to take into account the ISI due to the previous impulse response coefficients. These are referred to as the *precursor*. The ISI due to the *postcursor*, or the portion

of the impulse response *after* the ones in the impulse response coefficient matrix, is taken care of by the decision feedback equalizer. Interestingly, the techniques described in this chapter make it very simple to take the precursor into account. This procedure is described in Appendix 6.A.1. While optimizing the prefilter and the postfilter, the precursor term adds another term to the noise, and this term has essentially the same form as cyclostationary crosstalk. In all our simulations, the precursor was taken into account.

We first compare the performance with synchronization between adjacent loops, i.e., the crosstalk noise is cyclostationary, and without synchronization between adjacent loops, which implies that the crosstalk noise is wide-sense stationary. We performed these simulations over the 12kft, 24 gauge loop, with an input power limitation per transmitted symbol. When the noise is the dominant impairment, we found that both schemes gave essentially the same throughput. However, when the noise is low enough so that crosstalk is the dominant impairment, the throughput under the assumption of cyclostationary crosstalk was higher than the throughput for the wide-sense stationary crosstalk noise case. However, the difference in performance was just of the order of a few percent in the cases simulated. Hence, we tentatively state one of the main results: Synchronization does not appear to get us a whole lot. The model used for the crosstalk is the one in equation (6.4.1), with values for the various parameters being taken from [11]. Eight parallel channels were used in these calculations.

The results for this simulation are shown in Table 4.1 and Table 4.2. In Table 4.1, we show the comparative throughputs of the scheme for the two cases of crosstalk noise for different transmission schemes ranging from simple PAM to the most complicated one that achieves capacity. The input power is assumed to be 10mW and the variance of the white noise is assumed to be 10^{-14}W/Hz. In Table 4.2, we show similar results when using an input power of 20mW. This is equivalent to using a lower noise variance, since an increase in input power also increases the crosstalk noise by the same amount. We note that in addition to coding gain, the

use of a high dimensional code gives us the ability to transmit a fractional number of bits per dimension on each channel. For a further discussion of this aspect, see [10]. We find that the throughputs are slightly higher in the case of cyclostationary crosstalk but the difference in throughput is not very high. This indicates that there is not a whole lot to be gained in terms of throughput by synchronizing transmission on different loops in the same binder group. In Tables 4.3 and 4.4, we present similar results for a different crosstalk transfer function for a 9kft, 26-gauge loop. The impulse responses for this latter case were obtained experimentally by Dr.D. D. Falconer's research group at Carleton University, Ottawa, Canada. We acknowledge the help of Brent Petersen of Carleton University in obtaining this data.

Scheme Used	CSS Crosstalk	WSS Crosstalk
PAM	960 Kb/s	960 Kb/s
$4-d$ Trellis Code	1.48 Mb/s	1.48 Mb/s
$8-d$ Trellis Code	1.58 Mb/s	1.58 Mb/s
Capacity	1.941 Mb/s	1.936 Mb/s

Table 4.1. Throughputs over the 12kft,24-gauge loop with 10mW Input Power and Two Cases of Crosstalk

Scheme Used	CSS Crosstalk	WSS Crosstalk
PAM	960 Kb/s	960 Kb/s
$4-d$ Trellis Code	1.52 Mb/s	1.5 Mb/s
$8-d$ Trellis Code	1.63 Mb/s	1.61 Mb/s
Capacity	1.982 Mb/s	1.971 Mb/s

Table 4.2. Throughputs over the 12kft,24-gauge loop with 20mW Input Power and Two Cases of Crosstalk

Scheme Used	CSS Crosstalk	WSS Crosstalk
PAM	880 Kb/s	880 Kb/s
$4-d$ Trellis Code	1.46 Mb/s	1.44 Mb/s
$8-d$ Trellis Code	1.57 Mb/s	1.54 Mb/s
Capacity	1.92 Mb/s	1.89 Mb/s

Table 4.3. Throughputs over the 9kft,26-gauge loop with 10mW Input Power and Two Cases of Crosstalk

Scheme Used	CSS Crosstalk	WSS Crosstalk
PAM	880 Kb/s	880 Kb/s
$4-d$ Trellis Code	1.56 Mb/s	1.49 Mb/s
$8-d$ Trellis Code	1.65 Mb/s	1.58 Mb/s
Capacity	1.99 Mb/s	1.93 Mb/s

Table 4.4. Throughputs over the 9kft,26-gauge loop with 20mW Input Power and Two Cases of Crosstalk

We also determined the throughput with different input power constraints and a squared crosstalk transfer function of $Kf^{3/2}$ with $K = 10^{-13}$ and a white noise power spectral density of 10^{-14}W/Hz. We performed this calculation over two loops the carrier serving area, the 12 kft,24-gauge loop and the 9kft,26-gauge loop. These loops have been reported to be at the lossy end of the carrier serving area. We found that T1 transmission is possible over these loops at nominal input powers by using powerful multidimensional trellis codes. The 4-d,16-state code was used in these calculations.

No. of Channels	12kft,24-gauge loop	9kft,26-gauge loop
8	1.48 Mb/s	1.42 Mb/s
16	1.54 Mb/s	1.51 Mb/s
24	1.56 Mb/s	1.5133 Mb/s

Table 4.5 Throughputs over the two loops
with 10mW Input Power,$Kf^{3/2}$ Crosstalk, $K = 10^{-13}$
using the 4-d, 16-state Trellis Code

No. of Channels	12kft,24-gauge loop	9kft,26-gauge loop
8	1.52 Mb/s	1.48 Mb/s
16	1.6 Mb/s	1.56 Mb/s

Table 4.6 Throughputs over the two loops
with 20mW Input Power,$Kf^{3/2}$ Crosstalk, $K = 10^{-13}$
using the 4-d, 16-state Trellis Code

No. of Channels	12kft,24-gauge loop	9kft,26-gauge loop
8	1.9 Mb/s	1.9 Mb/s
16	2.02 Mb/s	2.03 Mb/s

Table 4.7 Throughputs over the two loops
with 10mW Input Power,$Kf^{3/2}$ Crosstalk, $K = 10^{-14}$
using the 4-d, 16-state Trellis Code

We also calculated the throughputs for the two loops with 24 channels and using an 8-dimensional trellis code, which doubles the minimum distance, while doubling of the number of the levels in 8 dimensions [7]. On the 12kft,24-gauge loop a rate of 1.677 Mb/s could be obtained using this code and the corresponding rate on the 9kft,26-gauge loop was 1.623 Mb/s. These results suggest that T1 transmission can be obtained over a large subset of the carrier serving area by using multidimensional trellis codes.

4.8 Conclusions

In this chapter, we determined the optimum filters for block data transmission over the ISDN subscriber loop. The main impairment over this channel was crosstalk, which depended on the input being transmitted. This led to a joint problem of determining the optimum inputs and the corresponding optimum filters. We considered two cases for the crosstalk noise; when transmission is synchronized on all loops in a binder group, the crosstalk noise is cyclostationary, but with a lack of synchronization, the noise is wide-sense stationary. We characterized the correlation of the crosstalk noise as a function of the input correlation matrix and the crosstalk transfer function in both these cases. For both cases, we presented methods to solve the problem exactly when all subchannels had positive input powers and proposed an iterative solution for the case when the input powers over some of the subchannels were zero.

We found that T1 transmission was possible over some of the most lossy loops in the carrier serving area using input powers of the order of 10mW. We also observed that the throughput was slightly higher when the dominant crosstalk noise is cyclostationary than when it is wide-sense stationary. However, the ensuing improvement in throughput does not seem to justify the effort of synchronizing transmission over the loops.

4.A.1 Appendix: What about Precursors?

In this appendix, we show how the proposed multichannel scheme is equipped to handle precursors. We demonstrate that the interference caused by the precursor is statistically similar to crosstalk noise; hence the techniques we derived in this chapter can be directly applied to derive optimum filters in the presence of precursor ISI.

Let the channel matrix be given by

$$\mathbf{C}(z) = \sum_{i=1}^{K-1} \mathbf{C}_i z^{-i} + \mathbf{C}_K z^{-K} + \sum_{i=K+1}^{\infty} \mathbf{C}_i z^{-i}. \tag{4A1.1}$$

Here $\mathbf{C}_i$, $i = 1, \ldots, K-1$ constitute the precursor, $\mathbf{C}_K$ is the cursor matrix and $\mathbf{C}_i$, $i = K+1, \ldots, \infty$ constitute the postcursor.

The relationship between the input and the output (see Fig. 3.2) is

$$\begin{aligned} \mathbf{v}(n) = &\sum_{k=1}^{K-1} \mathbf{B}\mathbf{C}_\mathbf{k}\mathbf{A}\ \mathbf{x}(n-1) + \sum_{k=K+1}^{\infty} \mathbf{B}\mathbf{C}_\mathbf{k}\mathbf{A}\ \mathbf{x}(n-k) \\ &+\mathbf{B}\mathbf{C}_\mathbf{K}\mathbf{A}\ \mathbf{x}(n-K) + \mathbf{B}\mathbf{w}(n) + \sum_{k=K+1}^{\infty} \mathbf{D}_\mathbf{k}\hat{\mathbf{x}}(n-k). \end{aligned} \tag{4A1.2}$$

We know that $\mathbf{x}(n)$ is correlated within blocks with

$$E[\mathbf{x}(n)\mathbf{x}(m)] = \mathbf{R}_{xx}\delta_{nm}. \tag{4A1.3}$$

If we choose the decision feedback optimally as described in Chapter 3, we can cancel the ISI due to the $\mathbf{C}_\mathbf{k}$'s for $k > K$, i.e., the postcursor. The resulting mean-squared error is given by

$$\mathcal{E} = Tr[(\mathbf{B}\mathbf{C}_\mathbf{K}\mathbf{A} - \mathbf{I})\mathbf{R}_{xx}(\mathbf{B}\mathbf{C}_\mathbf{K}\mathbf{A} - \mathbf{I})^T + \sum_{k=1}^{K-1} \mathbf{B}\mathbf{C}_\mathbf{k}\mathbf{A}\mathbf{R}_{xx}\mathbf{A}^T\mathbf{C}_\mathbf{k}{}^T\mathbf{B}^T + \mathbf{B}\mathbf{R}_w\mathbf{B}^T] \tag{4A1.4}$$

where we have used the fact that $\mathbf{x}(n)$ is correlated only within blocks. This can be rewritten as

$$\mathcal{E} = Tr[(\mathbf{B}\mathbf{C}_\mathbf{K}\mathbf{A} - \mathbf{I})\mathbf{R}_{xx}(\mathbf{B}\mathbf{C}_\mathbf{K}\mathbf{A} - \mathbf{I})^T + \mathbf{B}\Big(\sum_{k=1}^{K-1} \mathbf{C}_\mathbf{k}\mathbf{A}\mathbf{R}_{xx}\mathbf{A}^T\mathbf{C}_\mathbf{k}{}^T + \mathbf{R}_w\Big)\mathbf{B}^T]. \tag{4A1.5}$$

From equation (4A1.5), it seems evident that the interference term due to the precursor adds as an extra noise term. The form of the noise added due to the precursor indicates that it is quite like crosstalk noise. Indeed, a noise vector with such a correlation matrix can be obtained by passing a random process $\mathbf{g}(n)$, one which has the same autocorrelation as $\mathbf{x}(n)$, i.e.,

$$E[\mathbf{g}(n)\mathbf{g}(m)] = \mathbf{R}_{xx}\delta_{nm}, \tag{4A1.3}$$

through a filter with impulse response

$$\begin{aligned} \mathbf{H}(k) &= \mathbf{C}_k, \qquad k = 1, \ldots, K-1 \\ &= 0, \qquad \text{otherwise.} \end{aligned} \tag{4A1.6}$$

Thus, it is evident that the noise due to the precursor can be modeled as a form of crosstalk noise. This chapter has essentially dealt with obtaining the optimum filters in the presence of crosstalk noise, so the same techniques could be applied in the presence of the precursor too.

References

[1] P.Crespo and M. L. Honig, "Pole-Zero Decision Feedback Equalization for the Digital Subscriber Loop," *IEEE Globecom'90 Conference Record*, pp. 1166-1171.

[2] J. W. Lechleider, "Spectrum Management in Telephone Loop Cables, II: Signal Constraints That Depend on Shape," *IEEE Trans. Commun.*, vol. 34, no. 8, pp. 737-743, Aug. 1986.

[3] D. G. Messerschmitt, "Design Issues in the ISDN U-Interface Transceiver," *IEEE JSAC,* vol. SAC-4, no. 8, pp. 1281-1293, Nov. 1986.

[4] Athanasios Papoulis, *Probability, Random Variables, and Stochastic Processes*, McGraw-Hill, 1985.

[5] Vinay Sathe and P. P. Vaidyanathan, "Efffects of Multirate Systems on the Statistical Properties of Random Inputs," presented at the IEEE ICASSP'91, Toronto, Canada, May 1991.

[6] P.P. Vaidyanathan and S.K. Mitra, "Polyphase Networks, Block Digital Filtering, LPTV Systems, and Alias-Free QMF Banks: A Unified Approach Based on Pseudocirculants," *IEEE Trans. on Acoustics, Speech and Signal Processing,* vol. 36, no. 3, pp. 381-391, March 1988.

[7] G. D. Forney Jr., "Coset Codes- Part I: Introduction and Geometrical Classification," *IEEE Trans. on Info. Theory,* vol. 34, no. 5, pp. 1123-1151, Sept. 1988.

[8] L. D. Landau and E. M. Lifshitz, *Quantum Mechanics: Non-Relativistic Theory,* Addison-Wesley Pub. Co., Reading, Mass., 1958.

[9] Joel Franklin, *Methods of Mathematical Economics : Linear and Non-linear Programming, Fixed-Point Theorems*, Springer-Verlag New York Inc., 1980.

[10] J. C. Tu and J. M. Cioffi, "A Loading Algorithm for the Concatenation of Coset Codes with Multichannel Modulation Methods," *IEEE Globecom'90*, Conference Record, pp. 1183-1187.

[11] M. L. Honig, K. Steiglitz and B. Gopinath, "Multichannel Signal Processing for Data Communications in the Presence of Crosstalk," *IEEE Trans. Commun.*, vol. 38, no. 4, pp. 551-558, April 1990.

[12] G. P. Dudevoir, "Equalization Techniques for High Rate Digital Transmission on Spectrally Shaped Channels," Ph.D. Dissertation, Stanford University, Dept. of Electrical Eng., December 1989.

Chapter 5 Conclusions and the Future

The reader will probably heave a sigh of relief, having come to this point in the thesis; the author certainly did. In this *final* chapter, we briefly summarize our results and present suggestions for further work. Our work is barely the tip of the iceberg in an interesting and increasingly important area, and there are a host of problems for future researchers to tackle. This chapter will describe some of the interesting unsolved problems in mathematics and communications that arose in the course of this research.

5.1 Summary and Conclusions

In this thesis, we were mainly concerned with the transmission of data over channels with intersymbol interference and colored noise. Our objective was to derive good transmit and receive filters to improve the efficiency of data transmission over these channels. Motivated by the Water-Pouring Theorem from Information theory, we proposed a parallel multichannel scheme for data transmission over these channels. The basic idea was that by partitioning the input signal into various frequency bands, we could control the signal power in each frequency band, thereby shaping the signal spectrum.

In Chapter 2, we introduced the scheme to be used and derived simple equivalent circuits for the scheme by applying Multirate Signal Processing techniques. This led to an equivalent structure where the prefilter, the postfilter and the channel could be represented as matrix transfer functions. By recognizing this, we were able to propose simple equalization schemes for channels with ISI by using theorems from matrix theory. We demonstrated certain interesting properties of these equalization schemes, and showed how some of their properties could lead to interesting methods of coding over ISI channels. In particular, we showed how codes designed for the $1-D$ channel could be used over the $1+D$ channel. A pleasing aspect of this research is that the tool we used, viz., the Smith Form Decomposition, has hitherto only found application as a theoretical tool, but we have been able to propose a practical application for it.

In Chapter 3, we derived optimum finite-length filters for the transmission of data over channels with ISI and colored noise. We assumed that the prefilters and the postfilters took care of the ISI within a block and we used block decision-feedback equalization to tackle the ISI outside the block. In a sense, the optimum prefilter could be viewed as the Karhunen-Loeve transform of a combination of the channel and noise autocorrelations. We derived the performance of the mutichannel schemes when using the optimal prefilter and postfilter and found that the multichannel scheme was superior in performance to a single channel scheme employing

decision-feedback equalization. We explored the reasons for this improved performance and conjectured that the performance improvement is a result of the spectral shaping obtained due to the scheme.

In Chapter 4, we applied the multichannel scheme to the special case of the ISDN digital subscriber loop channel. This is an ISI channel where the noise is predominantly crosstalk due to adjacent loops in the same binder group. Hence, we had a channel where the noise depended on the transmitted signal. Depending on whether transmission over different loops in the same bundle was synchronized or not, the crosstalk noise could be modeled as cyclostationary or wide-sense stationary. For both these cases, we presented methods to obtain the correlation of the crosstalk noise and showed how to derive the optimum filters and the optimum input power distribution. We then applied these results to some representative loops from a subset of the ISDN subscriber loop called the Carrier Serving Area. We found that T1 transmission over these loops is definitely a feasibility. Also, synchronization between different loops seemed to improve throughput, but not by enough to make it worthwhile.

Our main conclusion is that optimum multichannel techniques seem to be an attractive way of achieving efficiency of transmission over practical channels. We hope that this work will stimulate interest in the application of these techniques to practice and the building of products and services involving these techniques.

5.2 Suggestions for Future Research

In the course of our research, we seem to have unearthed more problems than we could solve. We present a host of problems for future researches to tackle, these problems fall under the realms of mathematics and engineering.

In Chapter 2, we were originally interested in finding good analysis filters and synthesis filters which give a set of independent channels without any crosstalk between the channels and with a reasonably flat frequency response in each of the frequency bands. This problem has been solved as a variation of the QMF problem [1] in [2], but only for the case when the channel in between is ISI-free. Our aim was to generalize this result to the case of a channel with ISI, but we were unsuccessful. This problem remains for future research.

We also notice that our equivalent structure led to a polynomial matrix description of the channel. The Smith Form Decompostion we used was a tool to diagonalize the polynomial matrix, and it gave us a set of independent channels with no crosstalk. Do other such techniques exist for obtaining independent channels? In particular, we know of lossless matrices, which are a generalization of unitary matrices to the polynomial matrix domain. Does there exist a generalization of singular-value decomposition for polynomial matrices, where the premultiplying and postmultiplying matrices are lossless? These are questions in the theory of polynomial matrices that are unsolved to the best of our knowledge.

The Smith Form technique for equalization required knowledge of the channel characteristics. We have not investigated its application to a practical situation where the channel characteristics may be varying. The question of whether the Smith Form Decomposition could be done adaptively is also an open one.

In Chapter 3, we derived optimum filters for block data transmission with the knowledge of the channel and noise characteristics. Adaptive techniques for doing the same in the case of time-varying channels and non-stationary noise are worth investigating.

In Chapter 5, we showed how to obtain the optimum filters in the case when the noise is crosstalk. We assumed homogeneity of all the wires in a binder group and all loops transmitting using the same scheme. A question that could be asked is whether improvements can be obtained by transmitting using different schemes on different loops and exploiting this to mitigate crosstalk. We were able to present an exact method to find the optimum filters only in one special case, i.e, all channels had a positive input power. Our method to solve the problem in the other cases was a crude iterative method that was not guaranteed to give a solution. A method to solve the eigenvalue problem involved in finding the optimum filters in the crosstalk case is a problem of great interest, and we hope future researchers will attempt it. We have also noted that the decision-feedback equalizer could probably be simplified by using a pole-zero model for the loops; an investigation of this aspect may be an avenue for further research.

In summary, there is a host of problems available in this area for future researchers to tackle, and we hope they will have success in doing so.

References

[1] R. E. Crochiere and L. R. Rabiner, *Multirate Digital Signal Processing*, Prentice-Hall, 1983.

[2] R.D. Koilpillai, T.Q. Nguyen and P.P. Vaidyanathan, "Theory and Design of Perfect Reconstruction Transmultiplexers and their Relation to Perfect Reconstruction QMF Banks," Conference Record, *Twenty-third Asilomar Conference on Signals, Systems and Computers*, pp. 247-251, Oct.-Nov. 1989.